

OCRWM

DESIGN CALCULATION OR ANALYSIS COVER SHEET

1. QA: QA
2. Page 1

3. System: Emplacement Drifts
4. Document Identifier: 000-00C-SSE0-00500-000-00A

5. Title: Structural Stability of a Drip Shield Under Quasi-Static Pressure

6. Group: Waste Package and Components - Structural

7. Document Status Designation: Preliminary Final Cancelled

8. Notes/Comments
An AP-2.14Q review was completed on August 27, 2004.

The calculations contained in this document were developed by Waste Package and Components and are intended solely for the use of the Design and Engineering in its work regarding the drip shield. Yucca Mountain Project personnel from the Waste Package and Components should be consulted before use of the calculations for purposes other than those stated herein or use by individuals other than authorized personnel in the Design and Engineering.

Attachments	Total Number of Pages
See Section 8	

RECORD OF REVISIONS

9. No.	10. Reason For Revision	11. Total # of Pgs.	12. Last Pg. #	13. Originator (Print/Sign/Date)	14. Checker (Print/Sign/Date)	15. QER (Print/Sign/Date)	16. Approved/Accepted (Print/Sign)	17. Date
00A	Initial Issue	84	V1-2	Tim Schmitt <i>Tim Schmitt</i> 8/27/04	Zekai Ceylan <i>Zekai Ceylan</i> 8/27/04	Daniel J. Tunney <i>Daniel J. Tunney</i> 8/27/2004	Michael J. Anderson <i>Michael J. Anderson</i>	8/27/04

NOTICE OF OPEN CHANGE DOCUMENTS - THIS DOCUMENT IS IMPACTED BY THE LISTED CHANGE DOCUMENTS AND CANNOT BE USED WITHOUT THEM.

1) CACN-001, DATED 03/11/2008

CONTENTS

	Page
1. PURPOSE	7
2. METHOD	7
3. ASSUMPTIONS	8
4. USE OF COMPUTER SOFTWARE.....	10
5. CALCULATION	11
5.1 MATERIAL PROPERTIES	11
5.2 FINITE ELEMENT REPRESENTATION	12
6. RESULTS	19
7. REFERENCES	22
8. ATTACHMENTS.....	25

FIGURES

	Page
Figure 1. Full Finite Element Representation of the Drip Shield	13
Figure 2. One-Segment Finite Element Representation of the Drip Shield.....	13
Figure 3. Details of Finite Element Representation of the Drip Shield: (a) Top (inside view), and (b) Side (outside view)	14
Figure 4. Bilinear Elastoplastic Constitutive Representation (Notation: σ_y = yield strength, E = modulus of elasticity, E_1 = tangent modulus).....	15
Figure 5. Pressure Notation	16
Figure 6. Vertical (Y-) Displacement Evolution of the Apex Drip Shield Node for Realization 5 for Various Damping Levels.....	18
Figure 7. Location of Node 38 for the Vertical Displacement Evaluation	21
Figure II-1. Realization 1: (a) Final Drip Shield Configuration, and (b) Kinetic Energy of the Drip Shield	II-1
Figure II-2. Realization 2: (a) Final Drip Shield Configuration, and (b) Kinetic Energy of the Drip Shield	II-2
Figure II-3. Realization 3: (a) Final Drip Shield Configuration, and (b) Kinetic Energy of the Drip Shield	II-3
Figure II-4. Realization 4: (a) Final Drip Shield Configuration, and (b) Kinetic Energy of the Drip Shield	II-4
Figure II-5. Realization 5: (a) Final Drip Shield Configuration, and (b) Kinetic Energy of the Drip Shield	II-5
Figure II-6. Realization 6: (a) Final Drip Shield Configuration, and (b) Kinetic Energy of the Drip Shield	II-6
Figure II-7. Average of all Realizations with Density of Surrounding Rock Multiplied by 2.5: (a) Final Drip Shield Configuration, and (b) Kinetic Energy of the Drip Shield.....	II-7
Figure II-8. Average of all Realizations with Density of Surrounding Rock Multiplied by 3.0 (a) Final Drip Shield Configuration, and (b) Kinetic Energy of the Drip Shield....	II-8
Figure II-9. Average of all Realizations with Density of Surrounding Rock Multiplied by 4.0 (a) Final Drip Shield Configuration, and (b) Kinetic Energy of the Drip Shield....	II-9
Figure II-10. Average of all Realizations with Density of Surrounding Rock Multiplied by 2.5 for Full Length Drip Shield (a) Final Drip Shield Configuration, and (b) Kinetic Energy of the Drip Shield.....	II-10
Figure III-1. Maximum Shear Stress (Pa) Plot for Realization 3	III-1
Figure III-2. Maximum Shear Stress (Pa) Plot of the Large Support Beam Realization 3	III-1
Figure III-3. Maximum Shear Stress History Plots of the Large Support Beam for Realization 3 (a) Maximum Shear Stress through the Cross-Section, and (b) Average of the Shear Stress through the Cross-Section.....	III-2
Figure III-4. Maximum Shear Stress (Pa) Plot of the Bulkhead for Realization 3.....	III-3
Figure III-5. Maximum Shear Stress History Plots of the Bulkhead for Realization 3 (a) Maximum Shear Stress through the Cross-Section, and (b) Average of the Shear Stress through the Cross-Section	III-4

Figure III-6. Maximum Shear Stress (Pa) Plot for the Average of all Realizations with Density of Surrounding Rock Multiplied by 2.5	III-5
Figure III-7. Maximum Shear Stress (Pa) Plot of the Large Support Beam for the Average of all Realizations with Density of Surrounding Rock Multiplied by 2.5	III-5
Figure III-8. Maximum Shear Stress History Plots of the Large Support Beam for the Average of all Realizations with Density of Surrounding Rock Multiplied by 2.5 (a) Maximum Shear Stress through the Cross-Section, and (b) Average of the Shear Stress through the Cross-Section	III-6
Figure III-9. Maximum Shear Stress (Pa) Plot of the Bulkhead for the Average of all Realizations with Density of Surrounding Rock Multiplied by 2.5	III-7
Figure III-10. Maximum Shear Stress History Plots of the Bulkhead for the Average of all Realizations with Density of Surrounding Rock Multiplied by 2.5 (a) Maximum Shear Stress through the Cross-Section, and (b) Average of the Shear Stress through the Cross-Section	III-8
Figure III-11. Maximum Shear Stress (Pa) Plot for the Average of all Realizations with Density of Surrounding Rock Multiplied by 3.0	III-9
Figure III-12. Maximum Shear Stress (Pa) Plot of the Large Support Beam for the Average of all Realizations with Density of Surrounding Rock Multiplied by 3.0	III-9
Figure III-13. Maximum Shear Stress History Plots of the Large Support Beam for the Average of all Realizations with Density of Surrounding Rock Multiplied by 3.0 (a) Maximum Shear Stress through the Cross-Section, and (b) Average of the Shear Stress through the Cross-Section	III-10
Figure III-14. Maximum Shear Stress (Pa) Plot of the Bulkhead for the Average of all Realizations with Density of Surrounding Rock Multiplied by 3.0	III-11
Figure III-15. Maximum Shear Stress History Plots of the Bulkhead for the Average of all Realizations with Density of Surrounding Rock Multiplied by 3.0: (a) Maximum Shear Stress through the Cross-Section, and (b) Average of the Shear Stress through the Cross-Section	III-12
Figure III-16. Maximum Shear Stress (Pa) Plot for the Average of all Realizations with Density of Surrounding Rock Multiplied by 4.0	III-13
Figure III-17. Maximum Shear Stress (Pa) Plot of the Large Support Beam for the Average of all Realizations with Density of Surrounding Rock Multiplied by 4.0	III-13
Figure III-18. Maximum Shear Stress History Plots of the Large Support Beam for the Average of all Realizations with Density of Surrounding Rock Multiplied by 4.0: (a) Maximum Shear Stress through the Cross-Section, and (b) Average of the Shear Stress through the Cross-Section	III-14
Figure III-19. Maximum Shear Stress (Pa) Plot of the Bulkhead for the Average of all Realizations with Density of Surrounding Rock Multiplied by 4.0	III-15
Figure III-20. Maximum Shear Stress History Plots of the Bulkhead for the Average of all Realizations with Density of Surrounding Rock Multiplied by 4.0: (a) Maximum Shear Stress through the Cross-Section, and (b) Average of the Shear Stress through the Cross-Section	III-16
Figure IV-1. Damaged Area of the Ti-7 Plates for Realization 1	IV-1
Figure IV-2. Damaged Area of the Ti-7 Plates for Realization 2	IV-1
Figure IV-3. Damaged Area of the Ti-7 Plates for Realization 3	IV-2
Figure IV-4. Damaged Area of the Ti-7 Plates for Realization 4	IV-2

Title: Structural Stability of a Drip Shield Under Quasi-Static Pressure

Document Identifier: 000-00C-SSE0-00500-000-00A

Page 5 of 26

Figure IV-5. Damaged Area of the Ti-7 Plates for Realization 5.....	IV-3
Figure IV-6. Damaged Area of the Ti-7 Plates for Realization 6.....	IV-3
Figure V-1. Details of Finite Element Representation of the Drip Shiled Support Beam: (a) The First Mesh, and (b) The Second Mesh.....	V-2
Figure V-2. Details of Finite Element Representation of the Drip Shiled Bulkhead: (a) The First Mesh, and (b) The Second Mesh	V-3
Figure VI-1. Vertical Displacement of Drip Shield Top: (a) LS-DYNA V960, and (b) LS-DYNA V970.....	V-1

TABLES

	Page
Table 1. Average Pressure Values on the Drip Shield for Quasi-Static Drift Degradation (0.2-m rock size)	17
Table 2. Vertical Displacement of the Drip Shield Top Plate	19
Table 3. Average Pressure Values on the Drip Shield for Quasi-Static Drift Degradation..... (Averaged Realizations with Increased Density).....	19
Table 4. Vertical Displacement of the Drip Shield Top Plate	20
(Averaged Realizations with Increased Density).....	20
Table 5. Stress Intensities in the Drip Shield Structural Components.....	20
Table 6. Damaged Area of the Drip Shield Top and Side Plates.....	21
Table 7. List of Electronic Files in Attachment VII	25
Table V-1. Volume of Typical Element for Two Different Finite Element Meshes.....	V-1
Table V-2. Maximum Vertical Displacement of Drip Shield Top for Two Different Finite Element Meshes	V-1
Table VI-1. Maximum Vertical Displacement of Drip Shield Top for Two Different LS- DYNA Versions.....	VI-2

1. PURPOSE

The objective of this calculation is to study structural stability of a drip shield subjected to quasi-static pressure. The pressure results from the quasi-static drift degradation in the lithophysal rock zone. The pressure varies along the drip shield contour (Figure 3) due to the stochastic nature of the drift degradation (i.e., formation of the rock blocks of irregular shapes and different sizes and their fall).

The scope of this document is limited to reporting whether or not the drip shield structural collapse (i.e., the loss of structural stability) occurs. If the structural collapse does not occur the scope is limited to reporting the calculation results in terms of the maximum vertical deflection of the drip shield top plate (the apex point at the symmetry plane), maximum steady-state stress intensities in the structural members (bulkhead and large support beams), and damage area (area of the top and side plates exceeding 50% of the yield strength).

This calculation is performed by Waste Package and Components group in support of the Total System Performance Assessment–License Application seismicity modeling. AP-3.12Q, *Design Calculations and Analyses* (Reference 2) is used to perform the calculation and develop the document. The drip shield is classified as a Safety Category item (Reference 4, p. A-5). Therefore, this calculation is subject to the requirements of *Quality Assurance Requirements and Description* (Reference 3).

The information provided by the sketch attached to this calculation (Attachment I) is that of the potential design of the drip shield considered in this calculation and provides the potential dimensions and materials for the drip shield design. All obtained results are valid for this design only.

2. METHOD

The calculations are performed by the finite element analysis method. The finite element calculations are performed by using the explicit solver† of the commercially available LS-DYNA Version (V) 960.1106 (Reference 1) and LS-DYNA V970.3858 D MPP-00 (Reference 5) finite element analysis codes (hereinafter referred to as LS-DYNA V960 and LS-DYNA V970, respectively‡). The LS-DYNA explicit solver uses the central difference method (Reference 12, Section 6.2.1 and Reference 13, Section 21.2) for time integration of the governing equations.

If the structural collapse does not occur the scope is limited to reporting the calculation results in terms of the maximum vertical deflection of the drip shield top plate (the apex point at the symmetry plane), maximum steady-state stress intensities in the structural members (bulkhead and large support beams), and damage area (area of the top and side plates exceeding 50% of the yield strength).

† For explicit methods see, for example, Reference 12, Section 6.2.

‡ LS-DYNA V960 and LS-DYNA V970 are referred to as LS-DYNA whenever it is unnecessary to make a distinction.

3. ASSUMPTIONS

In the course of developing this document, the following assumptions are made regarding the structural calculation.

- 3.1 The density and Poisson's ratio are not available for Ti-7 (Titanium Grade 7 [SB-265 R52400]) and Ti-24 (Titanium Grade 24 [SB-265 R56405]), except at room temperature (RT) (20 °C). (Note: In regard to UNS designation for Ti-24, note that Ti-24 has the same mechanical properties as Ti-5 since the compositions are almost identical; see Reference 14, Section II, Part B, SB-265, Table 2.) The RT density and RT Poisson's ratio are assumed for these materials. The impact of using RT density and RT Poisson's ratio is anticipated to be negligible. The rationale for this assumption is that the material properties in question do not have dominant impact on the calculation results. This assumption is used in Section 5.1 and corresponds to paragraph 5.2.8.6 of Reference 15.
- 3.2 The temperature-dependent material properties are not available for TSw2 (Topopah Spring Welded-Lithophysal Poor) rock except at RT. The TSw2 is used to represent the rigid invert (see Section 5.2) and the material properties are necessary only for the contact definitions. The corresponding RT material properties are assumed for this material. The impact of using RT material properties is anticipated to be negligible. The rationale for this assumption is that the material properties of the invert do not have a significant impact on the calculation results. This assumption is used in Section 5.1 and corresponds to paragraph 5.2.16.1 of Reference 15.
- 3.3 The modulus of elasticity and Poisson's ratio of the TSw2 are characterized by significant scatter of data. For the purpose of the present calculation modulus of elasticity is assumed to be 33 GPa, and Poisson's ratio 0.21. The rationale for this assumption is that these values represent the mean values of the middle nonlithophysal zone (Ttptmn) the uppermost interval of the TSw2 unit (see Reference 26, Tables 6 and 5, respectively, DTN: MO402DQRIRPPR.003 Reference 16). This assumption is used in Section 5.1 and corresponds to paragraph 5.2.16.3 of Reference 15.
- 3.4 The density of the TSw2 is assumed to be $2370 \text{ kg}/\text{m}^3$. The rationale for this assumption is that this value agrees well with all Topopah Spring Welded rocks and is not exceeded by any of other rocks presented in Reference 17, Table 2. It should be noted that this assumption has no effect on the calculation results since density of the rock affects only masses of the rigid invert. This assumption is used in Section 5.1.
- 3.5 It is assumed that the dynamic (sliding) friction coefficient for the contact between the drip shield and invert is 0.4. The rationale for this assumption is that this friction coefficient represents a reasonable estimate based on available range for metal-on-stone friction coefficients, which is from 0.3 to 0.7 (see Reference 18, Table 8.1, p. 306). The friction coefficient used in this calculation is somewhat below the range average (that is used, for example, in Reference 10, Assumption 3.5) for the sake of conservatism of the drip shield stability assessment. This assumption is used in Section 5.2.

- 3.6 The variation of functional friction coefficient between the static and dynamic value as a function of relative velocity of the surfaces in contact is not available in literature for the materials used in this calculation (see Section 5.2). Therefore, the effect of relative velocity of the surfaces in contact is neglected in these calculations by assuming that the functional friction coefficient and static friction coefficient are both equal to the dynamic friction coefficient. The impact of this assumption on results presented in this document is negligible. The rationale for this conservative assumption is that it maximizes the relative motion of the drip shield with respect to the invert by minimizing the friction coefficient. This assumption is used in Section 5.2 and corresponds to paragraph 5.2.14.2 of Reference 15.
- 3.7 The temperature of the drip shield is assumed to be 150 °C. The rationale for this assumption is that this temperature is conservative for most of the regulatory period for high-temperature operating modes and strictly conservative for low-temperature operating modes. The waste package temperature remains below 150 °C for the 97% of the regulatory time period, 10,000 years (see Reference 19, Figure 6-3) and the drip shield temperature is less than the waste package temperature. This assumption is used in Section 5.1.
- 3.8 The thickness of the Ti-7 and T-24 plates are reduced by 2 mm (DTN: MO0306SPAGLCDS.001 [Reference 20], file name: 5-year CR-Data.pdf). The rationale for this assumption is that the maximum general corrosion of titanium in 10,000 years is conservatively determined using the corrosion rate for 100th percentile value for both sides of the titanium plate (see Reference 21 and Reference 22, Section 6.3.3.2). Furthermore, Reference 22, p. 12 states that Ti-16 was used as an analog of Ti-7 for the corrosion tests due to its compositional similarity to Ti-7. This assumption is used in Section 5.2.
- 3.9 The drip shield sides are assumed to be unconstrained in lateral direction during the 10,000-year regulatory period (with the exception of the lateral constraint provided by the emplacement pallet). The rationale for this assumption is that the gantry rail is made of steel sets (Reference 7, Attachment A-1), which are not anticipated to remain intact (eventually corrode away) during the 10,000-year regulatory period. This assumption is used in Section 5.2.
- 3.10 The drip shield connector assembly, lifting feature, and base are excluded from the finite element representation for simplicity. The rationale for this assumption is that the effect of these drip shield components on the calculation results is negligibly small. This assumption is used in Section 5.2.

4. USE OF COMPUTER SOFTWARE

The qualified finite element analysis computer codes used for this calculation are Livermore Software Technology Corporation LS-DYNA V960.1106 (Reference 1) and LS-DYNA V970.3858 D MPP-00 (Reference 5) (LS-DYNA V960 and LS-DYNA V970, respectively). Both LS-DYNA codes are obtained from Software Configuration Management in accordance with the appropriate procedure (Reference 6). LS-DYNA V960.1106 is identified by the Software Tracking Number 10300-960.1106-00, while LS-DYNA V970 D MPP-00 is identified by the Software Tracking Number 10300-970.3858 D MPP-00. LS-DYNA is appropriate for this calculation. The LS-DYNA calculations performed herein are fully within the range of the validation performed for LS-DYNA V960 code (Reference 11, Sections 4 and 5) and LS-DYNA V970 code (Reference 9, Sections 4 and 5). The calculations using the LS-DYNA V960 software are executed on six Hewlett-Packard (HP) 9000 series UNIX workstations (Operating System HP-UX 11.00), identified with Yucca Mountain Project (YMP) tag numbers 151665, 151664, 150691, 150689, 150690, 150688, located in Las Vegas, Nevada. The calculations using the LS-DYNA V970 software are executed on the HP Itanium2 (IA64) series UNIX workstations (Operating System HP-UX 11.22), identified with YMP tag number 501711, located in Las Vegas, Nevada. Access to the code is granted by the Software Configuration Management in accordance with the appropriate procedures.

TrueGrid V2.2 (XYZ Scientific Applications, Inc.) is used in this calculation solely to mesh geometric representations of the domain. Therefore, the use of TrueGrid V2.2 is exempt of the requirements defined in Reference 6 (Section 2.1.2). The mesh is created on the HP 9000 series UNIX workstation (Operating System HP-UX 11.00) identified with YMP tag number 150689, located in Las Vegas, Nevada.

LS-PREPOST V1.0 (Livermore Software Technology Corporation) is the postprocessor used for visual display and graphical representation of results that is exempt of the requirements defined in Reference 6 (Section 2.1.2). The postprocessing is performed on the HP Itanium2 (IA64) series UNIX workstations (Operating System HP-UX 11.22), identified with YMP tag number 501711, located in Las Vegas, Nevada.

5. CALCULATION

5.1 MATERIAL PROPERTIES

Material properties used in these calculations are listed in this section. The material properties are evaluated for 150 °C (Assumption 3.7). Some of the temperature-dependent material properties are not available for Ti-7, Ti-24, and TSw2 rock. Therefore, RT density and RT Poisson's ratio are used for Ti-7 and Ti-24 (see Assumption 3.1). The RT material properties are used for TSw2 rock (Assumption 3.2).

Note that the tangent (hardening) modulus, listed in this section, is a parameter of the bilinear elastoplastic constitutive representation used for the drip shield materials in this calculation. It is defined in Section 5.2.1 (see Figure 4).

SB-265 R52400 (Titanium Grade 7 [Ti-7]) (Note: All properties of Ti-7, with exception of Poisson's ratio, are obtained from Reference 10, Sections 5.1 through 5.1.3):

Density = 4520 kg/m^3 (at RT)

Yield strength = 209 MPa (at 150 °C)

Poisson's ratio = 0.32 (at RT) (Reference 27, Section "Mechanical Properties")

Modulus of elasticity = 101 *GPa* (at 150 °C)

Tangent (hardening) modulus = 0.448 *GPa* (at 150 °C)

SB-265 R56405 (Titanium Grade 24 [Ti-24]; in regard to this UNS designation, note that Ti-24 has the same mechanical properties with Ti-5 since the compositions are almost identical, see Ref. 14, Section II, Part B, SB-265, Table 2) (Note: All properties of Ti-24, with exception of density and Poisson's ratio, are obtained from Reference 10, Sections 5.1 through 5.1.3):

Density = 4430 kg/m^3 (at RT) (Reference 28, p. 620)

Yield strength = 750 MPa (at 150 °C)

Poisson's ratio = 0.34 (at RT) (Reference 28, p. 621)

Modulus of elasticity = 108 *GPa* (at 150 °C)

Tangent (hardening) modulus = 1.52 *GPa* (at 150 °C)

TSw2 Rock (Invert ballast material):

Density = 2370 kg/m^3 (at RT) (Assumption 3.4)

Poisson's ratio = 0.21 (at RT) (Assumption 3.3)

Modulus of elasticity = 33.0 GPa (at RT) (Assumption 3.3)

5.2 FINITE ELEMENT REPRESENTATION

The three-dimensional finite element representation that is used to perform the structural stability calculations is illustrated in Figure 2. This time-efficient finite element representation is limited to one segment of the drip shield (Figure 1 and Attachment I); thus, it is hereinafter referred to as the one-segment finite element representation. Appropriate boundary conditions, which are discussed later in this section, are specified at the end-sections A-A and B-B of the one-segment representation (Figure 2) to account for the removed part of the drip shield. Three calculations are also performed by using the full finite element representation of the drip shield (Figure 1) to verify the results obtained by using the one-segment finite element representation (Section 6).

The drip shield connector assembly, lifting feature, and base are excluded from the finite element representation (Assumption 3.10). The benefit of this simplification is to reduce the computer execution time while preserving the features of the problem most relevant to the structural response of the drip shield.

The thickness of the drip shield components is reduced by 2 mm (Assumption 3.8). Moreover, the overall thickness of the parts of the drip shield plates covered by the internal and external support plates is conservatively reduced by 4 mm, implying the thickness reduction of 2 mm per plate at each location.

In the finite element representations the drip shield is free to move laterally with exception of the constraint provided by the pallet sides (Figure 2) (Assumption 3.9). Note that this calculation is concerned with the quasi-static pressure. Thus, the pressure distribution along the drip shield contour is calculated from the drip shield that is in static equilibrium. The final deformed drip shield configuration, corresponding to static equilibrium under the specific pressure distribution, is different from the drip shield configuration before the pressure application. It is important to emphasize, though, that the equilibrium drip shield configuration may or may not be affected by the pallet lateral constraint depending on the pressure distribution.

As previously mentioned, another boundary condition is applied on the one-segment finite element representation (Figure 2). Specifically, all drip shield nodes belonging to end-sections A-A and B-B (Figure 2) are constrained from translating in the longitudinal (z-) direction and from rotating about the x-axis and y-axis. The rationale for this boundary condition is twofold: (1) the drip shield (as represented in Figure 1) has a plane of longitudinal symmetry and its geometry for the most part consists of the repeating segments, and (2) the pressure distribution is independent of the longitudinal (z-) coordinate.

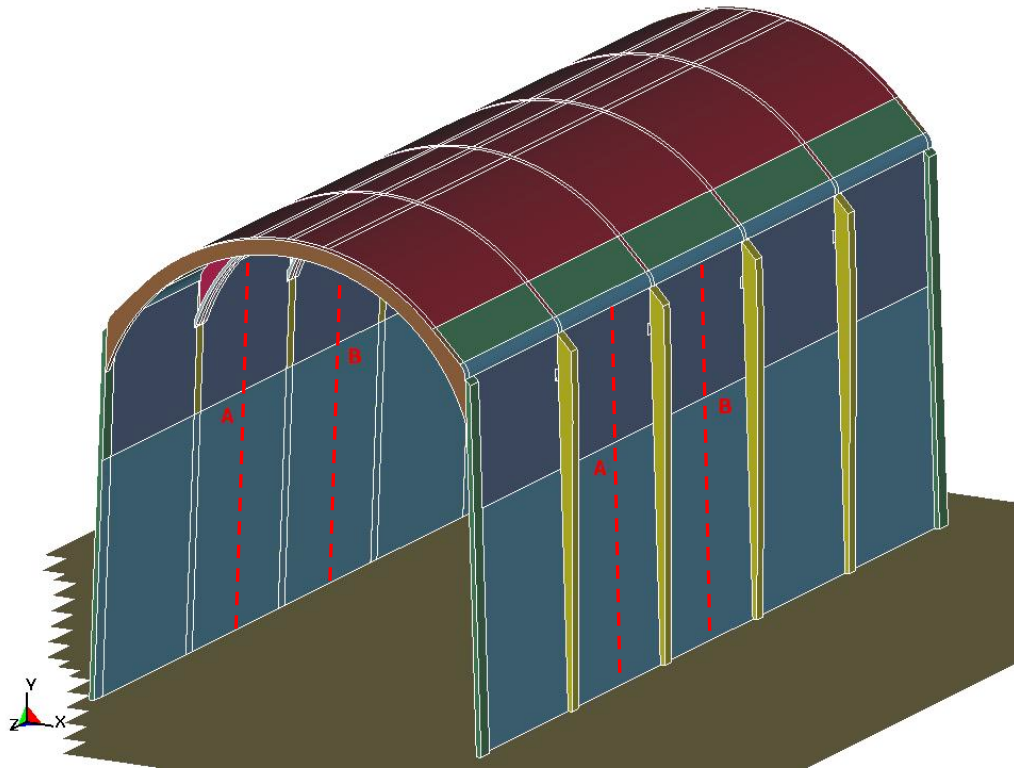


Figure 1. Full Finite Element Representation of the Drip Shield

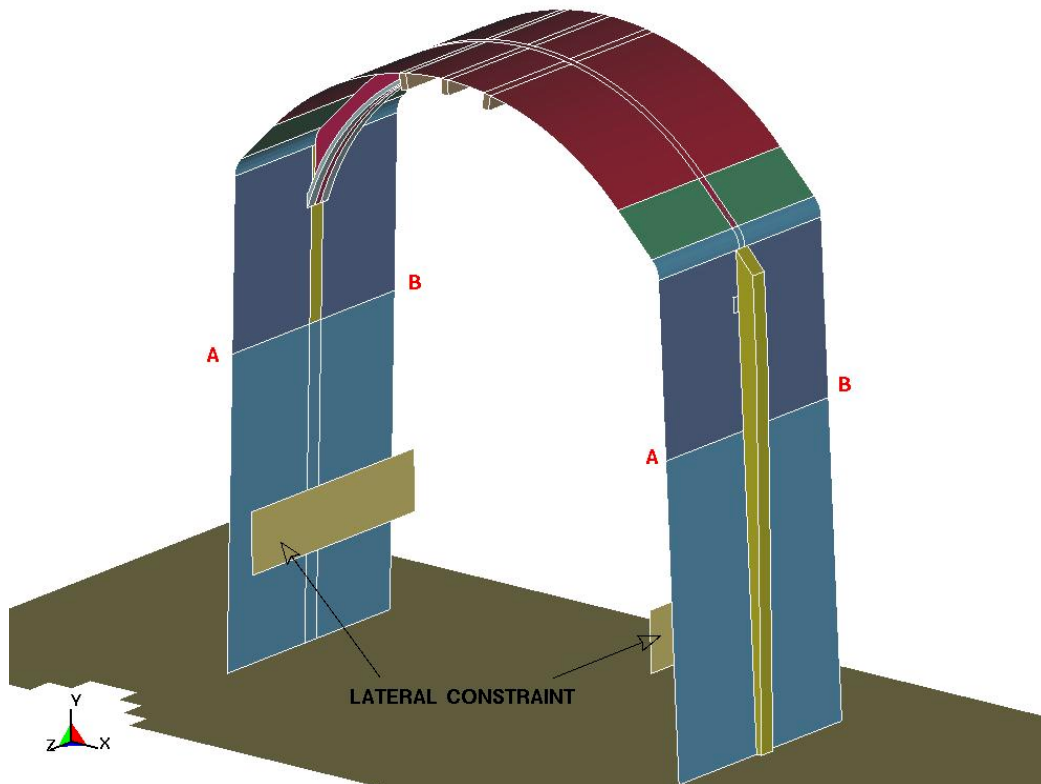


Figure 2. One-Segment Finite Element Representation of the Drip Shield

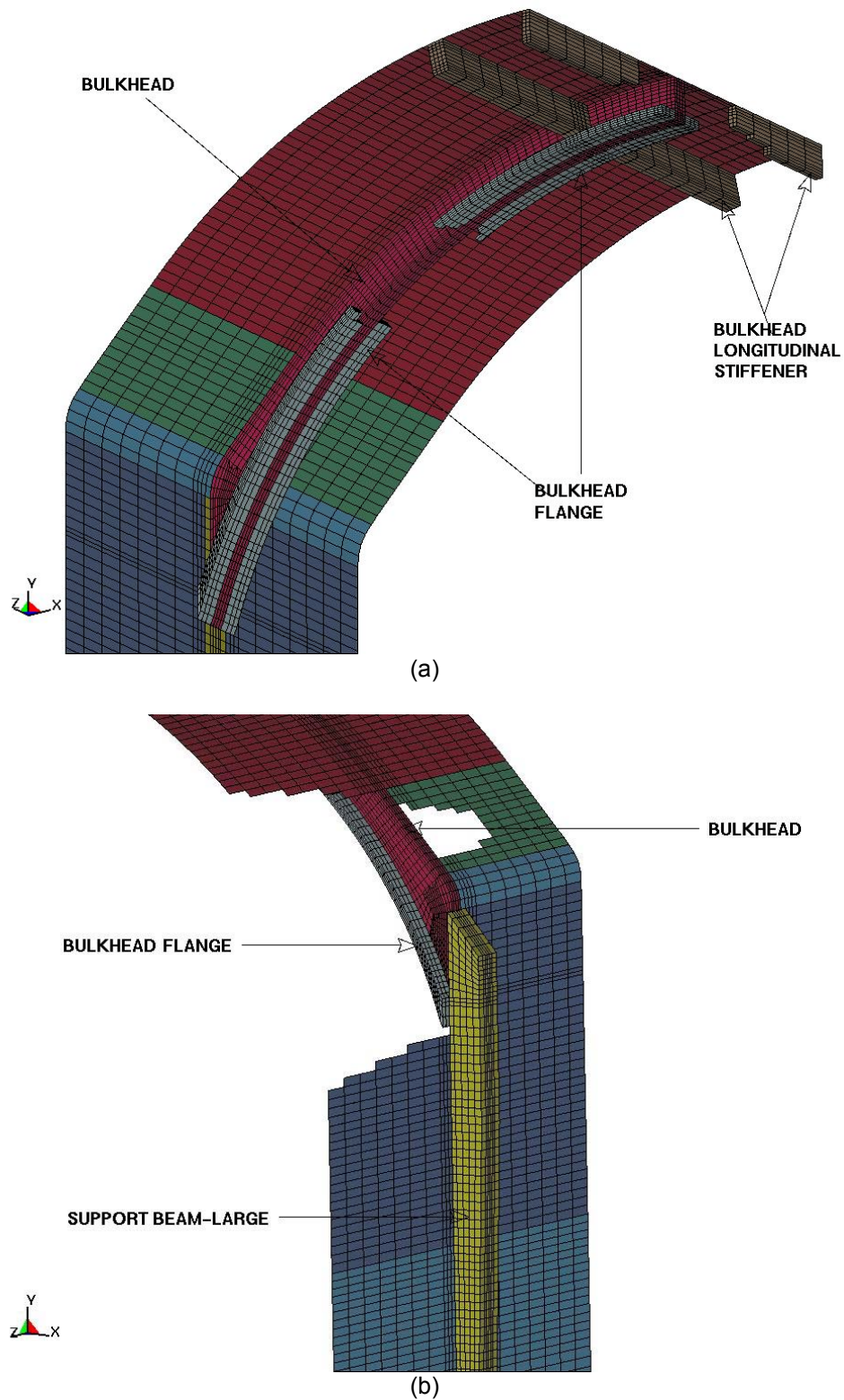


Figure 3. Details of Finite Element Representation of the Drip Shield: (a) Top (inside view), and (b) Side (outside view)

Note: Some drip shield parts are partially removed from Figure 3 to improve visibility.

The finite element representations are developed by using shell elements for the drip shield plates (specifically, DS plate-1, DS plate-2, and support plates), and solid (brick) elements for the rest of the structure (i.e., the support beams, bulkheads, bulkhead longitudinal stiffeners, and bulkhead flanges; see Attachment I). The details of the finite element representation are illustrated in Figure 3. The fully integrated four-node shell element (Reference 8, p. 26.22) and the constant-stress eight-node solid element (Reference 8, p. 26.30) are used for all calculations. Gauss integration and five through-thickness integration points (Reference 8, p. 26.23) are specified for the shell element. One-point Gaussian quadrature is used for the solid element (Reference 13, Section 3).

Contacts are specified between the drip shield and invert and the drip shield and lateral constraint. In absence of more specific data, the friction coefficient for all contacts is assumed to be 0.4 (see Assumption 3.5). Furthermore, the functional friction coefficient, static friction coefficient, and dynamic friction coefficient are assumed to be equal (Assumption 3.6). (It should be noted that these simulations are quasi-static and that the effect of the variation of friction coefficient between the static and dynamic value as a function of relative velocity of the surfaces in contact is not as important as in transient analysis.)

5.2.1 Constitutive Representation of the Drip Shield Materials

The LS-DYNA finite element code requires input in terms of true stress and strain definitions (for the true stress and strain definitions see Reference 23, Chapter 9). Also, the results of this simulation are required to include elastic and plastic deformations of the drip shield materials. When the materials are driven into the plastic range, the slope of the stress-strain curve continuously changes. Thus, a simplification for the stress-strain curve is needed to incorporate plasticity into the finite element analysis. A simple approximation often used in engineering is to use a straight line that connects the yield strength point and the ultimate strength point of the material (bilinear elastoplastic constitutive representation, Figure 4). The tangent (hardening) modulus represents the slope of the stress-strain curve in the plastic region.

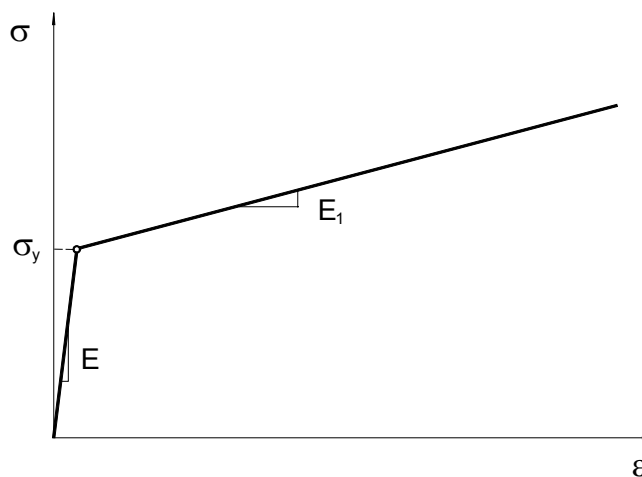


Figure 4. Bilinear Elastoplastic Constitutive Representation (Notation: σ_y = yield strength, E = modulus of elasticity, E_1 = tangent modulus)

5.2.2 Loads on the Drip Shield

The drift degradation in the lithophysal rock mass is a random process and, consequently, the drip shield loads are randomly distributed as well. The drip shield is subjected to an avalanche of small rocks. This series of small-energy impacts on the drip shield results in a pressure that varies along the drip shield contour (Figure 3). Thus, the pressure variability is due to the stochastic nature of the drift degradation (i.e., formation of the rock blocks of irregular shapes and different sizes and their fall). The variable loads of the collapsed rocks for six realizations are calculated using a two-dimensional UDEC software (Reference 29). This two-dimensional analysis does not provide variation of the load along the length of the drip shield. Applying the pressure uniformly along the length of the drip shield is conservative. In reality, the drip shield loads would vary along the length of the drip shield in the same way the loads vary along the cross-section. A discussion of the methods and results of finding the pressure distributions can be found in Section 6.4.2.5 of Reference 30.

For the purpose of this calculation, the pressure distribution along the drip shield contour (Reference 25) is discretized over 30 segments of approximately equal length as indicated in Figure 5. (Note that the even-number segments are omitted from Figure 5 to improve visibility.) The pressure distribution does not vary in the longitudinal (z-) direction in this calculation. In order to capture the quasi-static nature of the loading and minimize the oscillations of results, the applied loads (the pressure and gravitational acceleration) are ramped from 0 to 0.1 s and then held constant. (Thus, the load are applied in full intensity at 0.1 s.)

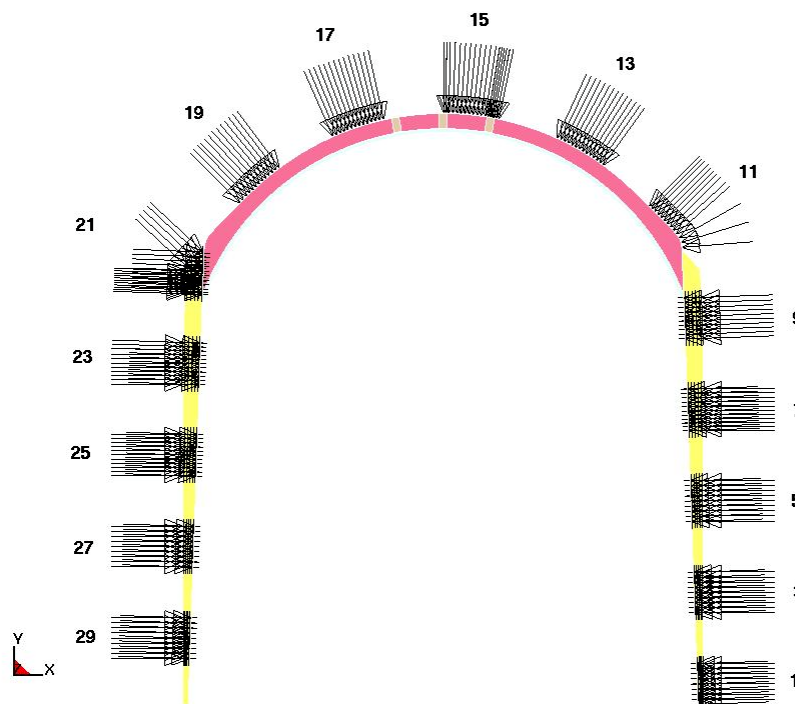


Figure 5. Pressure Notation

To assess dependence of the drip shield pressures on the stochastic nature of the rockfall, the problem of quasi-static drift collapse is solved for six realizations. The average pressures on the drip shield sides and top for all six cases are summarized in Table 1 (see Reference 25). The average pressure values presented in Table 1 vividly illustrate the random nature of the loading due to the rockfall in the lithophysal rock mass.

Table 1. Average Pressure Values on the Drip Shield for Quasi-Static Drift Degradation (0.2-m rock size)

Realization	Pressure (kPa)		
	Left	Top	Right
1	41.54	108.92	58.76
2	19.15	147.07	19.33
3	31.35	154.80	6.69
4	57.23	129.76	128.82
5	69.69	112.73	105.43
6	32.97	113.87	52.19

The simulations are terminated either when the static equilibrium of the drip shield is reached (based on the kinetic energy history), or when the loss of the drip shield structural stability occurs. Thus, the termination times are different for different realizations due to the stochastic nature of the pressure distribution.

5.2.3 System Damping

In order to obtain quasi-static results, it is necessary to apply system damping. The mass-proportional system damping is applied globally. As discussed in Reference 13 (Section 28.2), the most appropriate damping constant for the system is usually the critical damping constant. The critical damping constant for the drip shield, $DC = 116 \text{ rad/s}$, is calculated in Reference 24, Section 5.2.2. The damping constant used in this calculation is reduced to $DC = 100 \text{ rad/s}$ to ensure that the system is not over-damped. The appropriateness of the damping coefficient and the pressure ramp time (0.1 s) is confirmed by the character of the vertical-deflection time history presented in Figure 6 (see Attachment VII, folders RN5-960, RN5-DC=50, and RN5-nodamp) (i.e., the amplitude of the oscillations of the vertical-deflection time history around the steady-state solution decays fast).

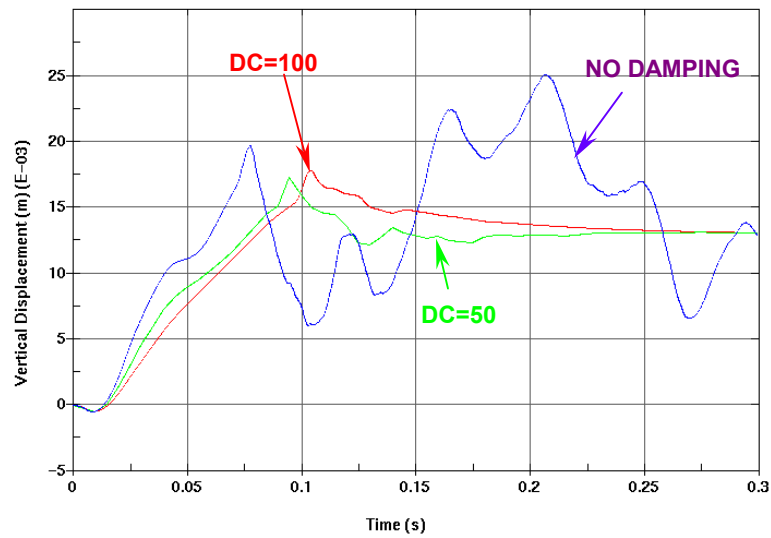


Figure 6. Vertical (Y-) Displacement Evolution of the Apex Drip Shield Node for Realization 5 for Various Damping Levels

Note that the quasi-static solution by definition corresponds to the steady-state value obtained by the end of the simulation (the solution is transient).

6. RESULTS

All six realizations indicate that the drip shield reaches static equilibrium without the loss of structural stability for the given quasi-static pressure distributions (Reference 25). Figures II-1a, II-2a, II-3a, II-4a, II-5a, II-6a illustrate the final drip shield configurations. The kinetic energy plots presented in Figures II-1b, II-2b, II-3b, II-4b, II-5b, II-6b demonstrate that the final configuration corresponds to the drip shield static equilibrium.

The results presented below are found by carefully examining each reported time step taken by LS-DYNA in the files of Attachment VII, which outputs stresses, strains, deflections, etc. at each step, for each defined part.

The maximum vertical deflections of the drip shield top plate (node 38, see Figure 7), along the vertical symmetry plane are presented in Table 2. Node 38 is located on the outside surface of the top plate above the bulkhead (see Figure 7). Note that a positive value in Table 2 indicates an upward displacement.

Table 2. Vertical Displacement of the Drip Shield Top Plate

Realization	Vertical Displacement (10^{-3} m)
1	4.4
2	-9.3
3	-8.2
4	23.1
5	13.1
6	3.9

Three additional simulations are performed in order to estimate the factor of safety of the drip shield with respect to the static load by the collapsed rock mass. In these cases each segment load is calculated as an average for the six pressure realizations with the density of the surrounding collapsed rock multiplied by 2.5, 3.0, and 4.0 (Reference 25, files: drip shield quasi-static pressures fs 2.5.xls, drip shield quasi-static pressures fs 3.xls, and drip shield quasi-static pressures fs 4.xls). The averaged pressures are summarized in Table 3.

Table 3. Average Pressure Values on the Drip Shield for Quasi-Static Drift Degradation (Averaged Realizations with Increased Density)

Density Multiplier	Pressure (kPa)		
	Left	Top	Right
2.5	69.86	263.73	80.98
3	82.98	314.81	89.54
4	105.74	415.97	109.03

As illustrated by Figures II-7 and II-8, the pressure as a result of the density multiplication by 2.5 and 3.0 times does not result in the loss of the drip shield structural stability. On the other hand, the

increase of the pressure values corresponding to the density multiplication by 4 times results in a severe deformation of the drip shield, illustrated by Figure II-9. Table 4 displays the same vertical displacements as in Table 2 for each of the averaged pressure distributions with the density multipliers.

The use of one-segment is justified by the simulation performed with the full finite element representation of the drip shield with the pressure of the averaged realizations with the surrounding rock density multiplied by 2.5 (see Figure II-10). The final configuration of the full finite element representation is nearly identical to the segmented drip shield with the same pressure load (see Figure II-7).

Table 4. Vertical Displacement of the Drip Shield Top Plate
(Averaged Realizations with Increased Density)

Density Multiplier	Vertical Displacement (10^{-3} m)
2.5	-1.8
3.0	8.1
4.0	0.8

The maximum shear stress contours and maximum shear stress history plots of the structural components (bulkhead and large support beam) are presented in Attachment III. These are shown for the three cases where the quasi-static pressure distribution is averaged for the six realizations with the density of the surrounding rock multiplied by 2.5, 3.0, and 4.0. Also presented for comparison is the maximum shear stress contours and maximum shear stress history plots for Realization 3. Realization 3 is chosen because it has the highest average vertical pressure. Table 5 summarizes the stress intensities in the structural components (see Attachment III).

Table 5. Stress Intensities in the Drip Shield Structural Components

Realization	Structural Component			
	Large Support Beam		Bulkhead	
	Maximum σ_{int} (MPa)	Average σ_{int} Through Thickness (MPa)	Maximum σ_{int} (MPa)	Average σ_{int} Through Thickness (MPa)
3	530	199	416	214
Averaged with Density x 2.5	595	280	708	320
Averaged with Density x 3.0	788	394	524	260
Averaged with Density x 4.0	848	760	810	440

Attachment III also contains a plot for each of cases with increased density pressure distributions showing the area in the Ti-7 plates where the 1st principal stress exceeds 50% of the yield strength of Ti-7 (see Section 5.1). The red color in the Figures presented in Attachment IV indicates the damaged area, which is defined as the area that the 1st principal stress exceeds 50% of the yield strength. Table 6 summarizes the damaged area.

Table 6. Damaged Area of the Drip Shield Top and Side Plates

Realization	Damaged Area (m ²)	% of Total area
1	0.64	9%
2	0.90	12%
3	0.21	3%
4	2.42	32%
5	1.51	20%
6	1.10	15%

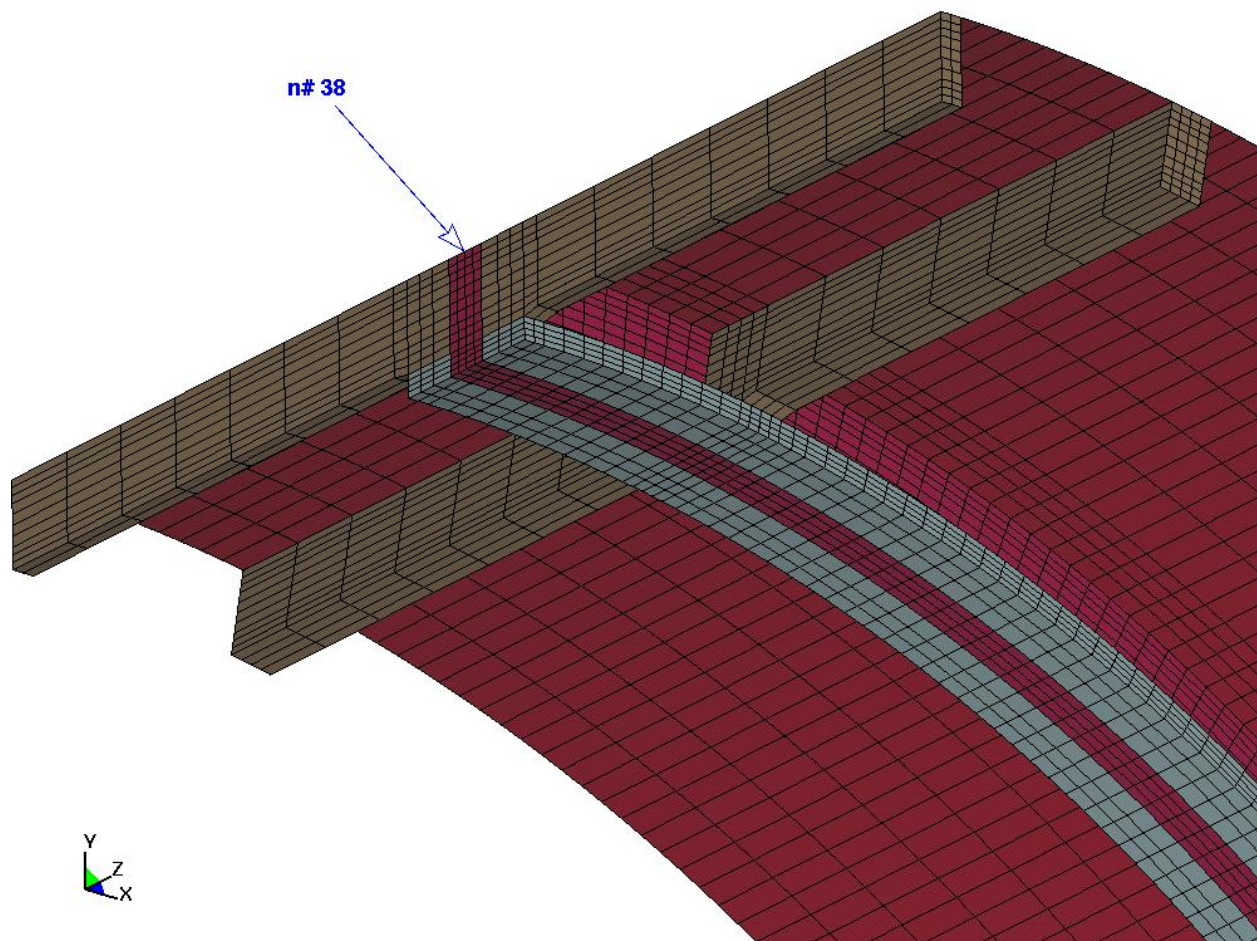


Figure 7. Location of Node 38 for the Vertical Displacement Evaluation

Based on engineering judgement, the output values of these calculations are reasonable for the given inputs. The results of these calculations are suitable for its intended use.

7. REFERENCES

1. BSC (Bechtel SAIC Company) 2002. *Software Code: LS-DYNA*. V960.1106. HP9000. 10300-960.1106-00.
2. AP-3.12Q, Rev. 2, ICN 2. *Design Calculations and Analyses*. Washington, D.C.: U.S. Department of Energy, Office of Civilian Radioactive Waste Management. ACC: DOC.20040318.0002.
3. DOE (U.S. Department of Energy) 2004. *Quality Assurance Requirements and Description*. DOE/RW-0333P, Rev. 16. Washington, D.C.: U.S. Department of Energy, Office of Civilian Radioactive Waste Management. ACC: DOC.20040823.0004.
4. BSC (Bechtel SAIC Company) 2004. *Q-List*. 000-30R-MGR0-00500-000-000 REV 00. Las Vegas, Nevada: Bechtel SAIC Company. ACC: ENG.20040721.0007.
5. BSC (Bechtel SAIC Company) 2003. *Software Code: LS-DYNA*. V.970.3858 D MPP. HP Itanium2, HP-UX 11.22. 10300-970.3858 D MPP-00.
6. LP-SI.11Q-BSC, Rev. 0. *Software Management*. Washington, D.C.: U.S. Department of Energy, Office of Civilian Radioactive Waste Management. ACC: DOC.20040225.0007.
7. BSC (Bechtel SAIC Company) 2004. *Steel Invert Structure - Emplacement Drifts*. 800-SSC-SSE0-00100-000-00B. Las Vegas, Nevada: Bechtel SAIC Company. ACC: ENG.20040519.0017.
8. Livermore Software Technology Corporation. 2003. *LS-DYNA Keyword User's Manual*. Version 970. Livermore, California: Livermore Software Technology Corporation. TIC: 254203.
9. DOE (U.S. Department of Energy) 2003. *Validation Test Report for LS-DYNA Version 970.3858 D MPP*. 10300-VTR-970.3858 D MPP-00. Las Vegas, Nevada: U.S. Department of Energy, Office of Repository Development. ACC: MOL.20031218.0337.
10. BSC (Bechtel SAIC Company) 2004. *Drip Shield Structural Response to Rock Fall*. 000-00C-SSE0-00300-000-00A. Las Vegas, Nevada: Bechtel SAIC Company. ACC: ENG.20040405.0019.
11. BSC (Bechtel SAIC Company) 2002. *LS-DYNA Version 960.1106 Validation Test Report*. Software Baseline Documentation Number: 10300-VTR-960.1106-00. Las Vegas, Nevada: Bechtel SAIC Company. ACC: MOL.20020515.1915.
12. Belytschko, T.; Liu, W.K.; and Moran, B. 2000. *Nonlinear Finite Elements for Continua and Structures*. New York, New York: John Wiley & Sons. TIC: 248840.
13. Hallquist, J.O. 1998. *LS-DYNA, Theoretical Manual*. Livermore, California: Livermore

- Software Technology Corporation. TIC: 238997.
14. ASME (American Society of Mechanical Engineers) 2001. *2001 ASME Boiler and Pressure Vessel Code (includes 2002 addenda)*. New York, New York: American Society of Mechanical Engineers. TIC: 251425.
 15. Mecham, D.C., ed. 2004. *Waste Package Component Design Methodology Report*. 000-30R-WIS0-00100-000-002. Las Vegas, Nevada: Bechtel SAIC Company. ACC: ENG.20040713.0003.
 16. MO0402DQRIRPPR.003. Intact Rock Properties Data on Poisson's Ratio and Young's Modulus. Submittal date: 02/19/2004.
 17. MO9808RIB00041.000. Reference Information Base Data Item: Rock Geomechanical Properties. Submittal date: 08/05/1998.
 18. Beer, F.P. and Johnston, E.R., Jr. 1977. *Vector Mechanics for Engineers, Statics*. 3rd Edition. New York, New York: McGraw-Hill Book Company. TIC: 247391.
 19. BSC (Bechtel SAIC Company) 2001. *Repository Multiple Waste Package Thermal Calculation*. CAL-WIS-TH-000010 REV 00. Las Vegas, Nevada: Bechtel SAIC Company. ACC: MOL.20010814.0330.
 20. MO0306SPAGLCDS.001. General Corrosion and Localized Corrosion of the Drip Shield. Submittal date: 05/28/2003.
 21. BSC (Bechtel SAIC Company) 2004. *D&E / PA/C IED Interlocking Drip Shield and Emplacement Pallet*. 800-IED-WIS0-00401-000-00D. Las Vegas, Nevada: Bechtel SAIC Company. ACC: ENG.20040503.0018.
 22. BSC (Bechtel SAIC Company) 2003. *General Corrosion and Localized Corrosion of the Drip Shield*. ANL-EBS-MD-000004 REV 01. Las Vegas, Nevada: Bechtel SAIC Company. ACC: DOC.20030626.0001.
 23. Dieter, G.E. 1976. *Mechanical Metallurgy*. 2nd Edition. Materials Science and Engineering Series. New York, New York: McGraw-Hill Book Company. TIC: 247879.
 24. BSC (Bechtel SAIC Company) 2003. *Structural Calculations of Drip Shield Exposed to Vibratory Ground Motion*. 000-00C-PEC0-00100-000-00A. Las Vegas, Nevada: Bechtel SAIC Company. ACC: ENG.20030618.0009.
 25. MO0407MWDDSLCR.000. Drip Shield Load in Collapsed Lithophysal Rock. Submittal date: 07/21/2004.
 26. BSC (Bechtel SAIC Company) 2004. *Data Qualification and Data Summary Report: Intact Rock Properties Data on Poisson's Ratio and Young's Modulus*. TDR-MGR-GE-

Title: Structural Stability of a Drip Shield Under Quasi-Static Pressure

Document Identifier: 000-00C-SSE0-00500-000-00A

Page 24 of 26

- 000004 REV 01 Errata 1. Las Vegas, Nevada: Bechtel SAIC Company. ACC: DOC.20040225.0001; DOC.20040419.0001.
27. MO0003RIB00073.000. Physical and Chemical Characteristics of TI Grades 7 and 16. Submittal date: 03/13/2000.
28. ASM International. 1990. *Properties and Selection: Nonferrous Alloys and Special-Purpose Materials*. Volume 2 of *ASM Handbook*. Formerly Tenth Edition, Metals Handbook. 5th Printing 1998. [Materials Park, Ohio]: ASM International. TIC: 241059.
29. Itasca Consulting Group. [2002]. *Itasca Software—Cutting Edge Tools for Computational Mechanics*. Minneapolis, Minnesota: Itasca Consulting Group. TIC: 252592.
30. BSC (Bechtel SAIC Company) 2004. *Drift Degradation Analysis*. ANL-EBS-MD-000027 Rev. 03A. Las Vegas, Nevada: Bechtel SAIC Company. ACC: MOL.20040513.0081. TBV-5841

8. ATTACHMENTS

Attachment I (24 pages): Design sketch (*Interlocking Drip Shield* [SK-0230 REV 00, 24 sheets])

Attachment II (10 pages): Plots of the Final Drip Shield Configurations and Kinetic Energy

Attachment III (16 pages): Plots of the Final Drip Shield Maximum Shear Stresses

Attachment IV (3 pages): Damaged Area

Attachment V (3 pages): Mesh Objectivity

Attachment VI (2 page): Comparison of Results Obtained by Using Different LS-DYNA Versions

Attachment VII (Compact Disc): Electronic files

Table 7 provides a list of files submitted on a compact disc as Attachment VII. The files with extensions “.tg” and “.inc” are the TrueGrid V2.2 input and output files, respectively. The files with extension “.k” and “.inc” are the LS-DYNA input files; d3hsp are the LS-DYNA output files.

Table 7. List of Electronic Files in Attachment VII

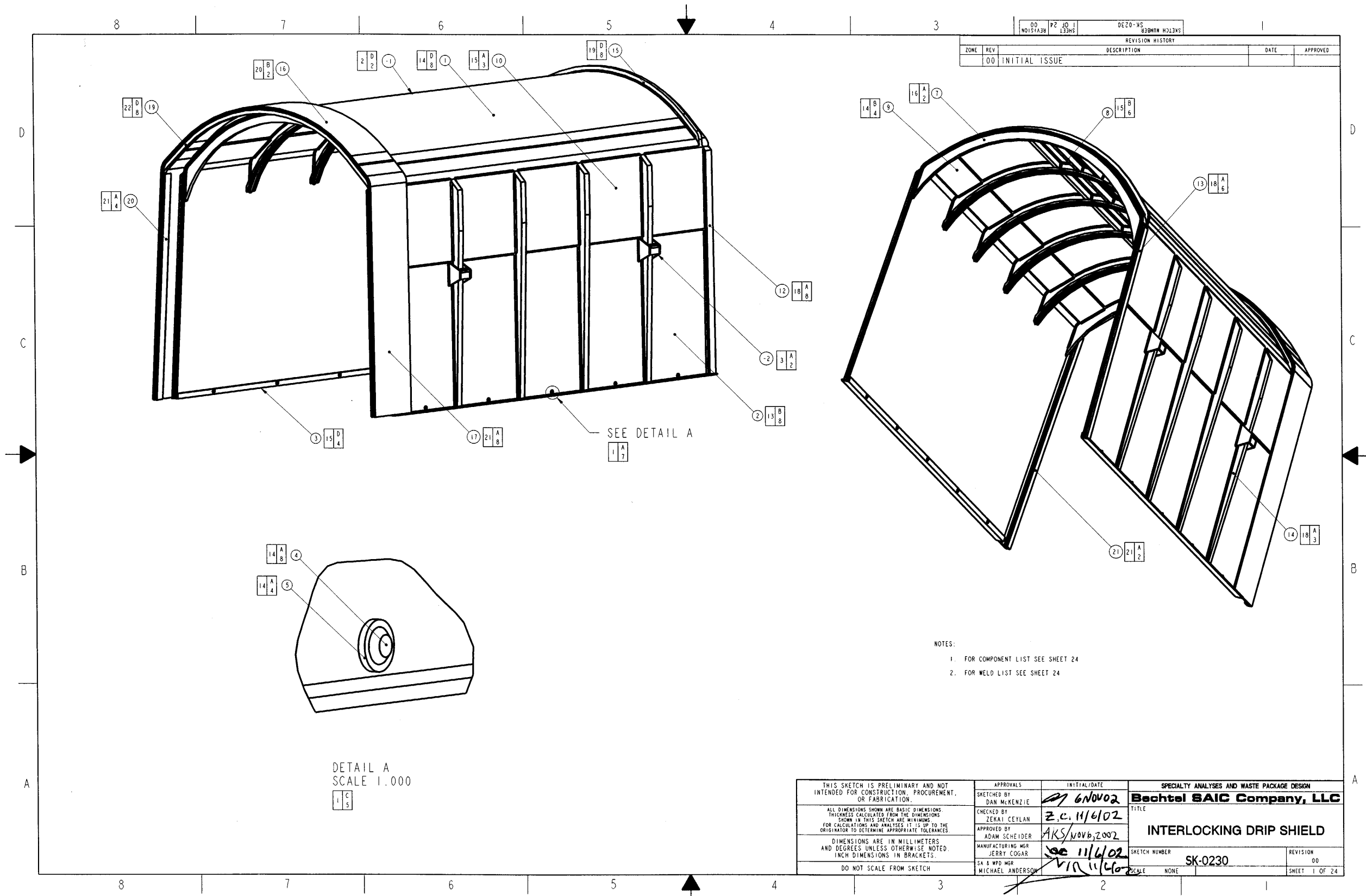
File Name	Size (kB)	Time	Date
Folder – RN1			
d3hsp	6,806	27 July 2004	07:35 am
DS_sing.inc	4,122	27 July 2004	07:35 am
DS_sing_div.tg	66	27 July 2004	07:35 am
qsdsB.k	6	27 July 2004	07:35 am
Folder – RN2			
d3hsp	6,800	27 July 2004	07:35 am
DS_sing.inc	4,122	27 July 2004	07:35 am
DS_sing_div.tg	66	27 July 2004	07:35 am
qsdsB.k	6	27 July 2004	07:35 am
Folder – RN3			
d3hsp	6,820	27 July 2004	07:37 am
d3hsp1	20	27 July 2004	07:37 am
DS_sing.inc	4,122	27 July 2004	07:37 am
DS_sing_div.tg	66	27 July 2004	07:37 am
qsdsB.k	6	27 July 2004	07:37 am
Folder – RN4			
d3hsp	36	27 July 2004	07:38 am
d3hsp0	6,793	27 July 2004	07:38 am
DS_sing.inc	4,122	27 July 2004	07:38 am
DS_sing_div.tg	66	27 July 2004	07:38 am
qsdsB.k	6	27 July 2004	07:38 am
Folder – RN5-960			
d3hsp	6,794	27 July 2004	07:38 am

DS_sing.inc	4,122	27 July 2004	07:38 am
DS_sing_div.tg	66	27 July 2004	07:38 pm
qsdsB.k	6	27 July 2004	07:38 pm
Folder – RN5-970			
d3hsp	8,266	27 July 2004	07:41 am
DS_sing.inc	4,122	27 July 2004	07:41 am
DS_sing_div.tg	66	27 July 2004	07:38 am
qsdsB.k	6	27 July 2004	07:41 am
Folder – RN5-DC=50			
d3hsp	6,804	27 July 2004	09:56 am
DS_sing.inc	4,122	27 July 2004	09:56 am
DS_sing_div.tg	66	27 July 2004	09:56 am
qsdsA.k	6	27 July 2004	09:56 am
Folder – RN5-nodamp			
d3hsp	6,794	27 July 2004	09:56 am
DS_sing.inc	4,122	27 July 2004	09:56 am
DS_sing_div.tg	66	27 July 2004	09:56 am
qsds.k	6	27 July 2004	09:56 am
Folder – RN6			
d3hsp	55	27 July 2004	07:39 am
d3hsp0	6,793	27 July 2004	07:39 am
DS_sing.inc	4,122	27 July 2004	07:39 am
DS_sing_div.tg	66	27 July 2004	07:39 am
qsdsB.k	6	27 July 2004	07:39 am
Folder – RNavg_ref			
d3hsp	13,929	27 July 2004	07:46 am
DS_sing_div_ref.tg	66	27 July 2004	07:47 am
DS_sing_ref.inc	7,123	27 July 2004	07:45 am
qsdsB.k	6	27 July 2004	07:45 am
Folder – RNavg2.5			
d3hsp	8,271	27 July 2004	07:40 am
DS_sing.inc	4,122	27 July 2004	07:40 am
DS_sing_div.tg	66	27 July 2004	07:35 am
qsdsB.k	6	27 July 2004	07:40 am
Folder – RNavg2.5full			
d3hsp	36,910	27 July 2004	07:44 am
d3hsp01	19	27 July 2004	07:44 am
DS_div1.inc	18,043	27 July 2004	07:42 am
DS_div1.tg	69	27 July 2004	07:47 am
qsdsB.k	6	27 July 2004	07:42 am
Folder – RNavg3			
d3hsp	8,278	27 July 2004	07:45 am
d3hsp01	34	27 July 2004	07:45 am
DS_sing.inc	4,122	27 July 2004	07:43 am
DS_sing_div.tg	66	27 July 2004	07:35 am
qsdsB.k	6	27 July 2004	07:43 am
Folder – RNavg4			
d3hsp	8,279	27 July 2004	07:41 am
DS_sing.inc	4,122	27 July 2004	07:41 am
DS_sing_div.tg	66	27 July 2004	07:35 am
qsdsB.k	6	27 July 2004	07:41 am

Note: The file sizes and times may vary with operating system.

ATTACHMENT I
DESIGN SKETCH

NAME: MCKENZIE D2 OBJECT: SK-0230_REV00_1 DATE: 06-Nov-02 12:38:33



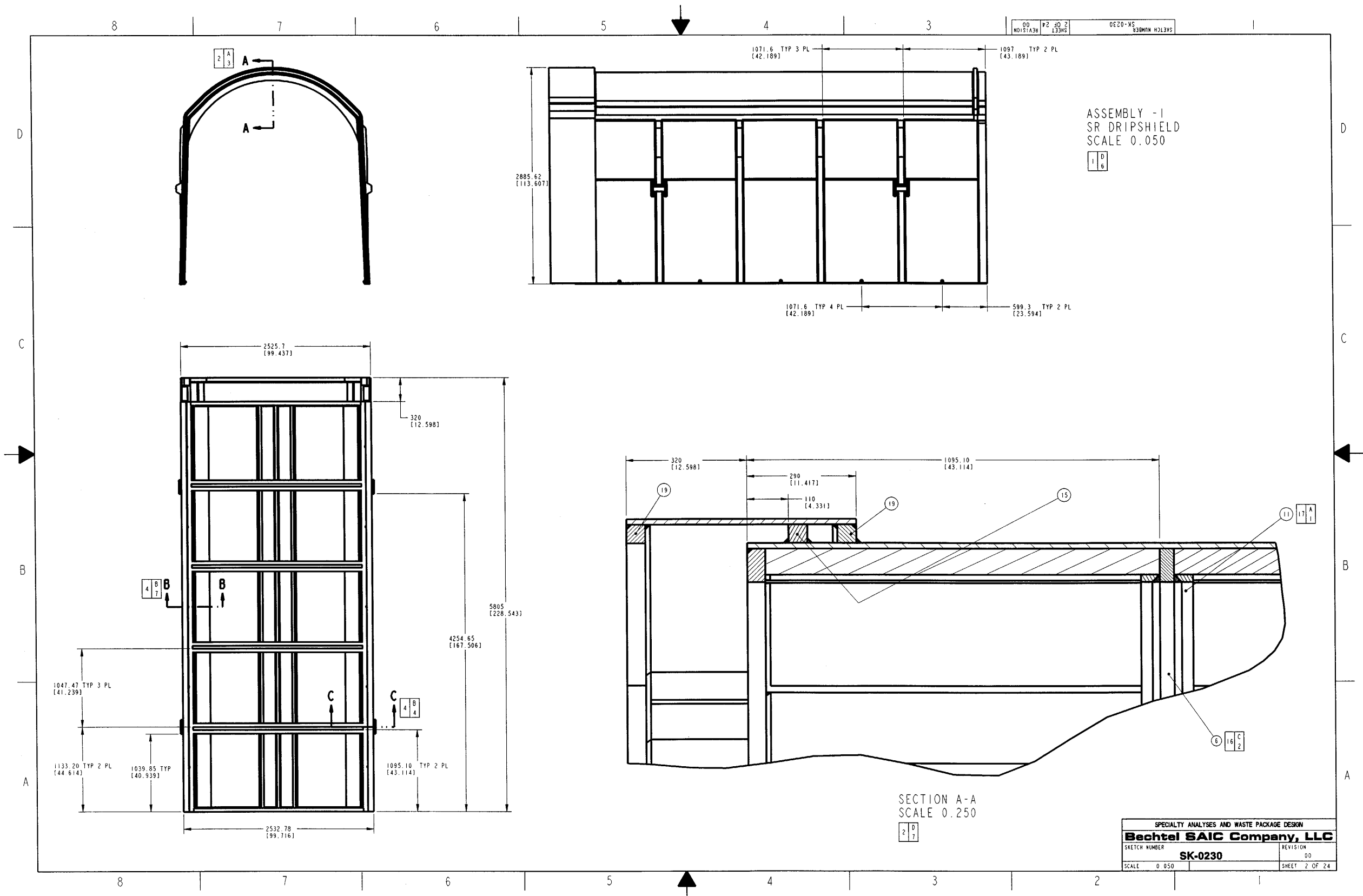
REVISION HISTORY		DATE	APPROVED
00	INITIAL ISSUE		

- NOTES:
1. FOR COMPONENT LIST SEE SHEET 24
 2. FOR WELD LIST SEE SHEET 24

THIS SKETCH IS PRELIMINARY AND NOT INTENDED FOR CONSTRUCTION, PROCUREMENT, OR FABRICATION. ALL DIMENSIONS SHOWN ARE BASIC DIMENSIONS. THICKNESSES CALCULATED FROM THE DIMENSIONS SHOWN IN THIS SKETCH ARE MINIMUMS FOR CALCULATIONS AND ANALYSES. IT IS UP TO THE ORIGINATOR TO DETERMINE APPROPRIATE TOLERANCES. DIMENSIONS ARE IN MILLIMETERS AND DEGREES UNLESS OTHERWISE NOTED. INCH DIMENSIONS IN BRACKETS. DO NOT SCALE FROM SKETCH	APPROVALS SKETCHED BY DAN MCKENZIE CHECKED BY ZEKAI CEYLAN APPROVED BY ADAM SCHEIDER MANUFACTURING MGR JERRY COGAR SA & WPD MGR MICHAEL ANDERSON	INITIAL/DATE 6/NOV02 Z.C. 11/6/02 AKS/NOV6,2002 see 11/6/02 via 11/6/02	SPECIALTY ANALYSES AND WASTE PACKAGE DESIGN Bechtel SAIC Company, LLC TITLE INTERLOCKING DRIP SHIELD SKETCH NUMBER SK-0230 REVISION 00 SHEET 1 OF 24
--	--	--	--

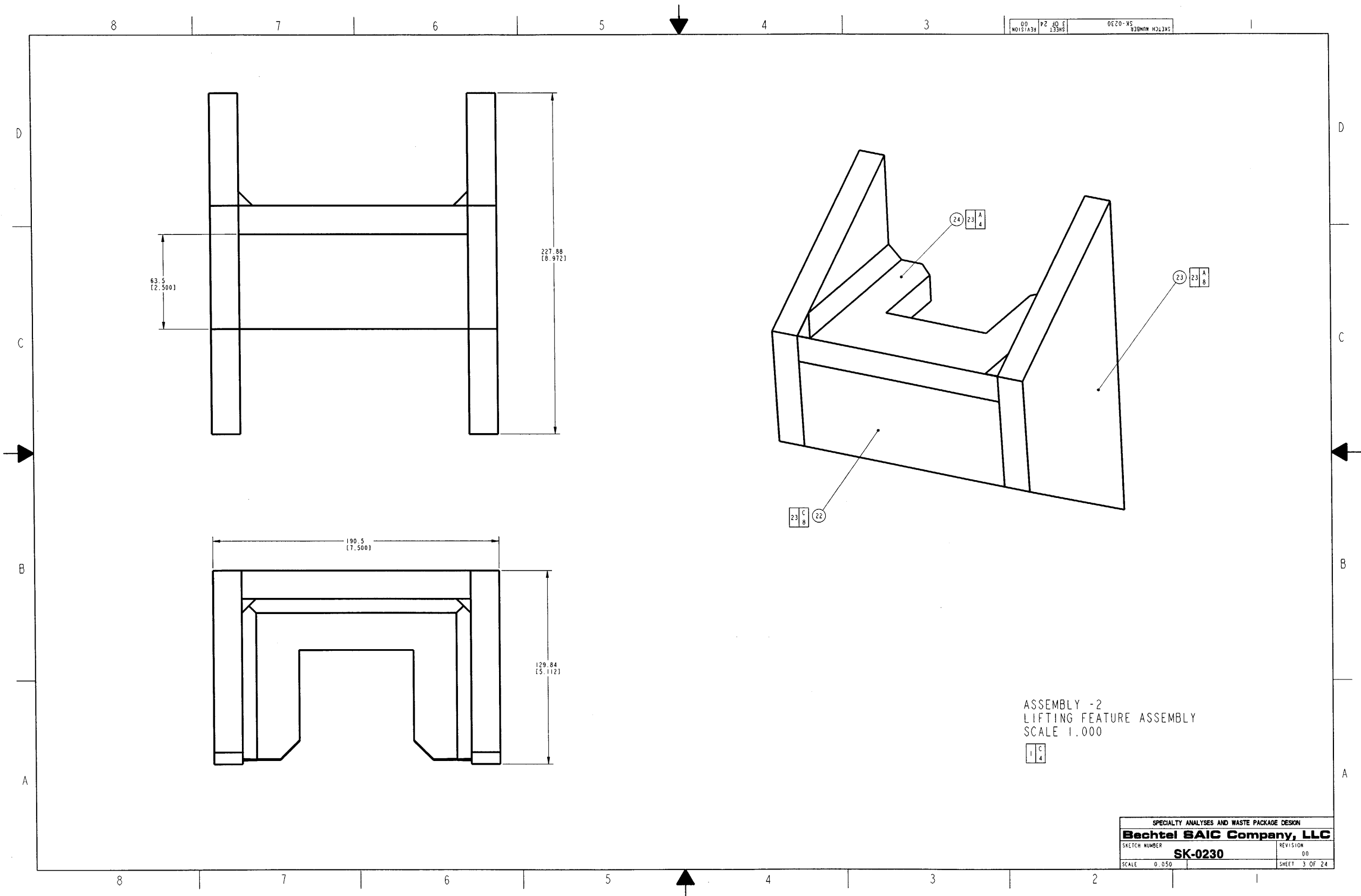
DETAIL A
SCALE 1.000

NAME: MCKENZIED2 OBJECT: SK-0230_REV00_2 DATE: 06-Nov-02 12:38:35



SPECIALTY ANALYSES AND WASTE PACKAGE DESIGN	
Bechtel SAIC Company, LLC	
SKETCH NUMBER	REVISION
SK-0230	00
SCALE 0.050	SHEET 2 OF 24

NAME: MCKENZIED2 OBJECT: SK-0230_REV00_3 DATE: 06-Nov-02 12:38:38



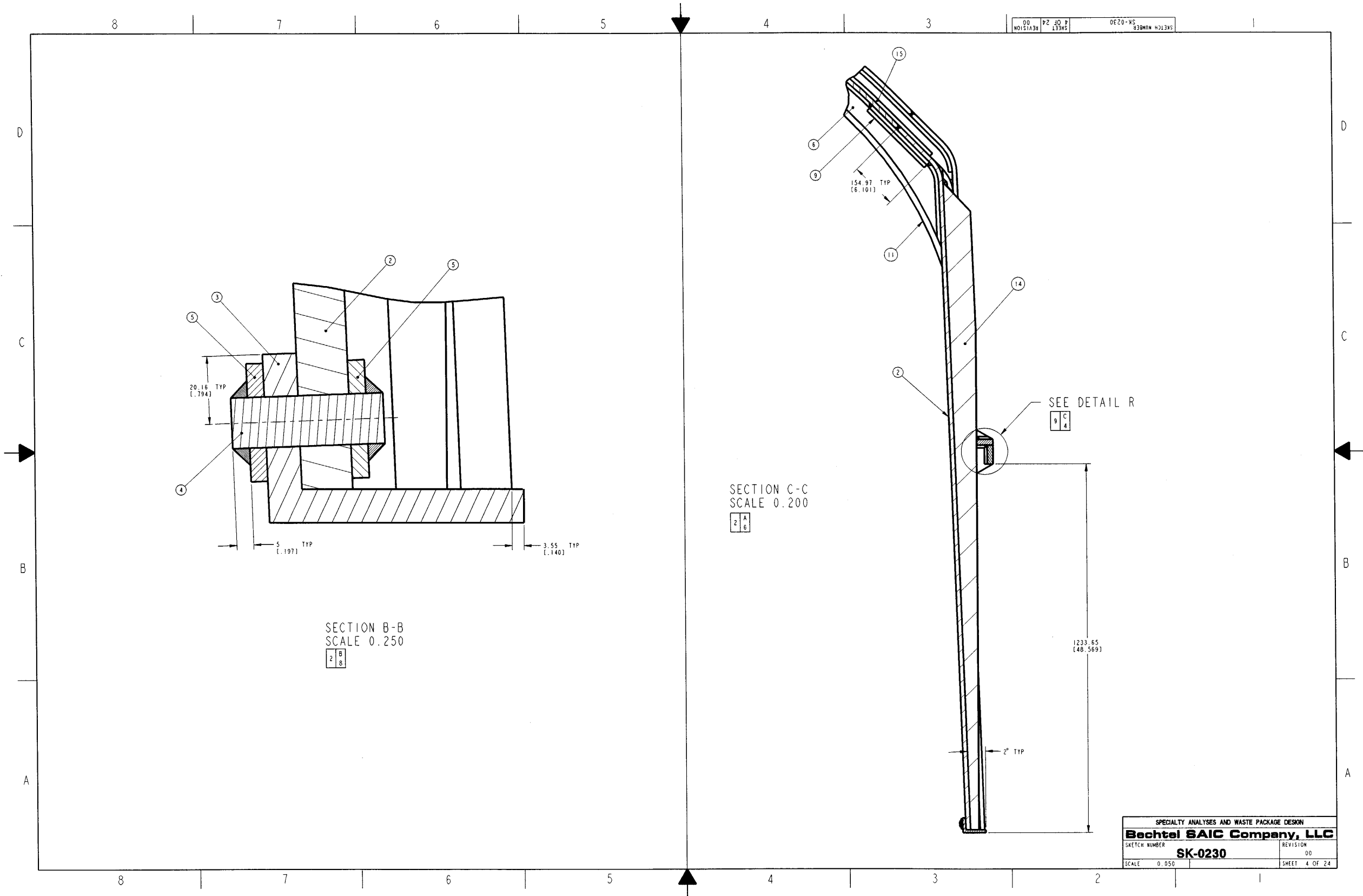
ASSEMBLY -2
LIFTING FEATURE ASSEMBLY
SCALE 1.000

1 C 4

SPECIALTY ANALYSES AND WASTE PACKAGE DESIGN	
Bechtel SAIC Company, LLC	
SKETCH NUMBER	REVISION
SK-0230	00
SCALE 0.050	SHEET 3 OF 24

SKETCH NUMBER SK-0230-W
SHEET 3 OF 24
REVISION 00

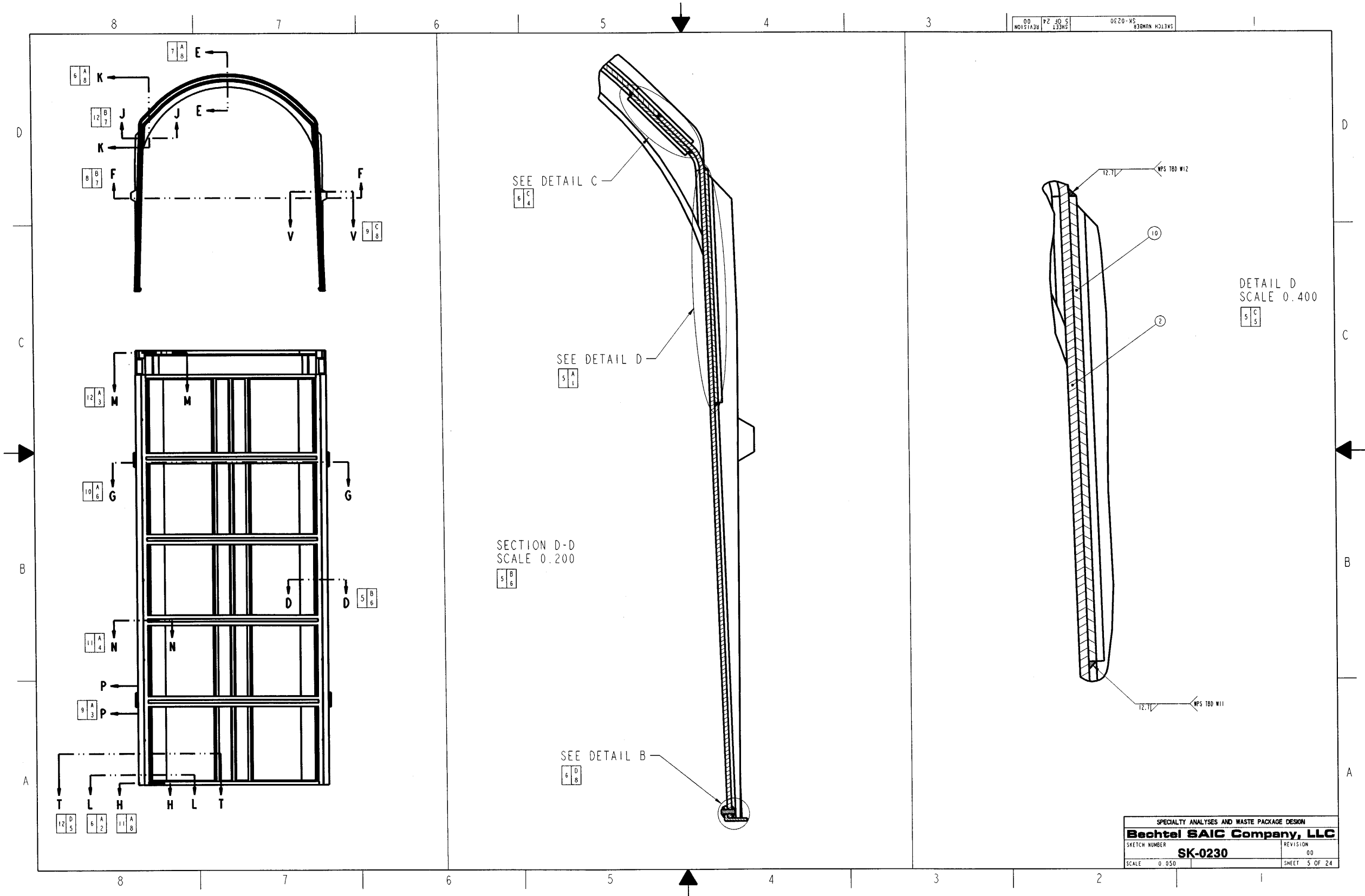
NAME: MCKENZIED2 OBJECT: SK-0230_REV00_4 DATE: 06-Nov-02 12:38:38



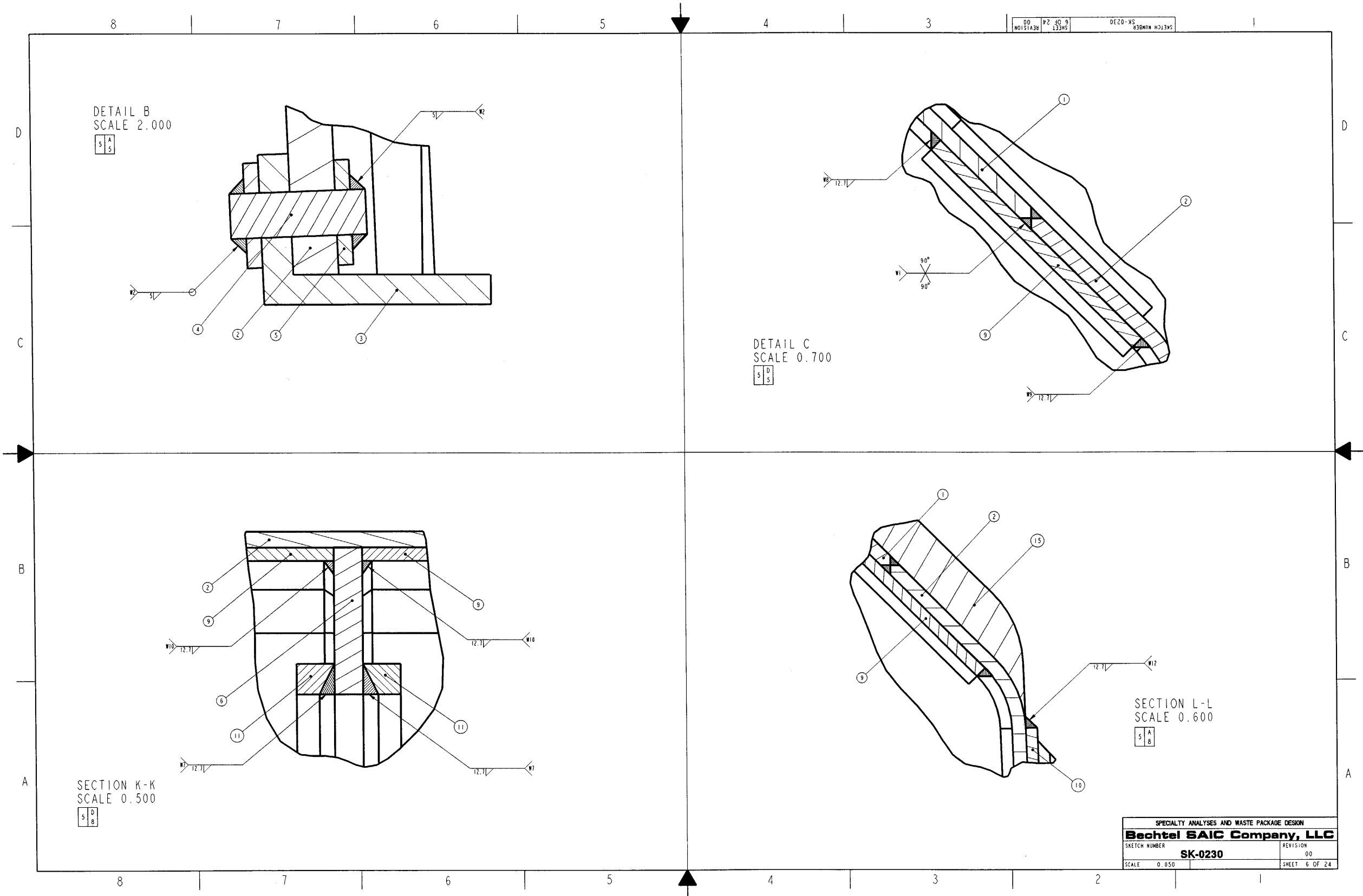
SKETCH NUMBER	00230
REVISION	00
SHEET	4 OF 24

SPECIALTY ANALYSES AND WASTE PACKAGE DESIGN	
Bechtel SAIC Company, LLC	
SKETCH NUMBER	REVISION
SK-0230	00
SCALE 0.050	SHEET 4 OF 24

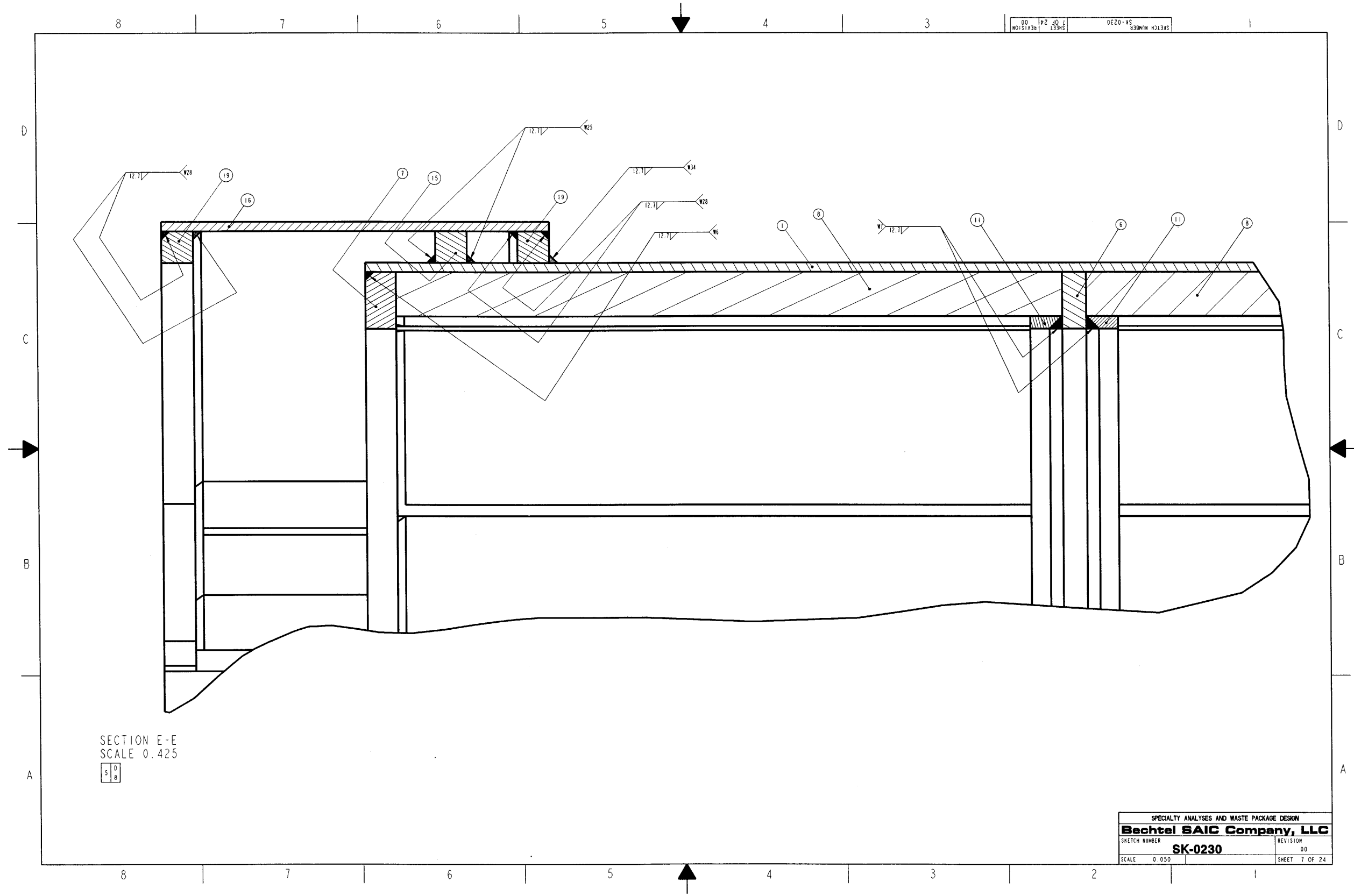
NAME: MCKENZIED2 OBJECT: SK-0230_REV00_5 DATE: 06-Nov-02 12:38:40



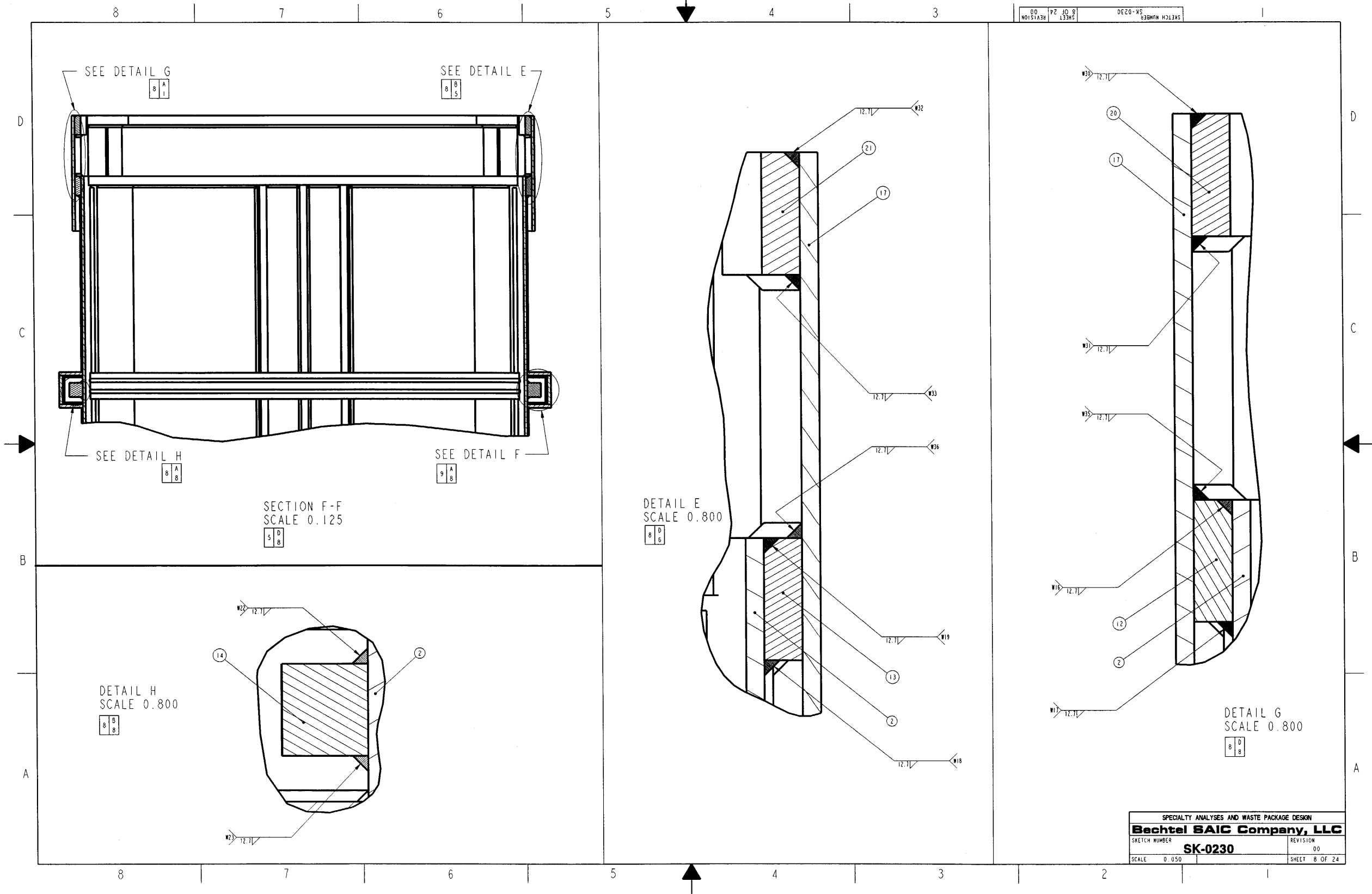
NAME: MCKENZIED2 OBJECT: SK-0230_REV00_6 DATE: 06-Nov-02 12:38:42



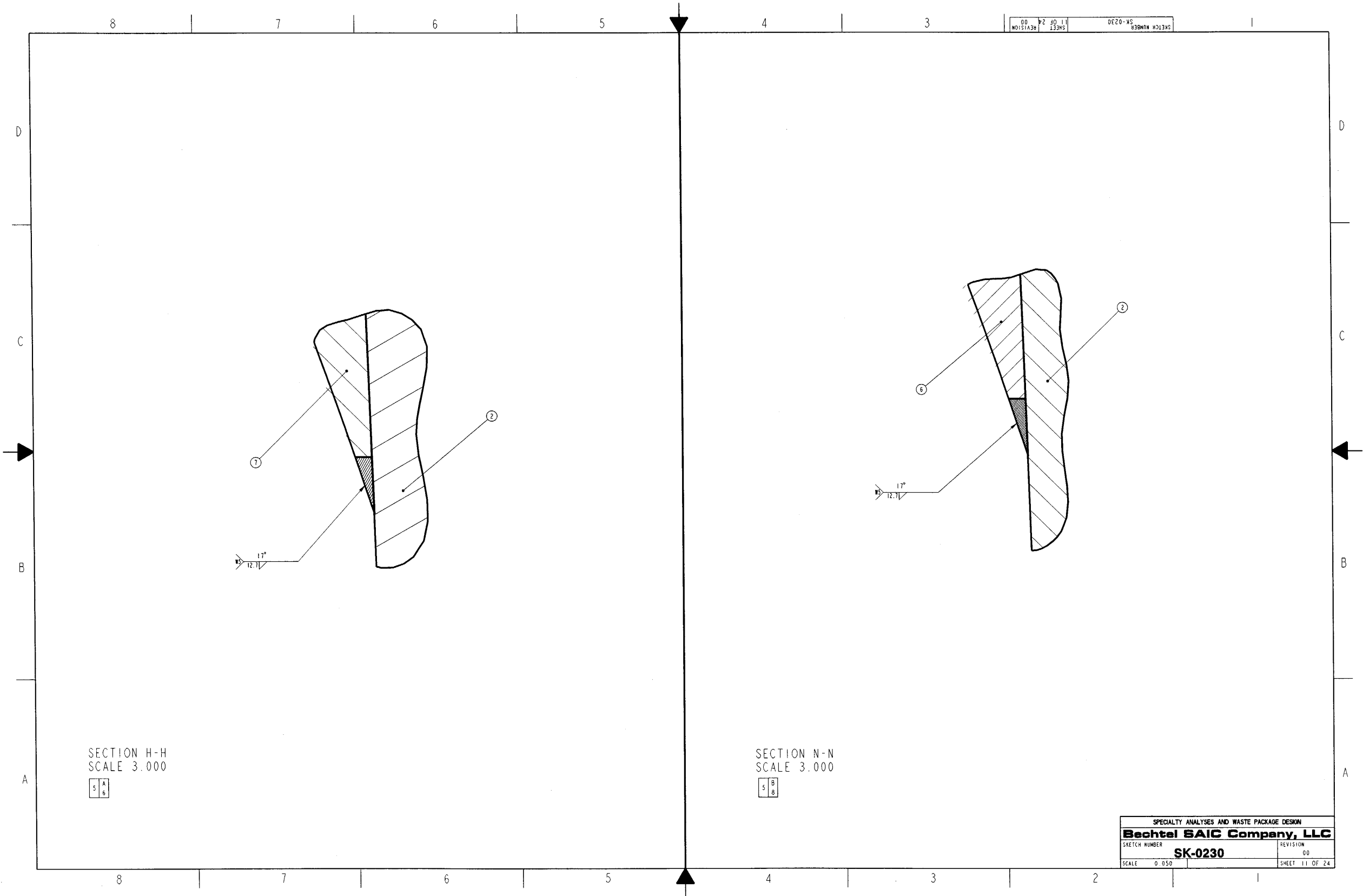
NAME: MCKENZIED2 OBJECT: SK-0230_REV00_7 DATE: 06-Nov-02 12:38:43



NAME: MCKENZIED2 OBJECT: SK-0230_REV00_8 DATE: 06-Nov-02 12:38:44



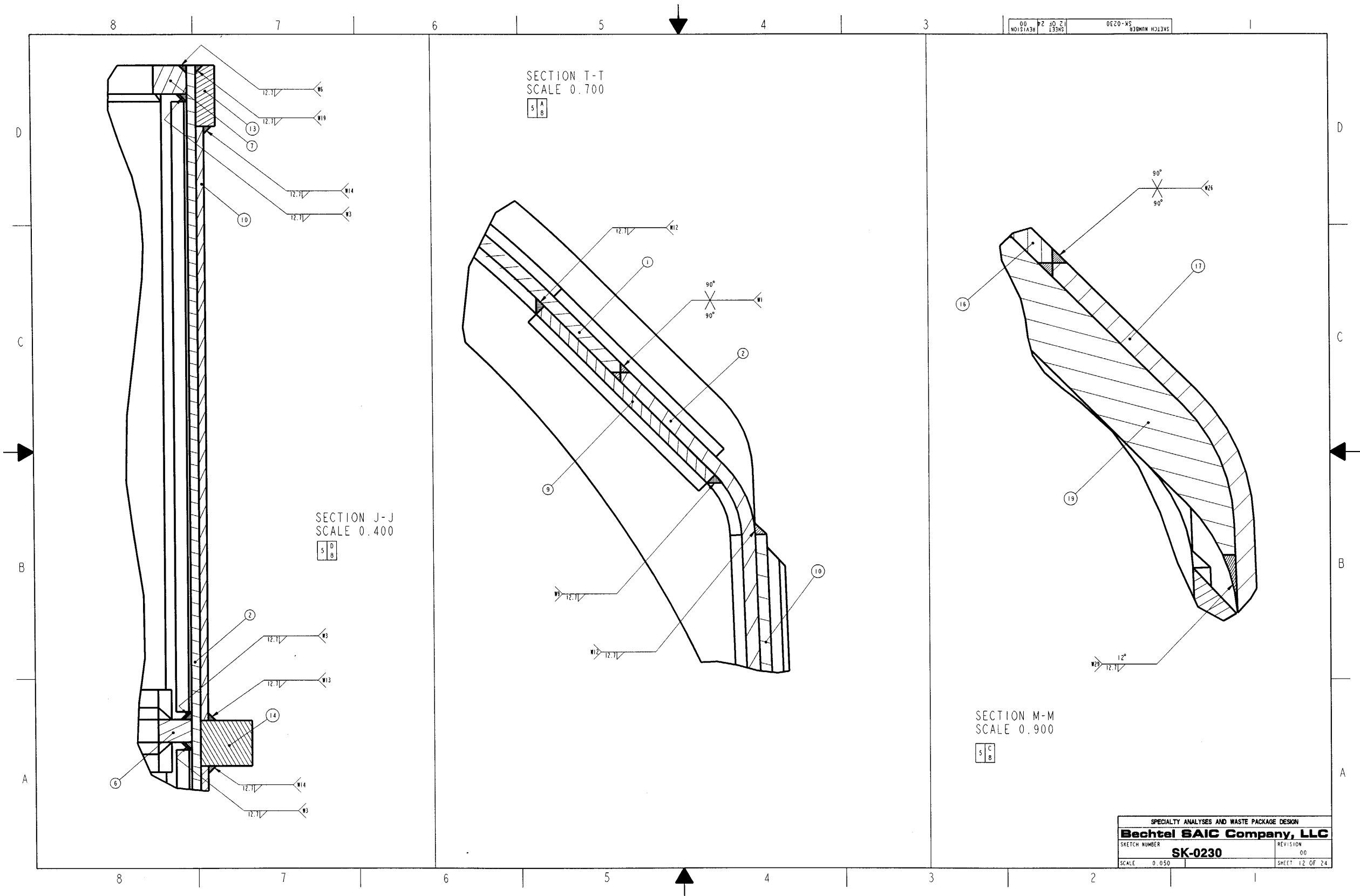
NAME: MCKENZIED2 OBJECT: SK-0230_REV00_11 DATE: 06-Nov-02 12:38:49



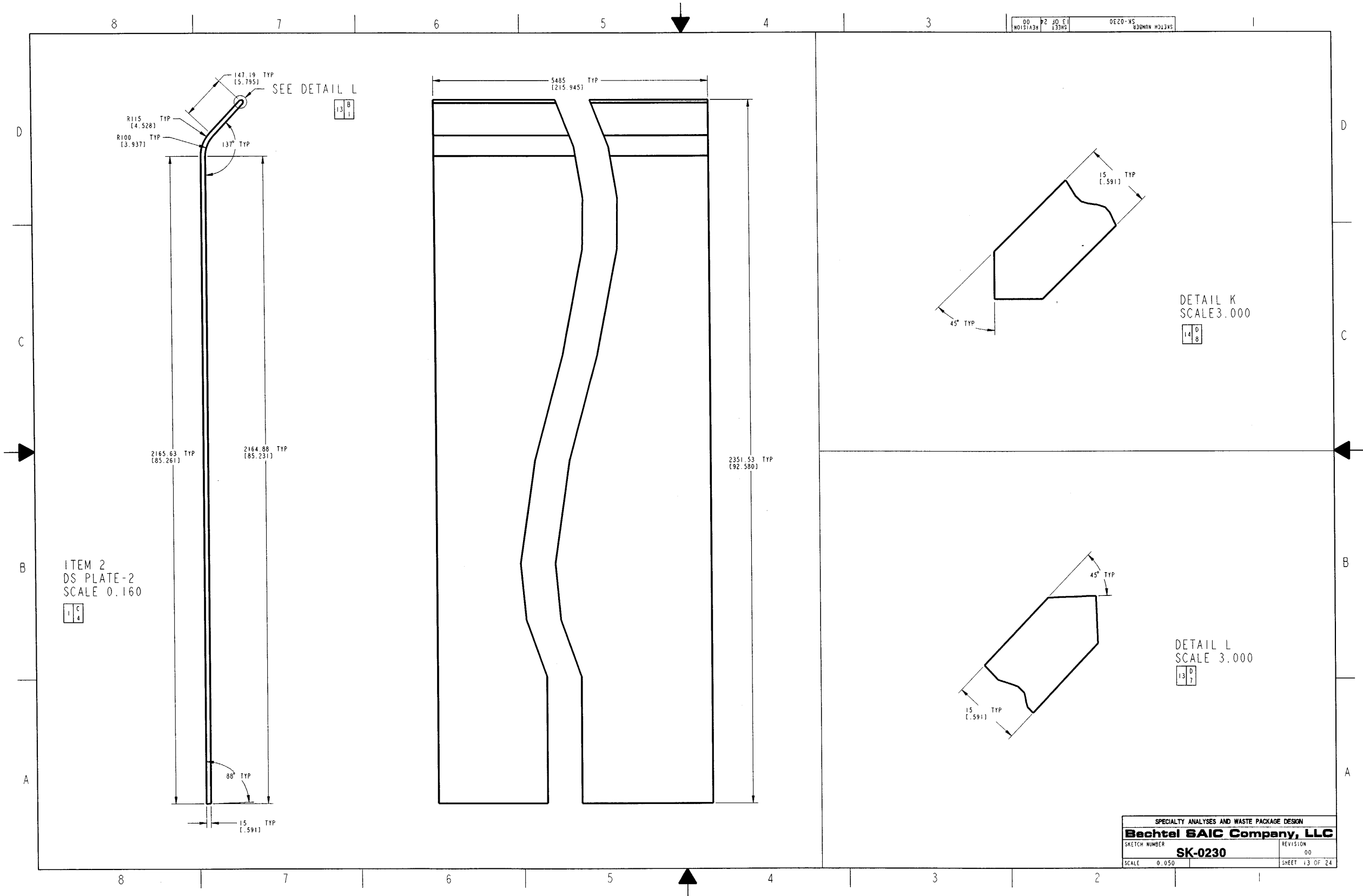
SKETCH NUMBER	SK-0230
REVISION	11
SHEET	11 OF 24

SPECIALTY ANALYSES AND WASTE PACKAGE DESIGN	
Bechtel SAIC Company, LLC	
SKETCH NUMBER	REVISION
SK-0230	00
SCALE 0.050	SHEET 11 OF 24

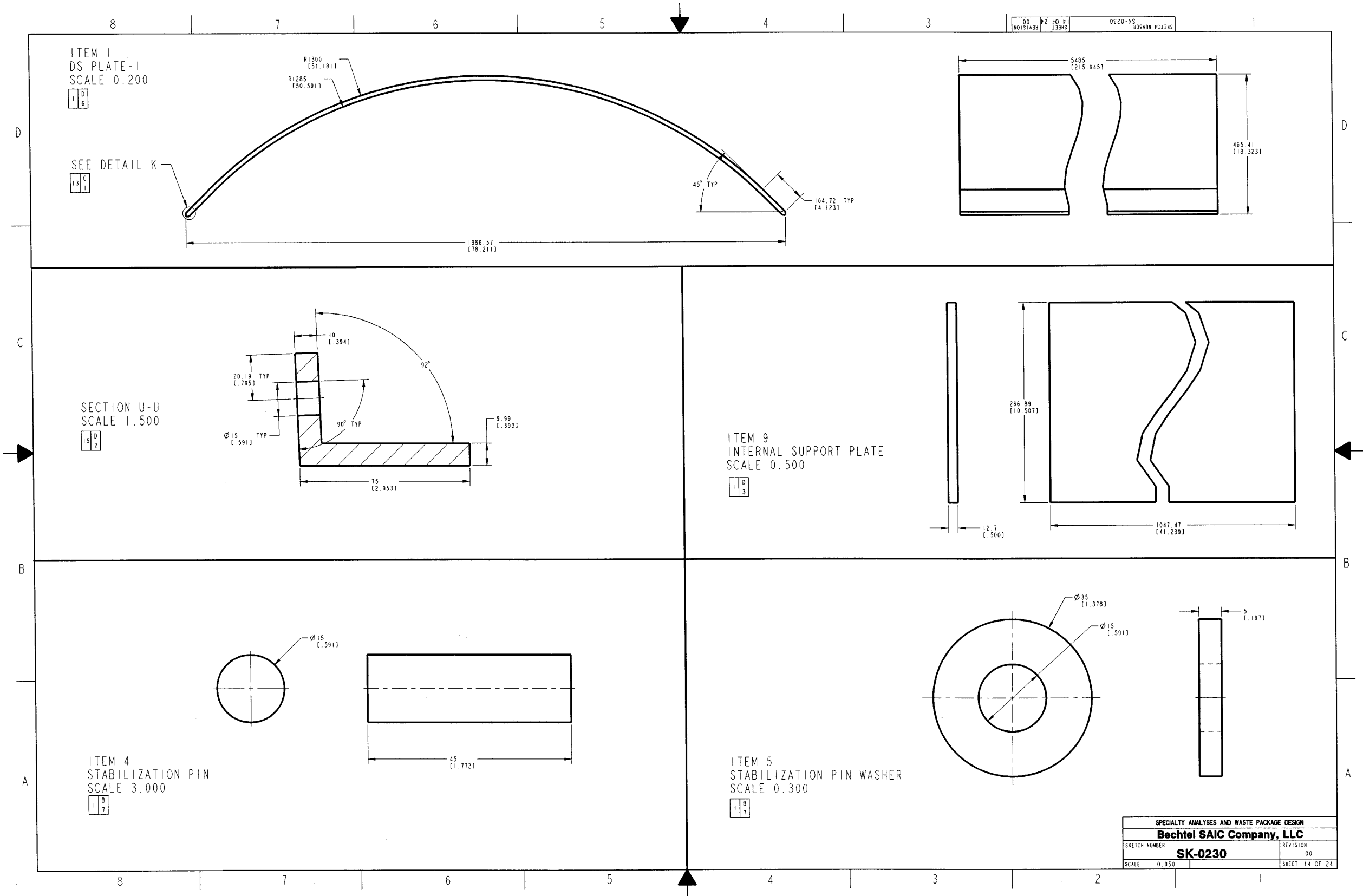
NAME: MCKENZIED2 OBJECT: SK-0230_REV00_12 DATE: 06-Nov-02 12:38:50



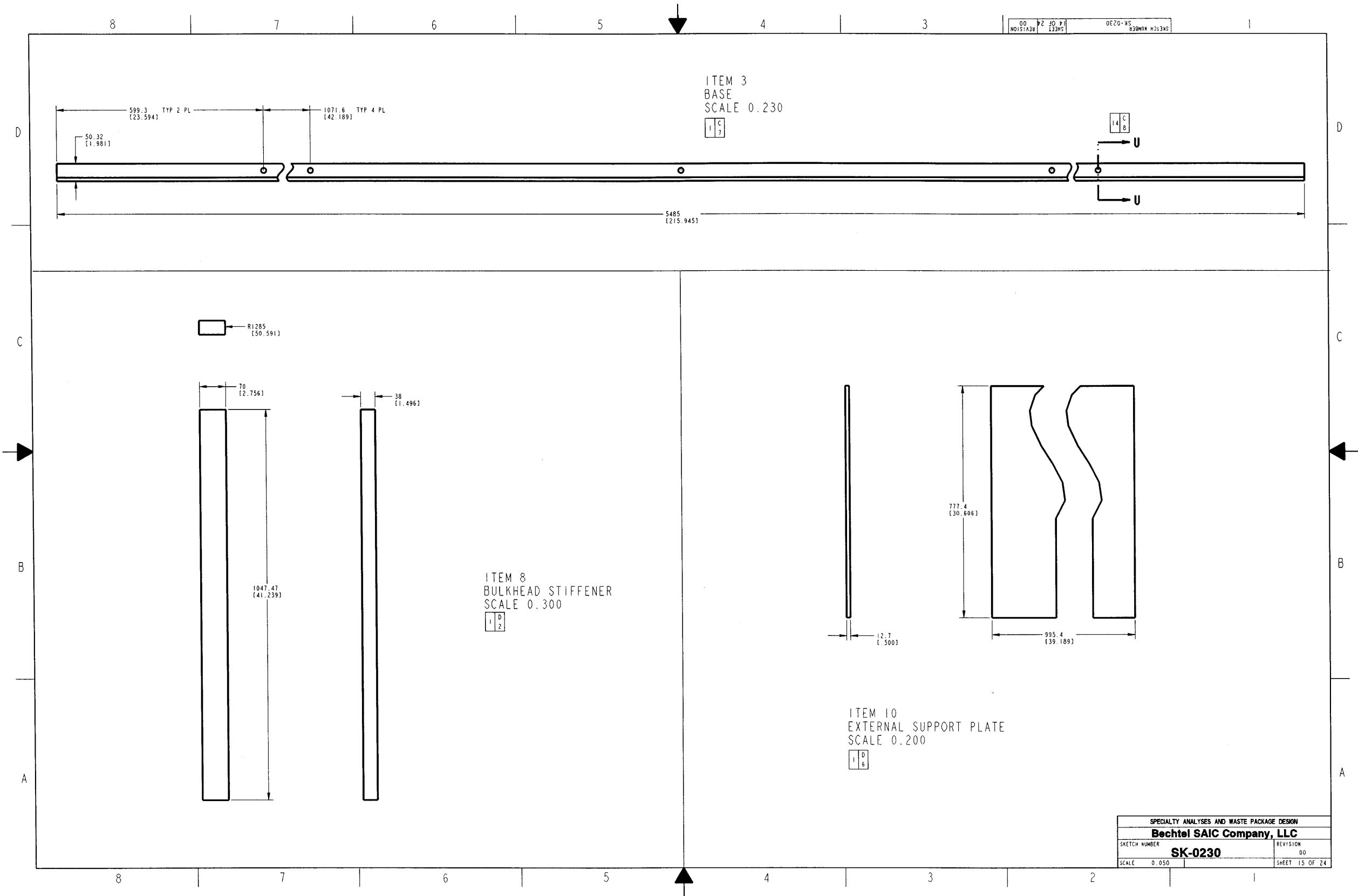
NAME: MCKENZIED2 OBJECT: SK-0230_REV00_13 DATE: 06-Nov-02 12:38:52



NAME: MCKENZIED2 OBJECT: SK-0230_REV00_14 DATE: 06-Nov-02 12:38:53

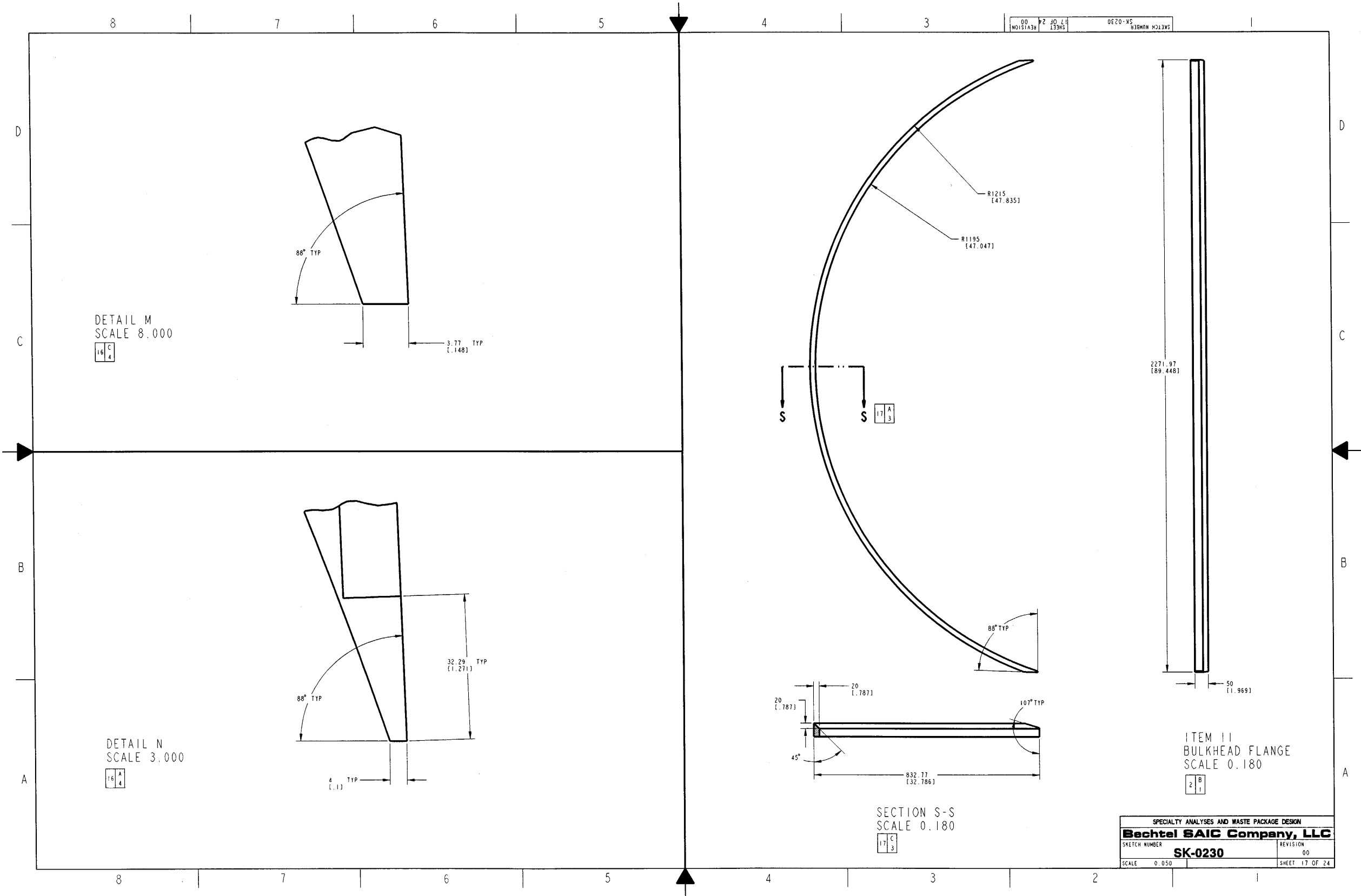


NAME: MCKENZIED2 OBJECT: SK-0230_REV00_15 DATE: 06-Nov-02 12:38:53

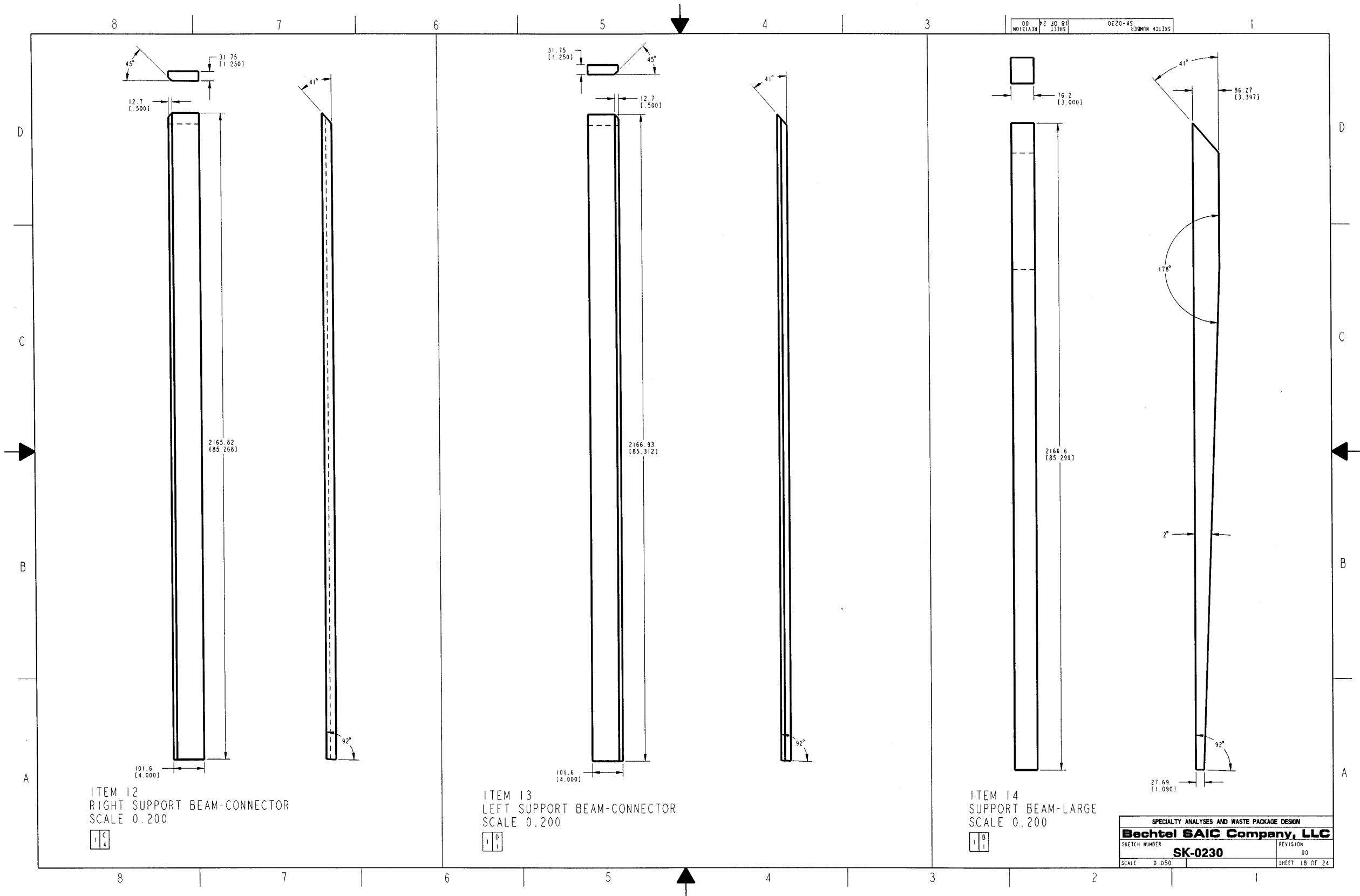


SPECIALTY ANALYSES AND WASTE PACKAGE DESIGN	
Bechtel SAIC Company, LLC	
SKETCH NUMBER SK-0230	REVISION 00
SCALE 0.050	SHEET 15 OF 24

NAME: MCKENZIED2 OBJECT: SK-0230_REV00_17 DATE: 06-Nov-02 12:38:54

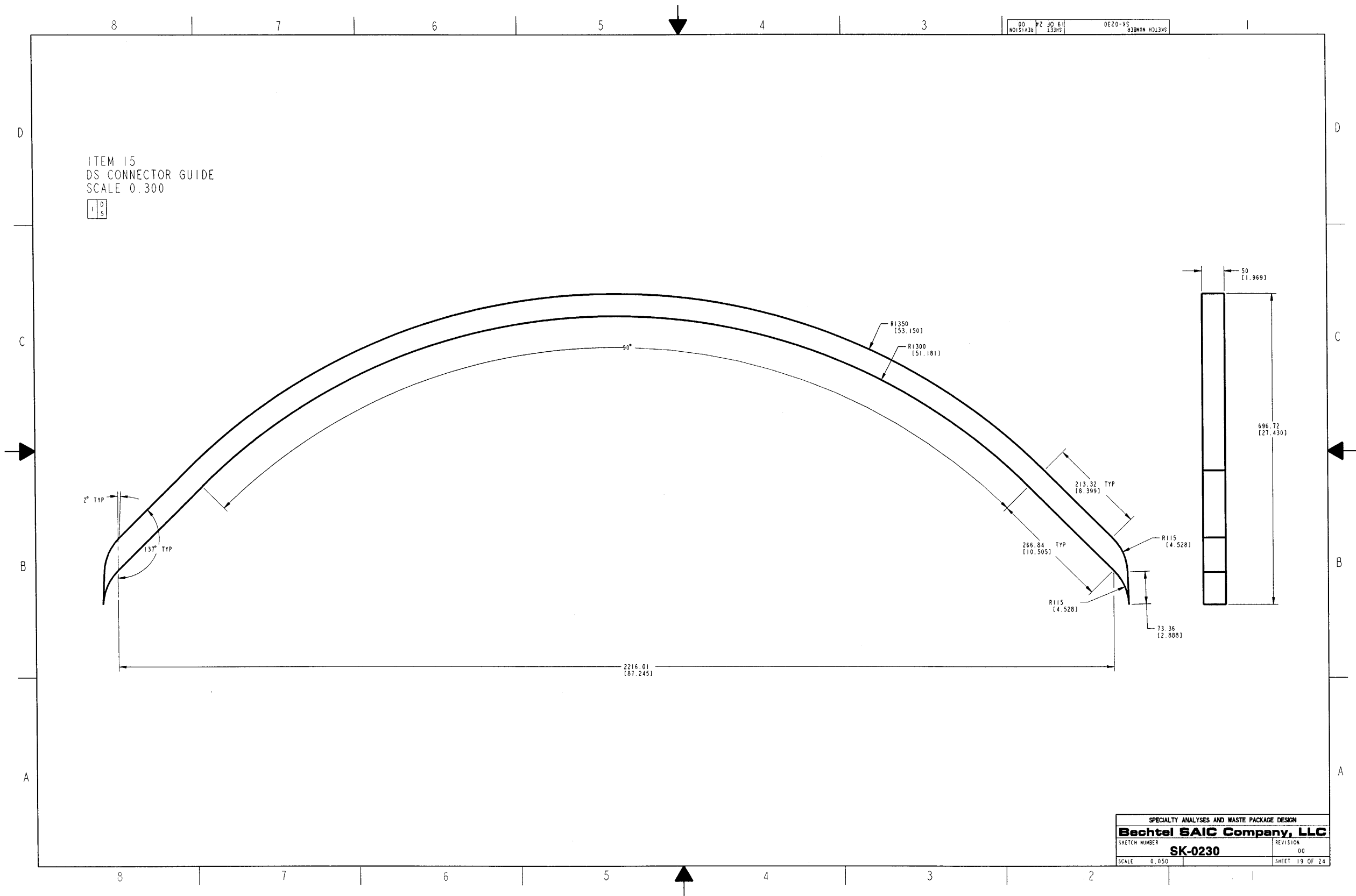


NAME: MCKENZIED2 OBJECT: SK-0230_REV00_18 DATE: 06-Nov-02 12:38:55

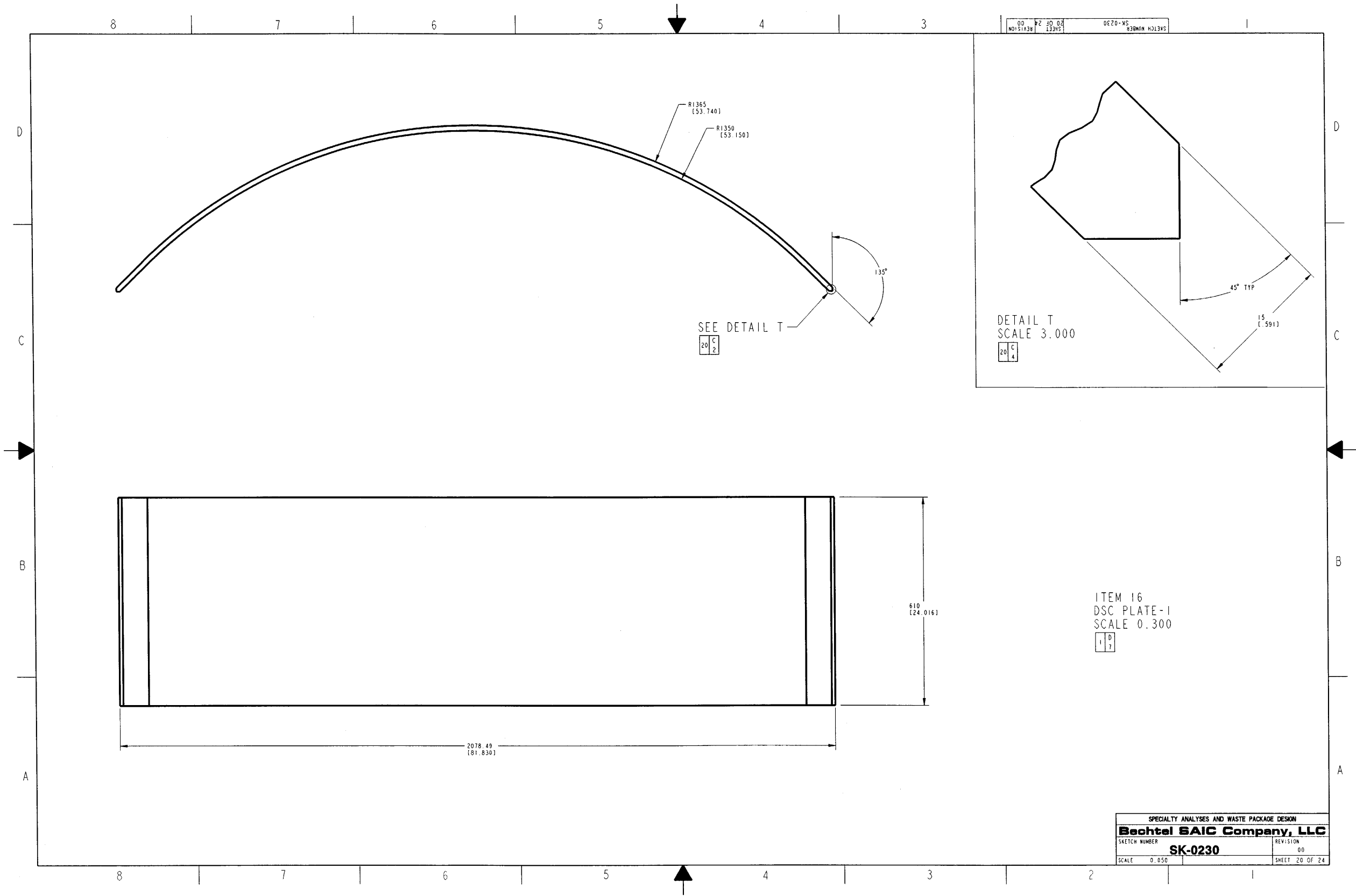


SPECIALTY ANALYSES AND WASTE PACKAGE DESIGN
Bechtel SAIC Company, LLC
 SKETCH NUMBER: SK-0230 REVISION: 00
 SCALE: 0.050 SHEET 18 OF 24

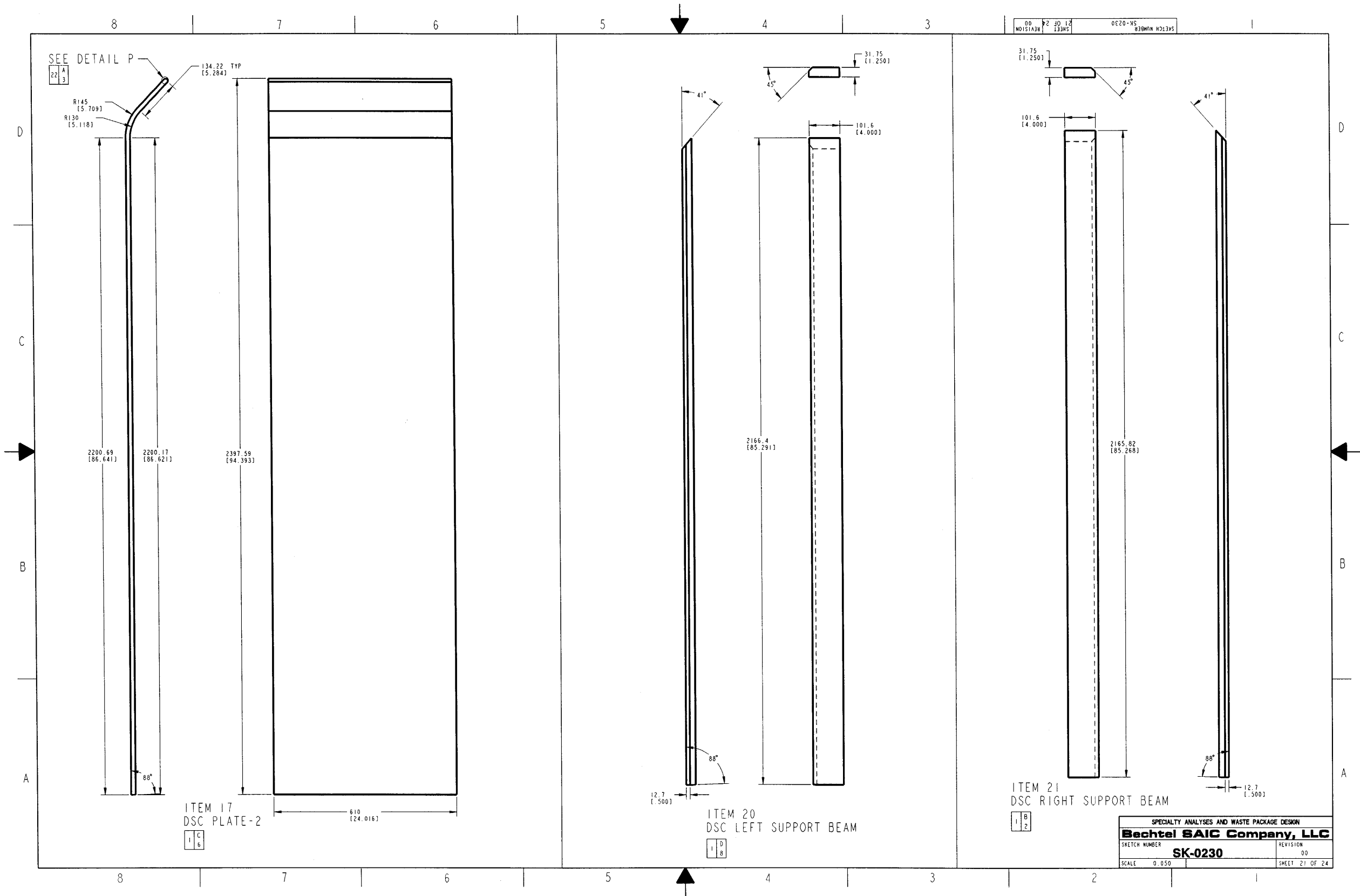
NAME: MCKENZIED2 OBJECT: SK-0230_REV00_19 DATE: 06-Nov-02 12:38:55



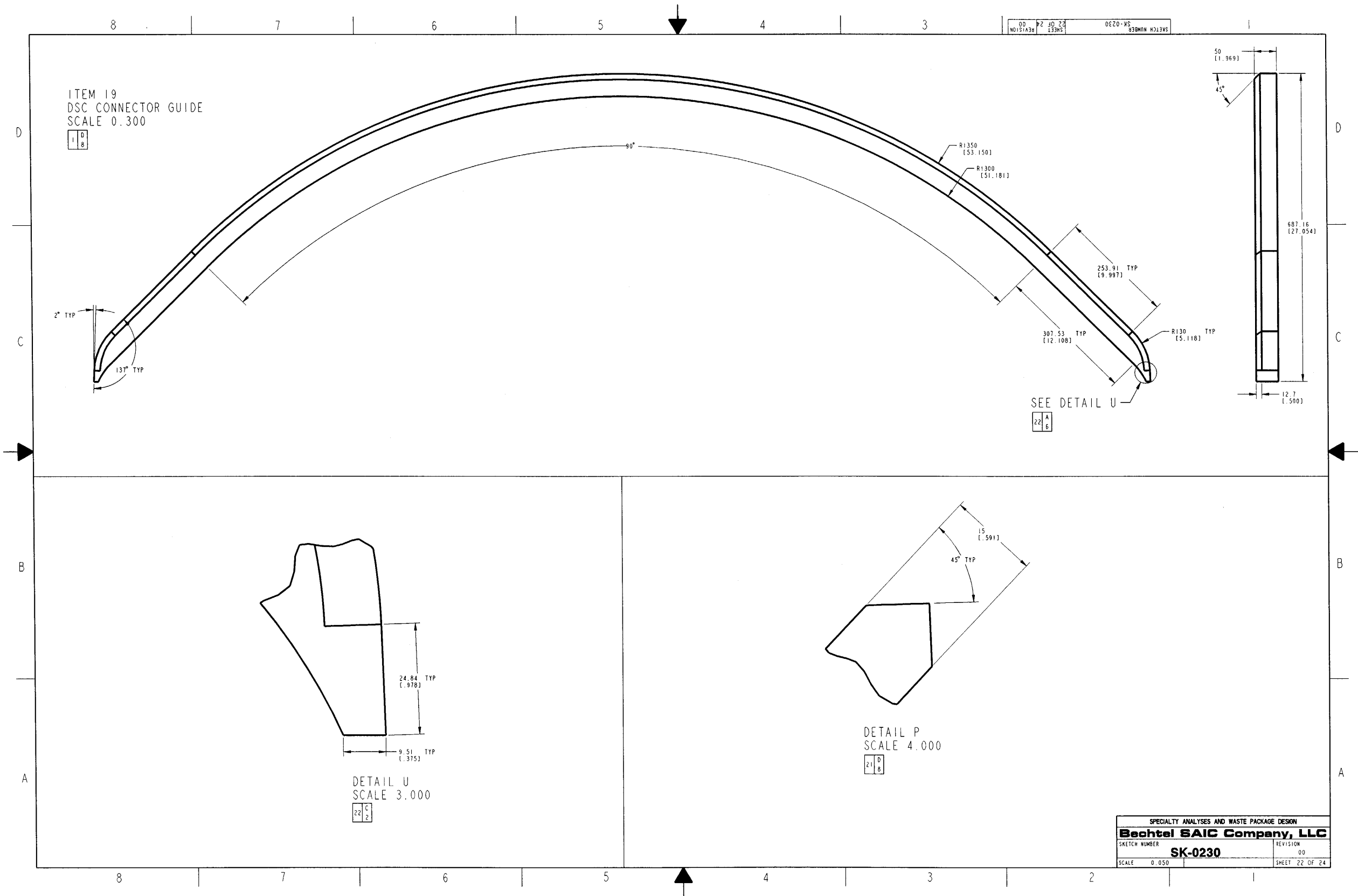
NAME: MCKENZIED2 OBJECT: SK-0230_REV00_20 DATE: 06-Nov-02 12:38:56



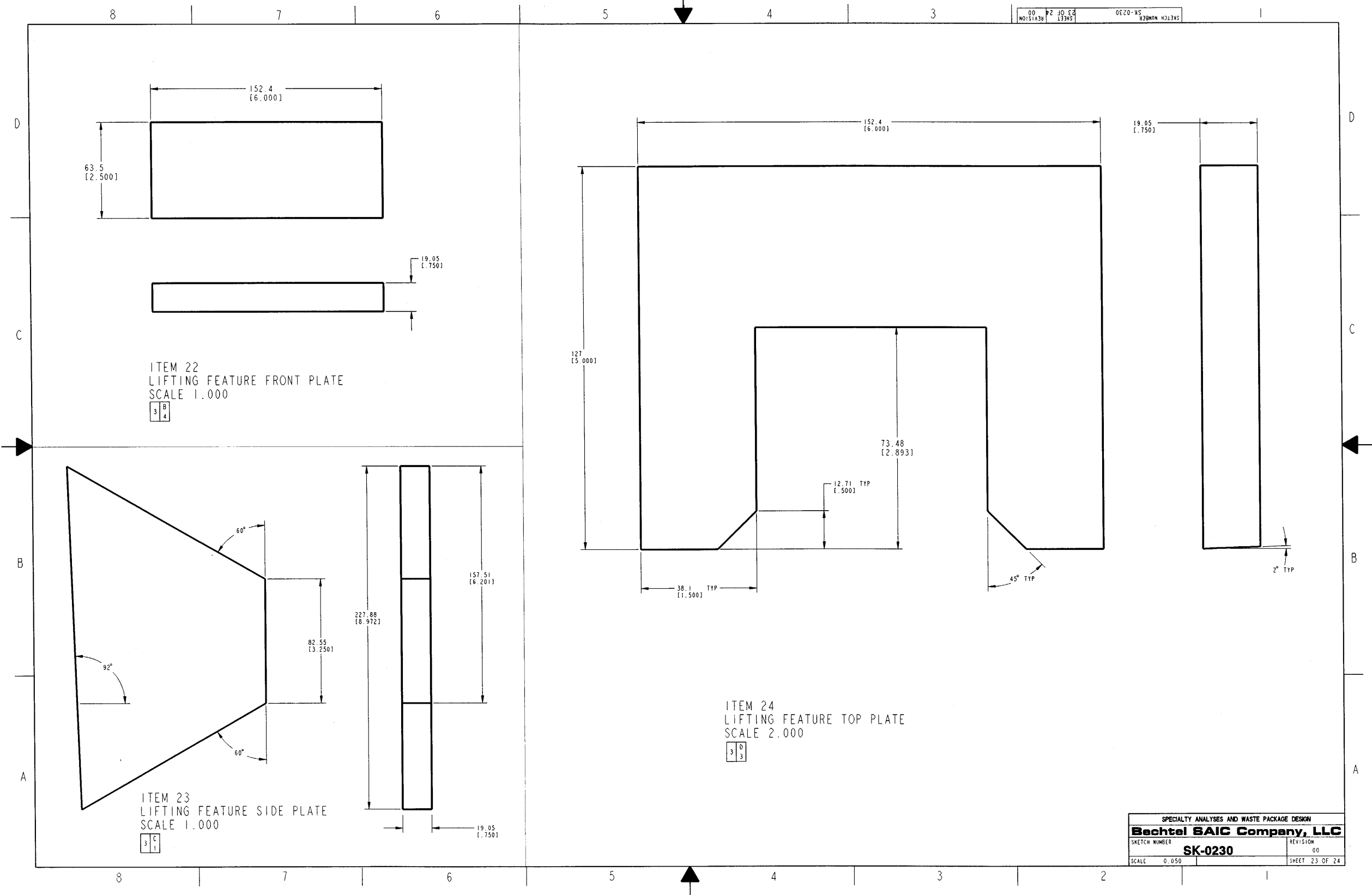
NAME: MCKENZIED2 OBJECT: SK-0230_REV00_21 DATE: 06-Nov-02 12:38:56



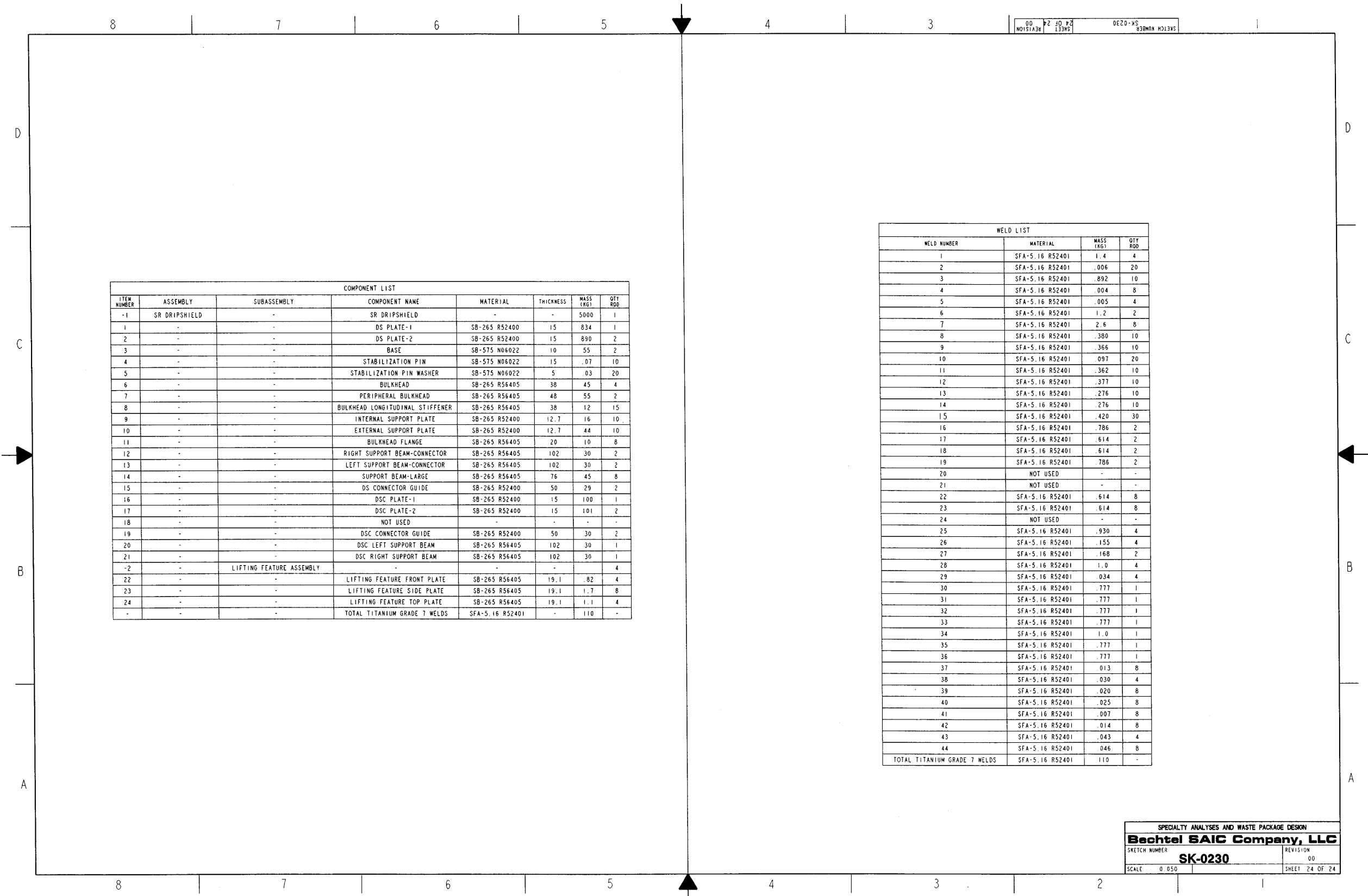
NAME: MCKENZIED2 OBJECT: SK-0230_REV00_22 DATE: 06-Nov-02 12:38:56



NAME: MCKENZIED2 OBJECT: SK-0230_REV00_23 DATE: 06-Nov-02 12:38:57



NAME: MCKENZIED2 OBJECT: SK-0230_REV00_24 DATE: 06-Nov-02 12:38:57



COMPONENT LIST							
ITEM NUMBER	ASSEMBLY	SUBASSEMBLY	COMPONENT NAME	MATERIAL	THICKNESS	MASS (KG)	QTY ROD
-1	SR DRIPSHIELD	-	SR DRIPSHIELD	-	-	5000	1
1	-	-	DS PLATE-1	SB-265 R52400	15	834	1
2	-	-	DS PLATE-2	SB-265 R52400	15	890	2
3	-	-	BASE	SB-575 N06022	10	55	2
4	-	-	STABILIZATION PIN	SB-575 N06022	15	.07	10
5	-	-	STABILIZATION PIN WASHER	SB-575 N06022	5	.03	20
6	-	-	BULKHEAD	SB-265 R56405	38	45	4
7	-	-	PERIPHERAL BULKHEAD	SB-265 R56405	48	55	2
8	-	-	BULKHEAD LONGITUDINAL STIFFENER	SB-265 R56405	38	12	15
9	-	-	INTERNAL SUPPORT PLATE	SB-265 R52400	12.7	16	10
10	-	-	EXTERNAL SUPPORT PLATE	SB-265 R52400	12.7	44	10
11	-	-	BULKHEAD FLANGE	SB-265 R56405	20	10	8
12	-	-	RIGHT SUPPORT BEAM-CONNECTOR	SB-265 R56405	102	30	2
13	-	-	LEFT SUPPORT BEAM-CONNECTOR	SB-265 R56405	102	30	2
14	-	-	SUPPORT BEAM-LARGE	SB-265 R56405	76	45	8
15	-	-	DS CONNECTOR GUIDE	SB-265 R52400	50	29	2
16	-	-	DSC PLATE-1	SB-265 R52400	15	100	1
17	-	-	DSC PLATE-2	SB-265 R52400	15	101	2
18	-	-	NOT USED	-	-	-	-
19	-	-	DSC CONNECTOR GUIDE	SB-265 R52400	50	30	2
20	-	-	DSC LEFT SUPPORT BEAM	SB-265 R56405	102	30	1
21	-	-	DSC RIGHT SUPPORT BEAM	SB-265 R56405	102	30	1
-2	-	LIFTING FEATURE ASSEMBLY	-	-	-	-	4
22	-	-	LIFTING FEATURE FRONT PLATE	SB-265 R56405	19.1	82	4
23	-	-	LIFTING FEATURE SIDE PLATE	SB-265 R56405	19.1	1.7	8
24	-	-	LIFTING FEATURE TOP PLATE	SB-265 R56405	19.1	1.1	4
-	-	-	TOTAL TITANIUM GRADE 7 WELDS	SFA-5.16 R52401	-	110	-

WELD LIST			
WELD NUMBER	MATERIAL	MASS (KG)	QTY ROD
1	SFA-5.16 R52401	1.4	4
2	SFA-5.16 R52401	.006	20
3	SFA-5.16 R52401	.892	10
4	SFA-5.16 R52401	.004	8
5	SFA-5.16 R52401	.005	4
6	SFA-5.16 R52401	1.2	2
7	SFA-5.16 R52401	2.6	8
8	SFA-5.16 R52401	.380	10
9	SFA-5.16 R52401	.366	10
10	SFA-5.16 R52401	.097	20
11	SFA-5.16 R52401	.362	10
12	SFA-5.16 R52401	.377	10
13	SFA-5.16 R52401	.276	10
14	SFA-5.16 R52401	.276	10
15	SFA-5.16 R52401	.420	30
16	SFA-5.16 R52401	.786	2
17	SFA-5.16 R52401	.614	2
18	SFA-5.16 R52401	.614	2
19	SFA-5.16 R52401	.786	2
20	NOT USED	-	-
21	NOT USED	-	-
22	SFA-5.16 R52401	.614	8
23	SFA-5.16 R52401	.614	8
24	NOT USED	-	-
25	SFA-5.16 R52401	.930	4
26	SFA-5.16 R52401	.155	4
27	SFA-5.16 R52401	.168	2
28	SFA-5.16 R52401	1.0	4
29	SFA-5.16 R52401	.034	4
30	SFA-5.16 R52401	.777	1
31	SFA-5.16 R52401	.777	1
32	SFA-5.16 R52401	.777	1
33	SFA-5.16 R52401	.777	1
34	SFA-5.16 R52401	1.0	1
35	SFA-5.16 R52401	.777	1
36	SFA-5.16 R52401	.777	1
37	SFA-5.16 R52401	.013	8
38	SFA-5.16 R52401	.030	4
39	SFA-5.16 R52401	.020	8
40	SFA-5.16 R52401	.025	8
41	SFA-5.16 R52401	.007	8
42	SFA-5.16 R52401	.014	8
43	SFA-5.16 R52401	.043	4
44	SFA-5.16 R52401	.046	8
TOTAL TITANIUM GRADE 7 WELDS	SFA-5.16 R52401	110	-

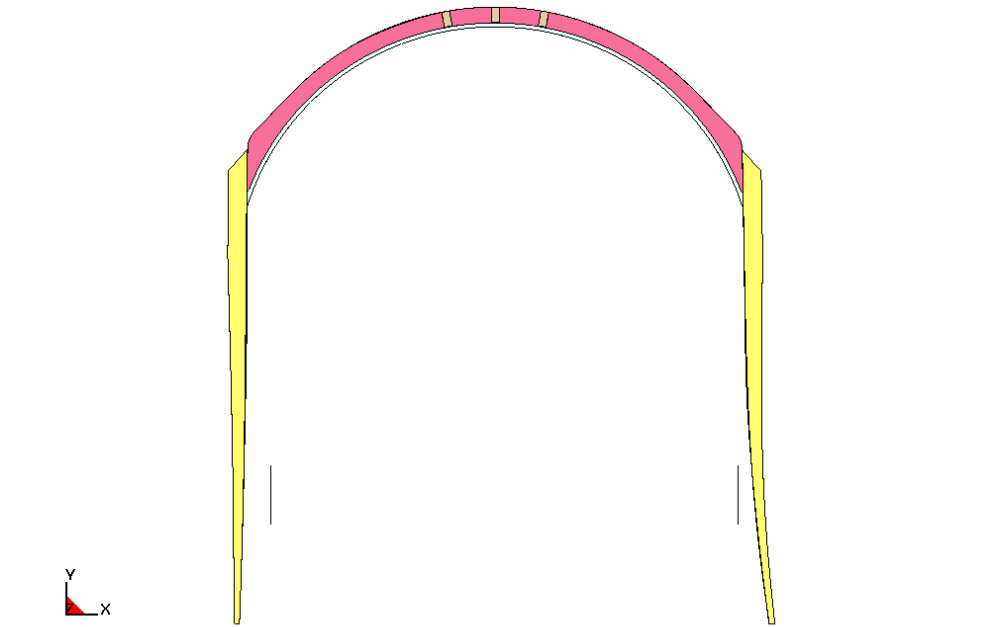
SPECIALTY ANALYSES AND WASTE PACKAGE DESIGN
Bechtel SAIC Company, LLC

SKETCH NUMBER	REVISION
SK-0230	00
SCALE 0.050	SHEET 24 OF 24

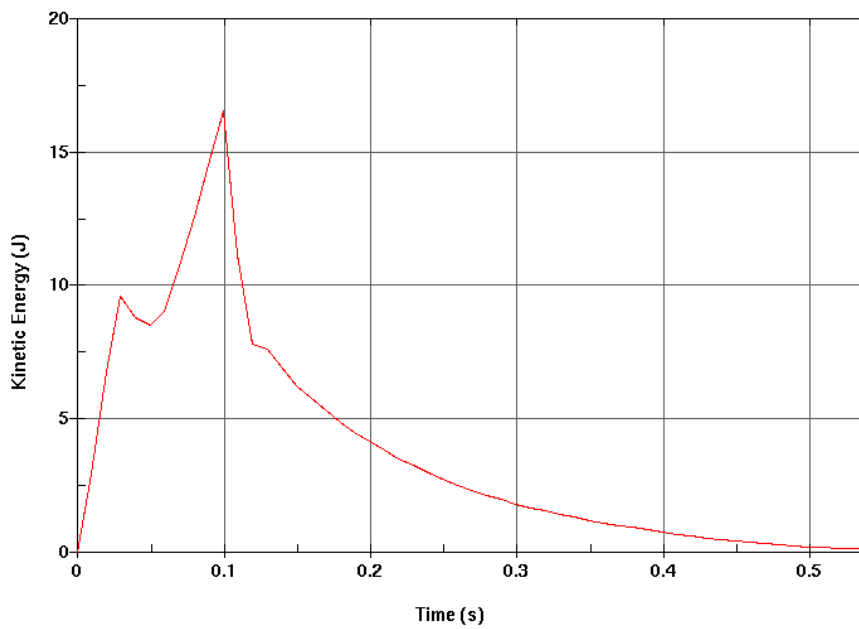
ATTACHMENT II

PLOTS OF FINAL DRIP SHIELD CONFIGURATIONS AND KINETIC ENERGY

Time = 0.5476

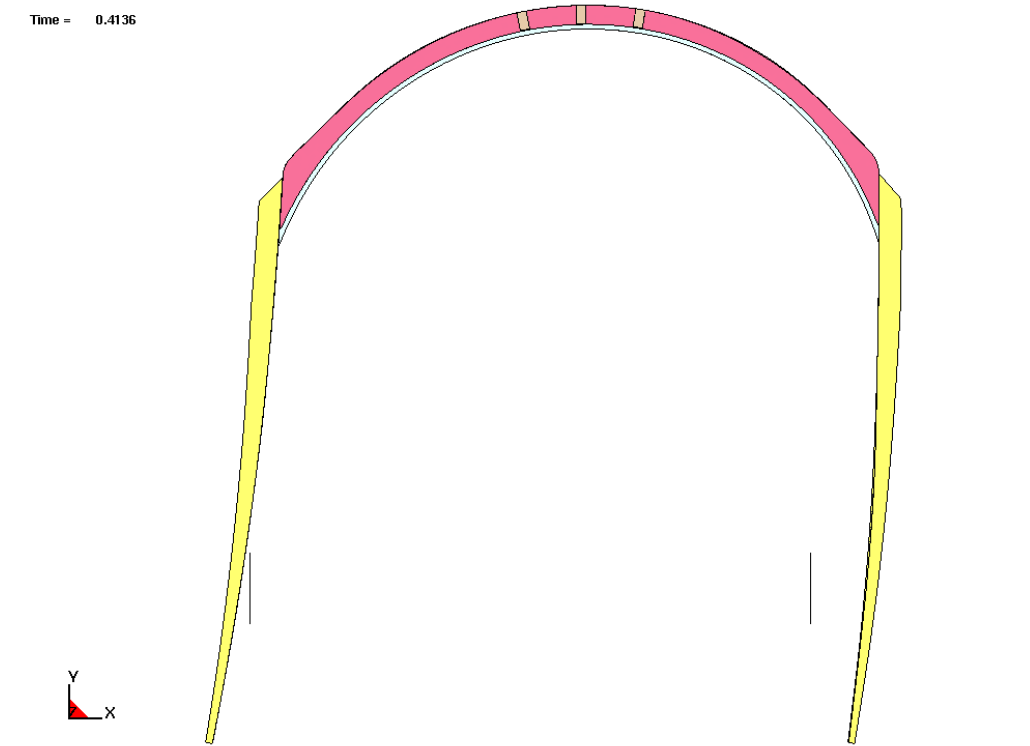


(a)

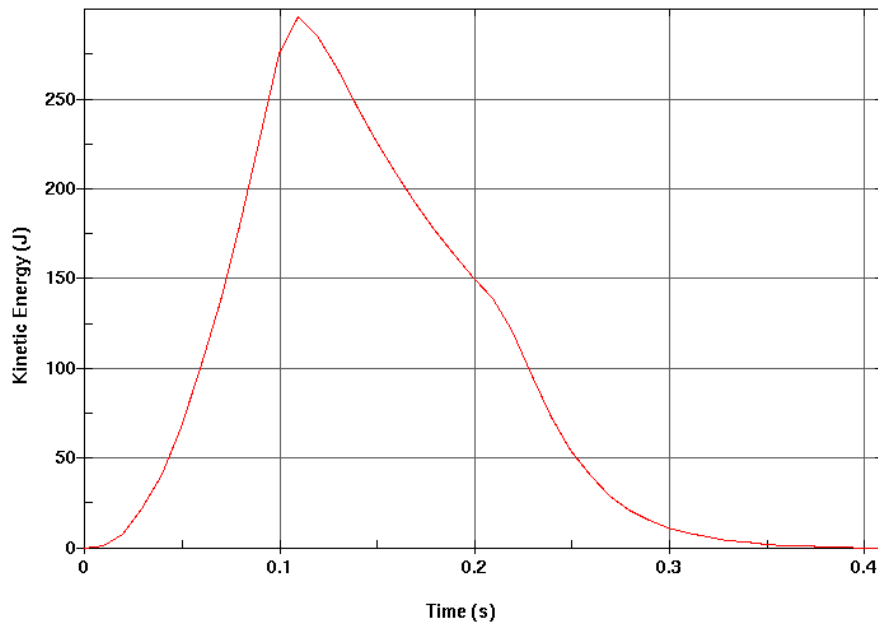


(b)

Figure II-1. Realization 1: (a) Final Drip Shield Configuration, and (b) Kinetic Energy of the Drip Shield

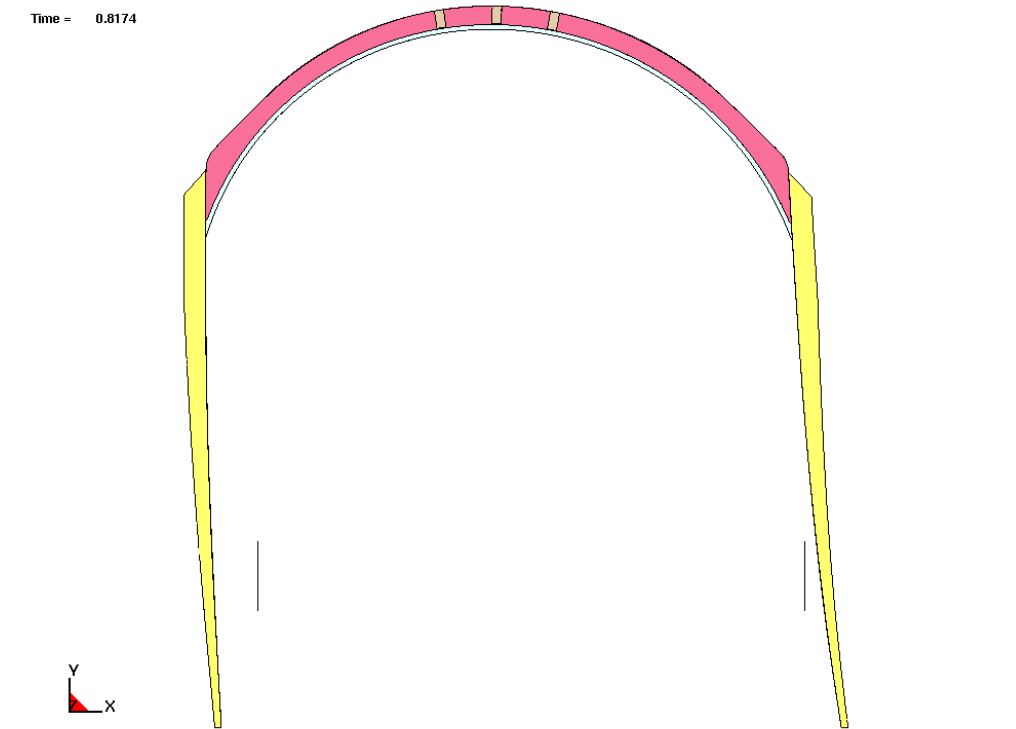


(a)

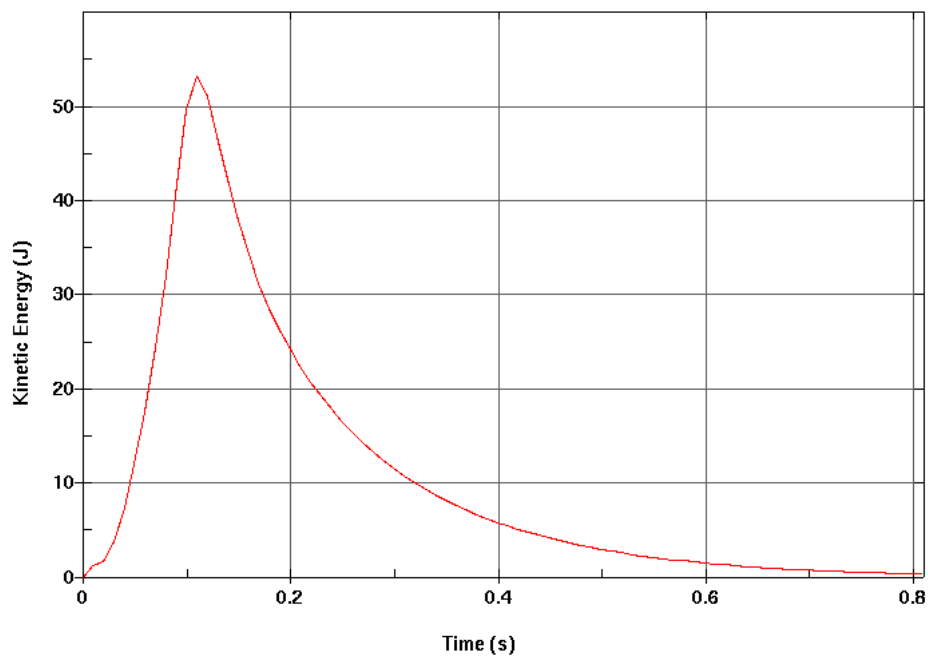


(b)

Figure II-2. Realization 2: (a) Final Drip Shield Configuration, and (b) Kinetic Energy of the Drip Shield

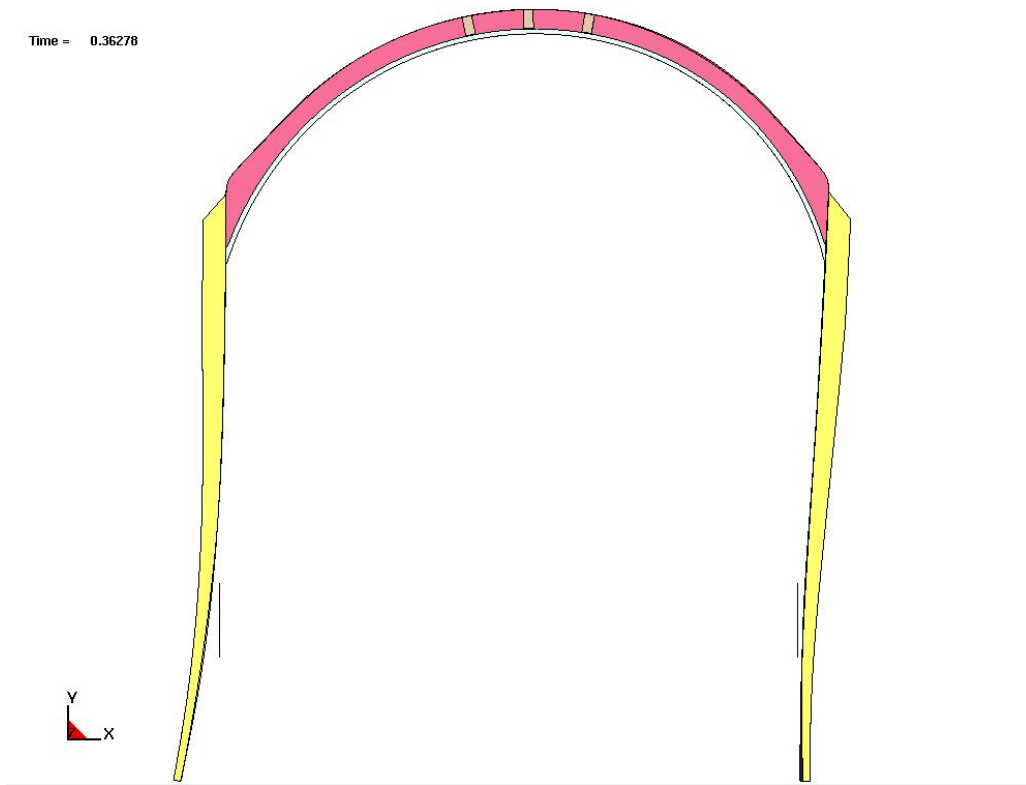


(a)

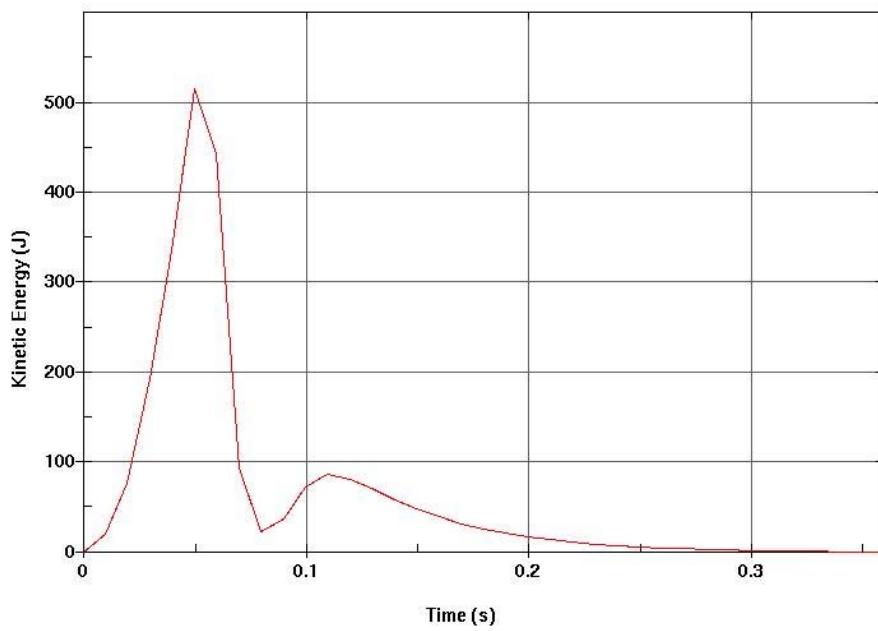


(b)

Figure II-3. Realization 3: (a) Final Drip Shield Configuration, and (b) Kinetic Energy of the Drip Shield



(a)



(b)

Figure II-4. Realization 4: (a) Final Drip Shield Configuration, and (b) Kinetic Energy of the Drip Shield

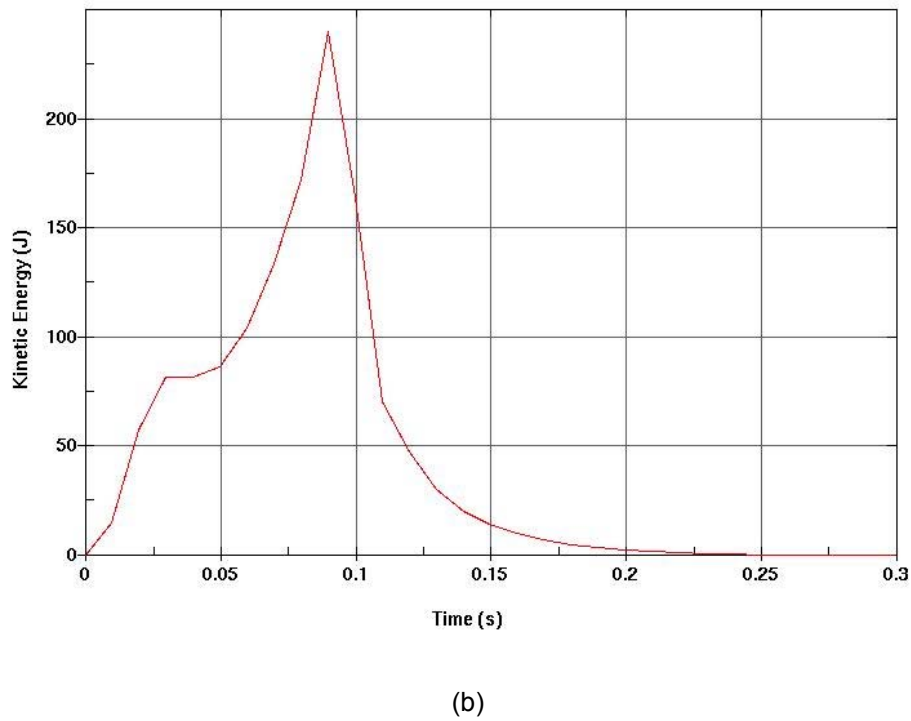
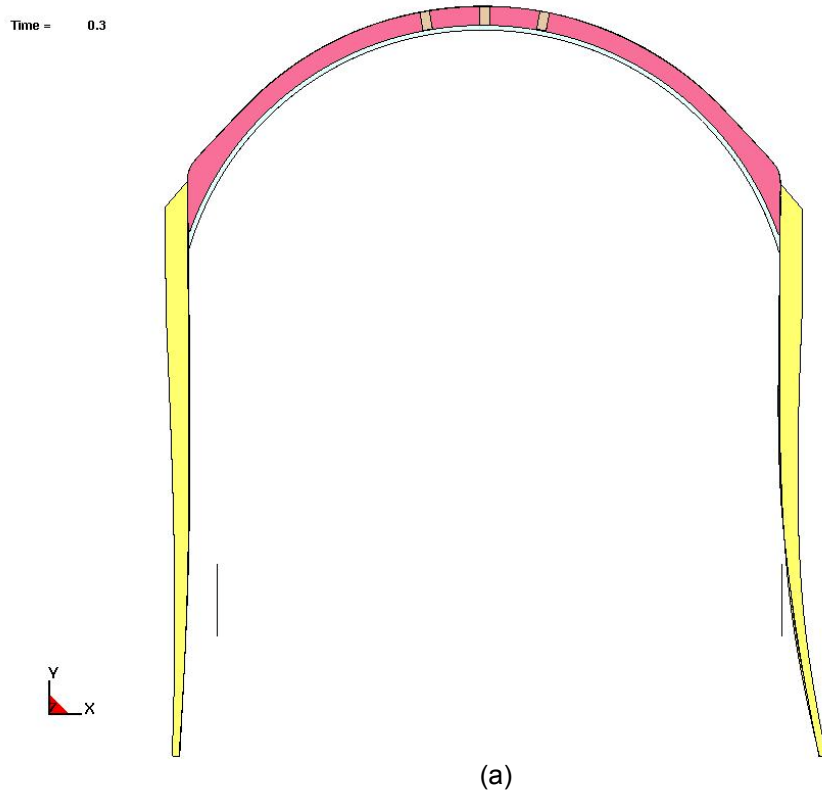


Figure II-5. Realization 5: (a) Final Drip Shield Configuration, and (b) Kinetic Energy of the Drip Shield

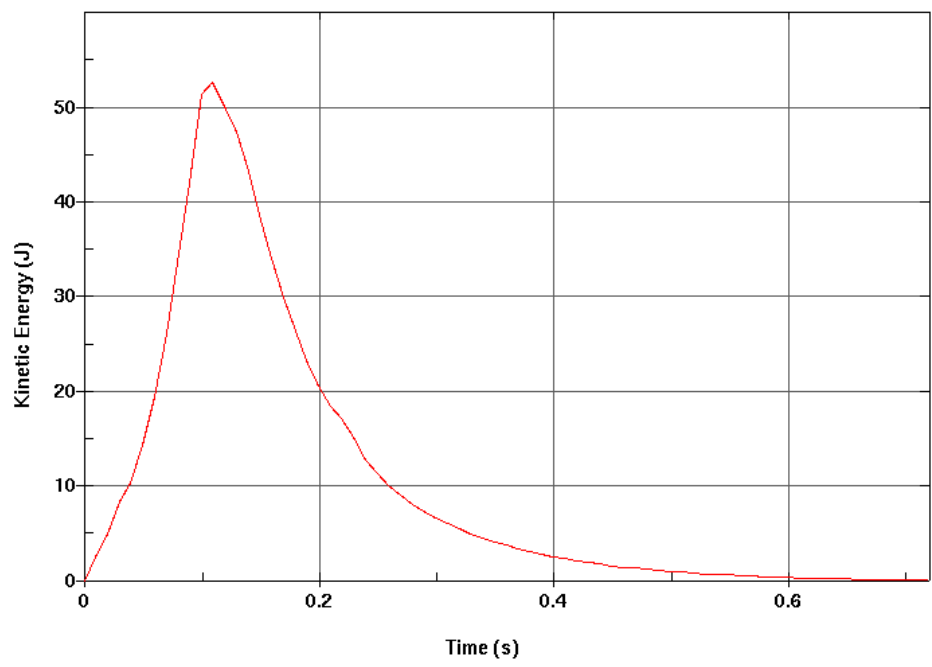
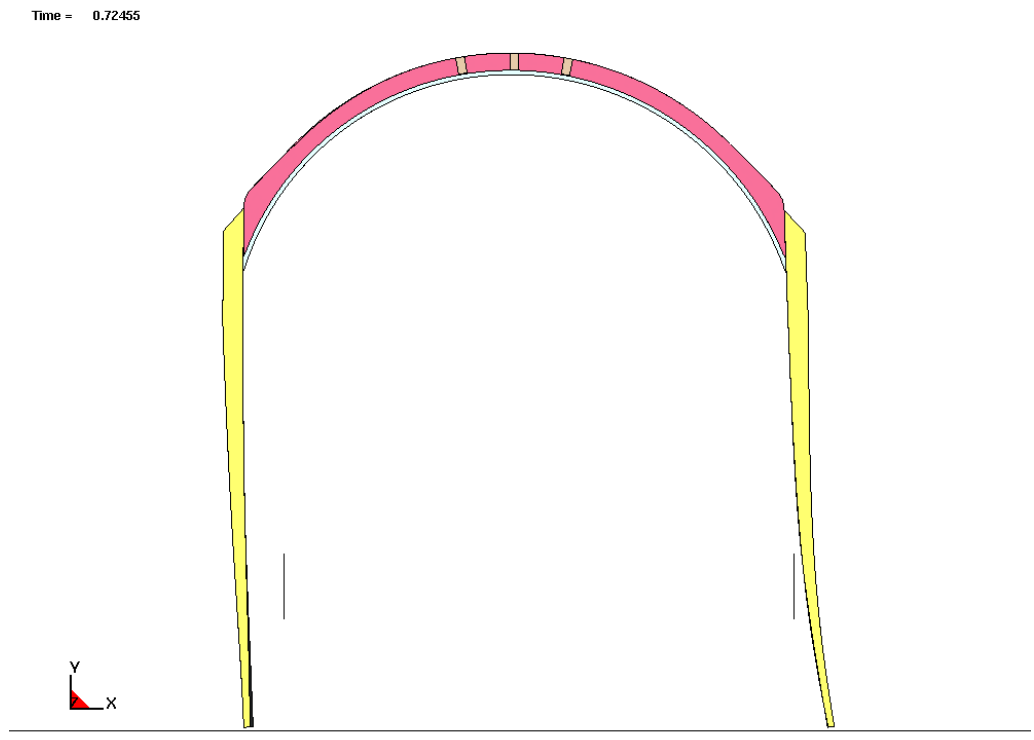
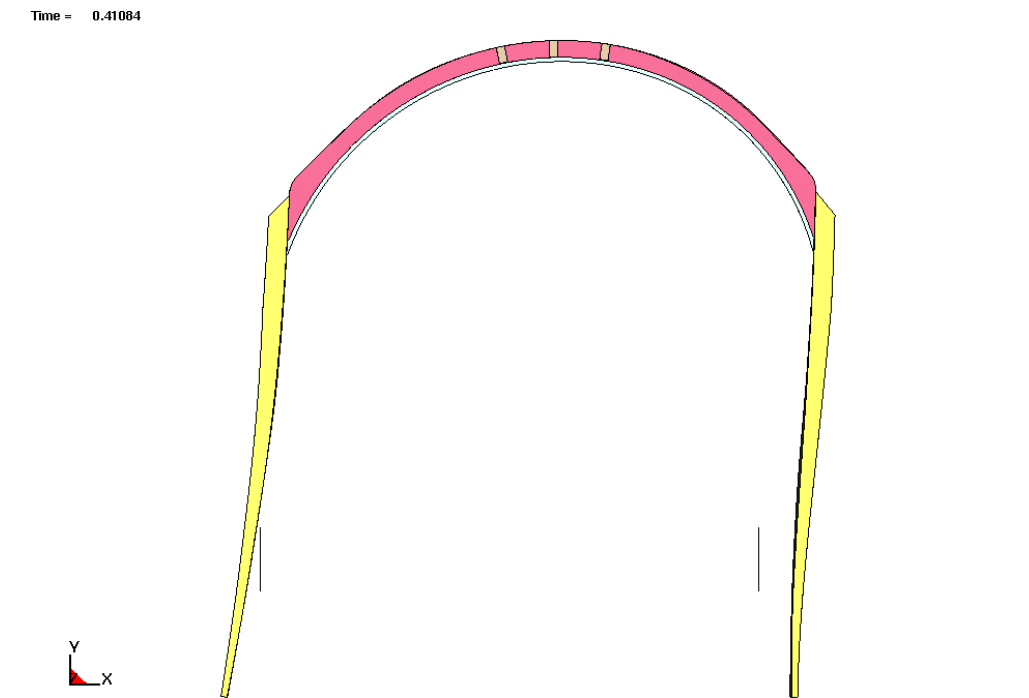
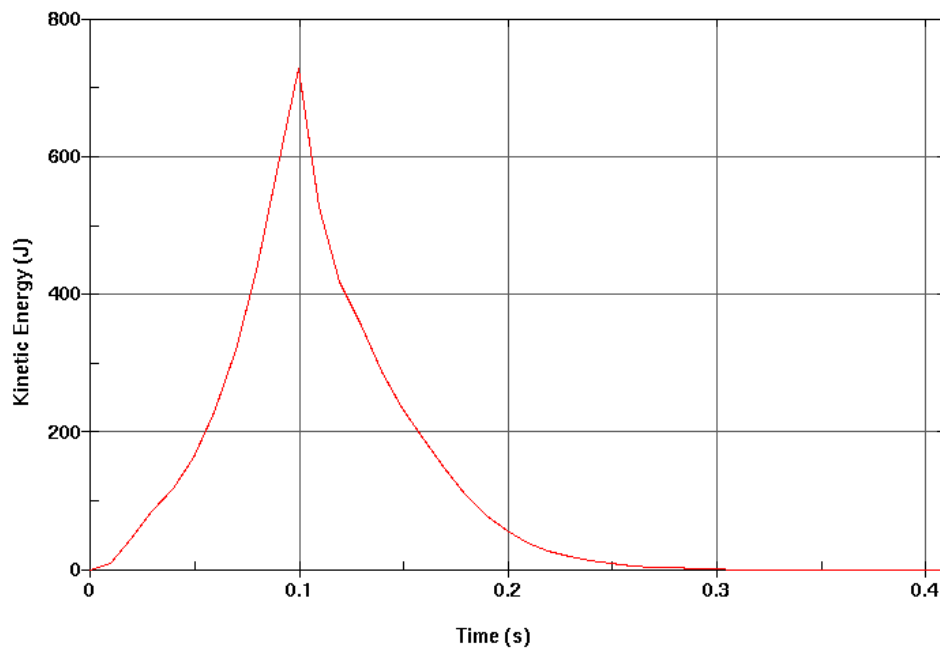


Figure II-6. Realization 6: (a) Final Drip Shield Configuration, and (b) Kinetic Energy of the Drip Shield

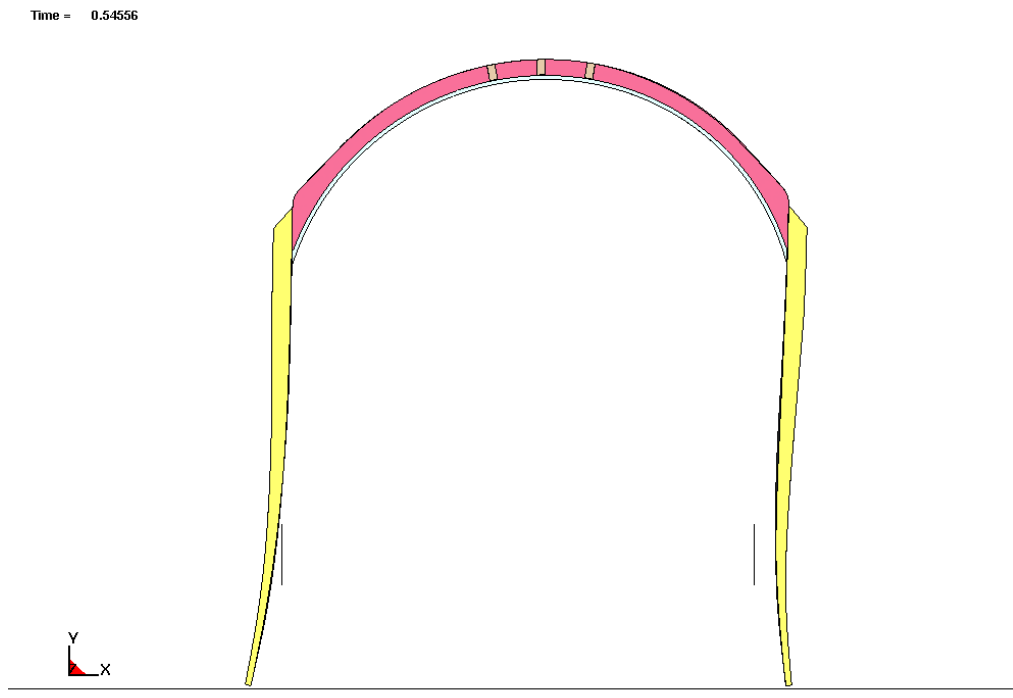


(a)

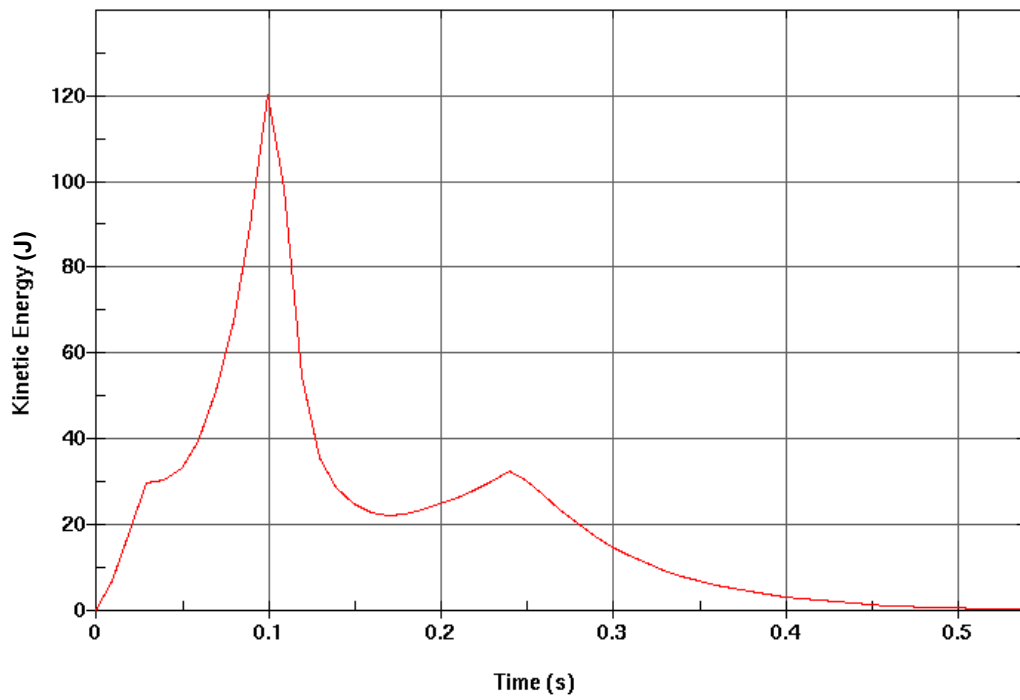


(b)

Figure II-7. Average of all Realizations with Density of Surrounding Rock Multiplied by 2.5:
(a) Final Drip Shield Configuration, and (b) Kinetic Energy of the Drip Shield



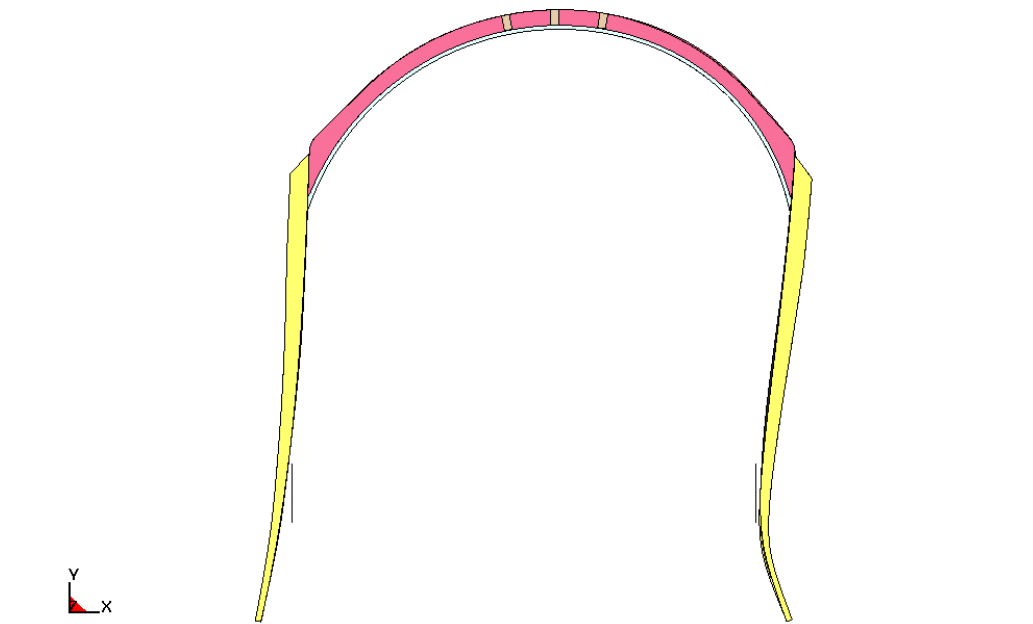
(a)



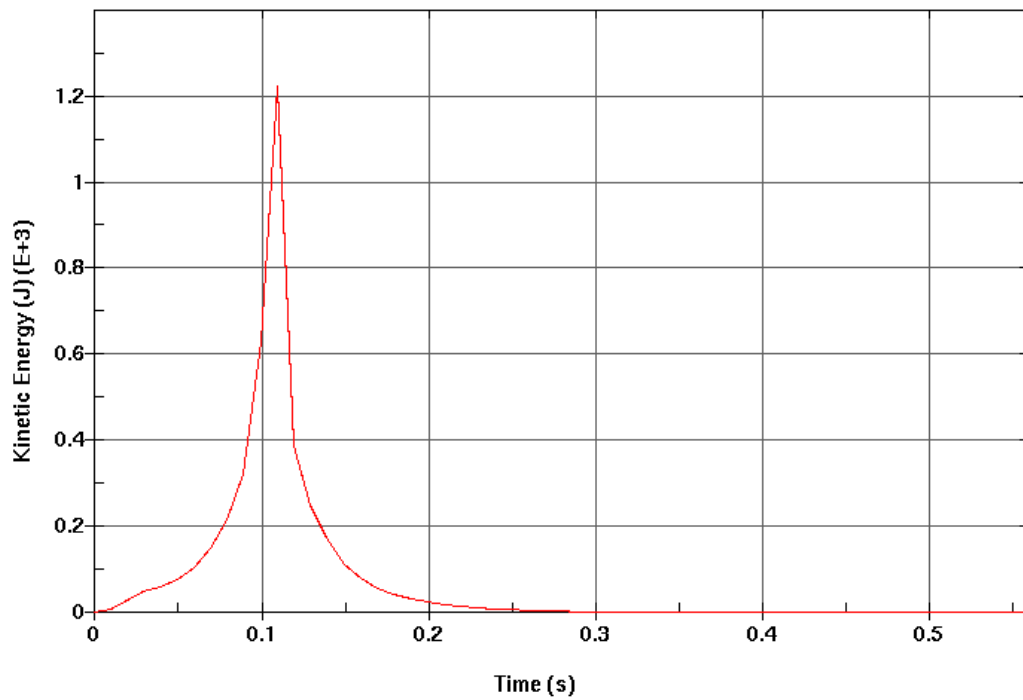
(b)

Figure II-8. Average of all Realizations with Density of Surrounding Rock Multiplied by 3.0:
(a) Final Drip Shield Configuration, and (b) Kinetic Energy of the Drip Shield

Time = 0.5662

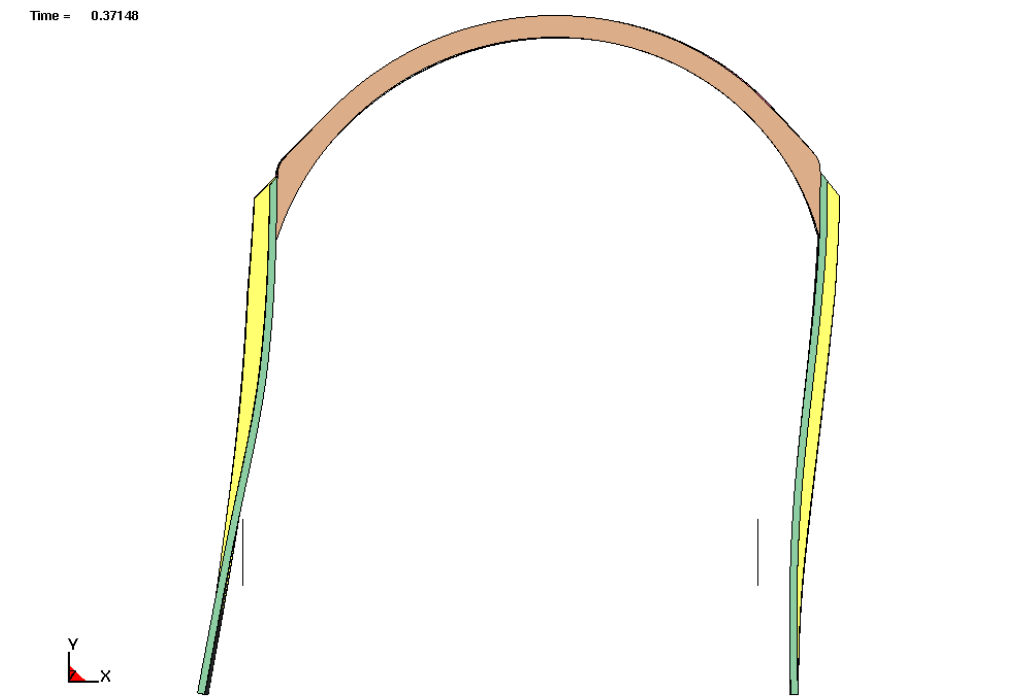


(a)

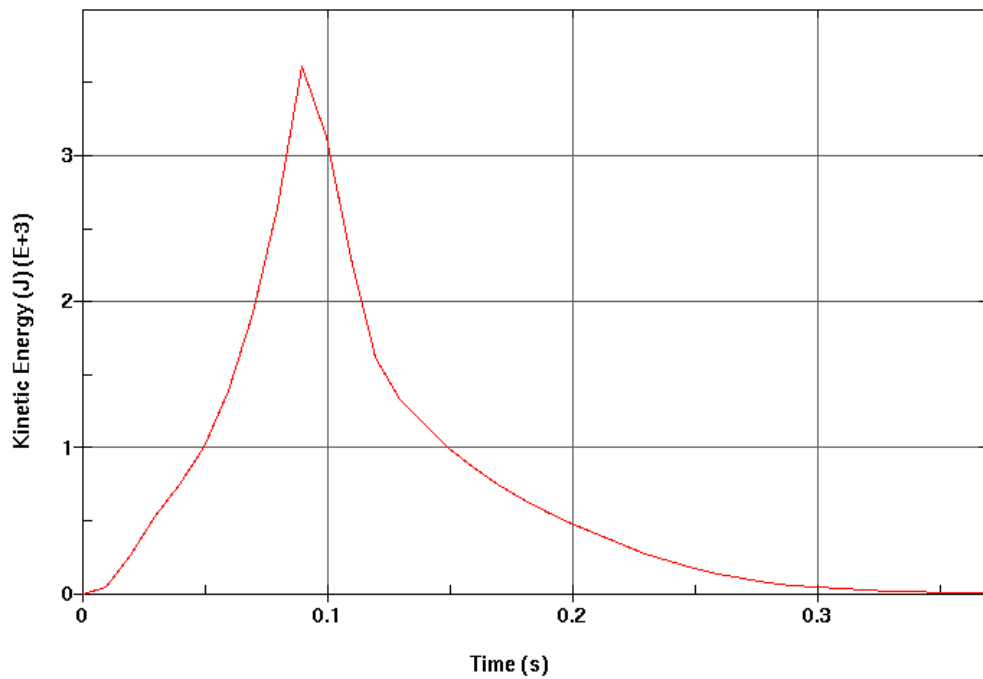


(b)

Figure II-9. Average of all Realizations with Density of Surrounding Rock Multiplied by 4.0: (a) Final Drip Shield Configuration, and (b) Kinetic Energy of the Drip Shield



(a)



(b)

Figure II-10. Average of all Realizations with Density of Surrounding Rock Multiplied by 2.5 for Full Length Drip Shield:

(a) Final Drip Shield Configuration, and (b) Kinetic Energy of the Drip Shield

ATTACHMENT III

PLOTS OF FINAL DRIP SHIELD MAXIMUM SHEAR STRESSES

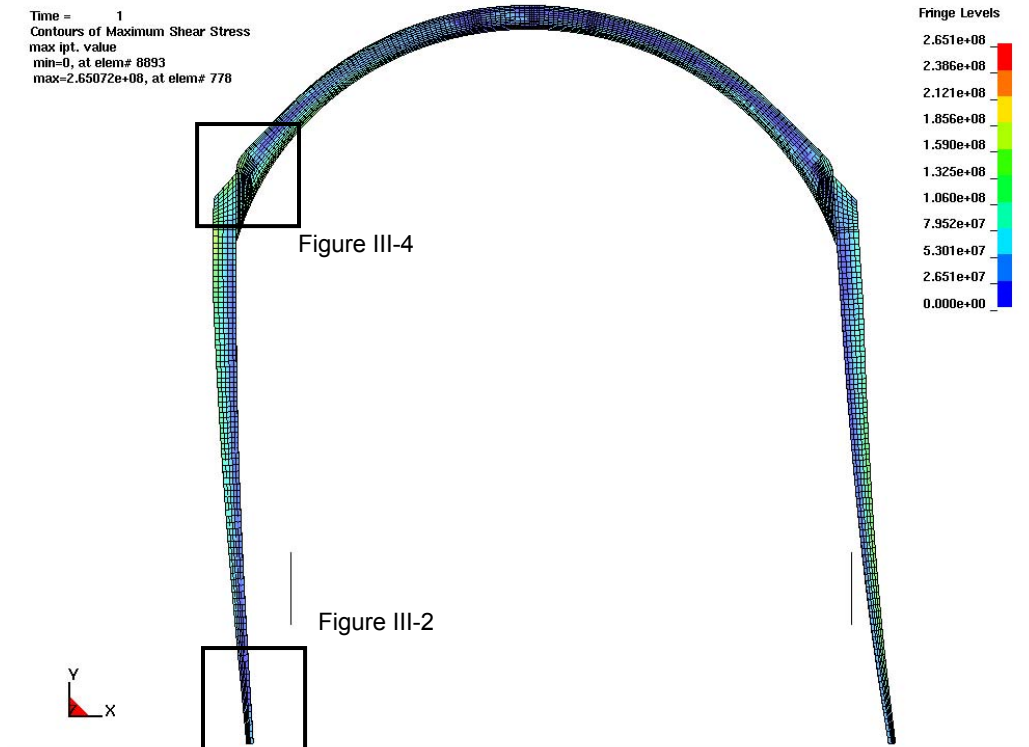


Figure III-1. Maximum Shear Stress (Pa) Plot for Realization 3

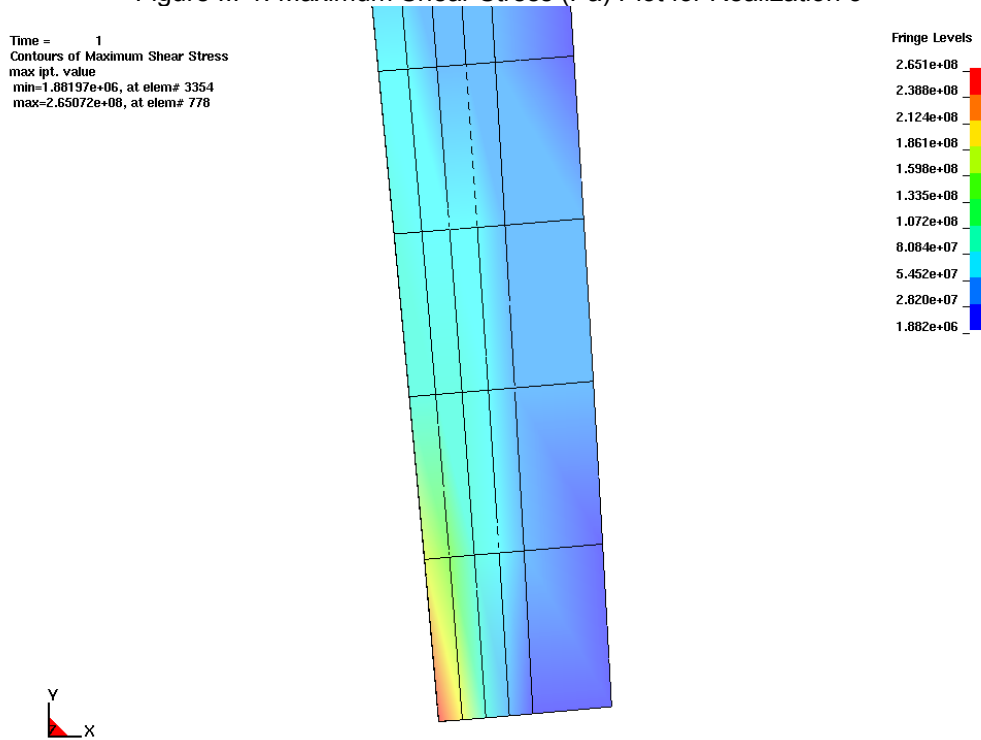


Figure III-2. Maximum Shear Stress (Pa) Plot of the Large Support Beam Realization 3

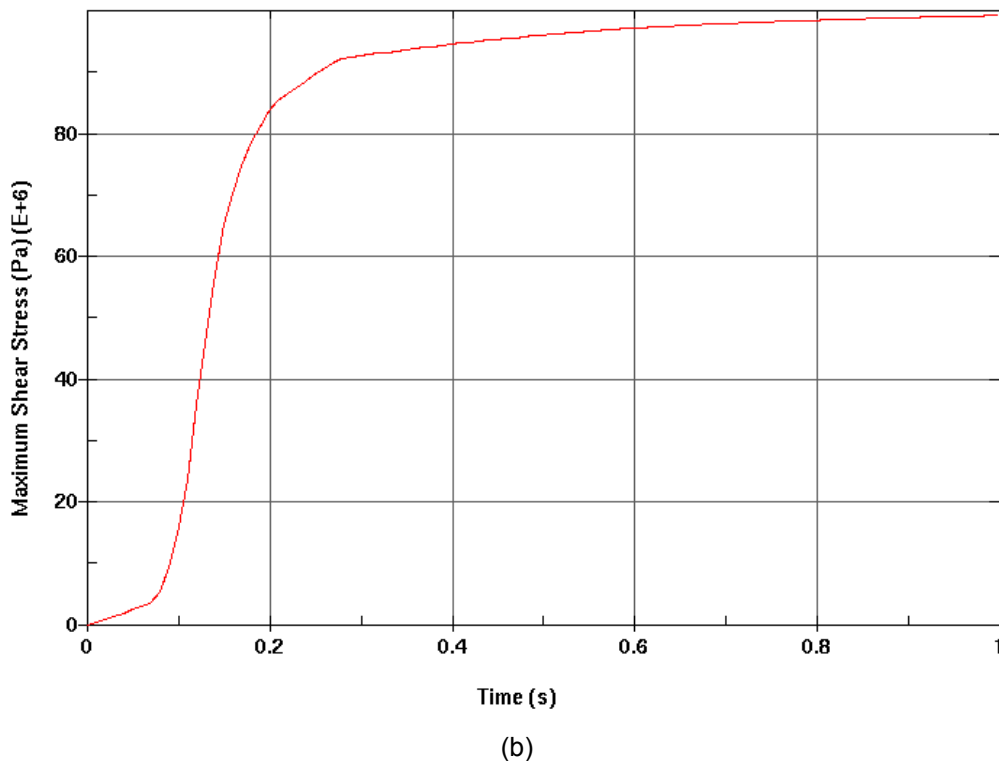
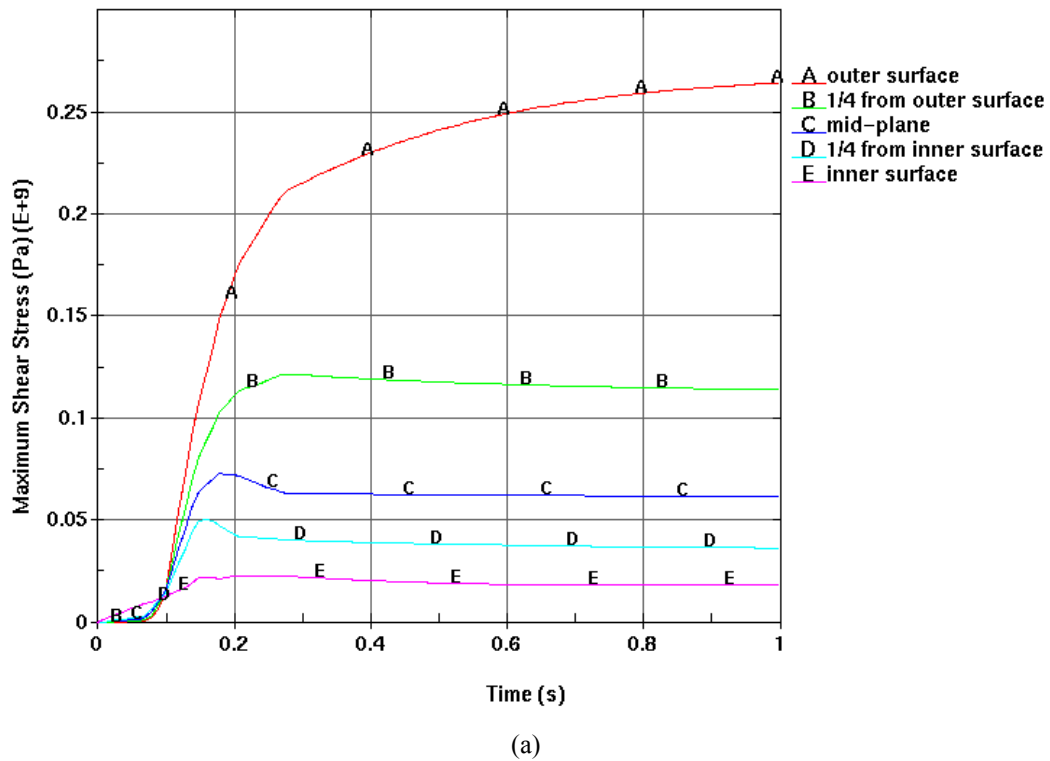


Figure III-3. Maximum Shear Stress History Plots of the Large Support Beam for Realization 3: (a) Maximum Shear Stress through the Cross-Section, and (b) Average of the Shear Stress through the Cross-Section

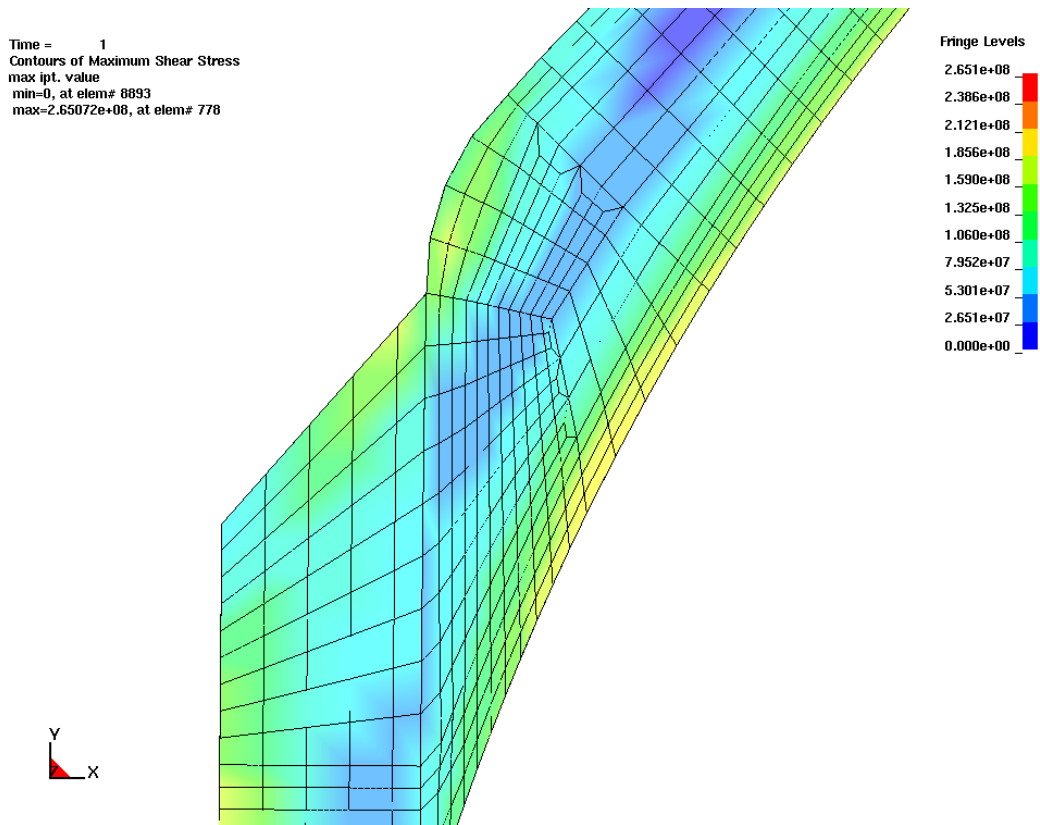
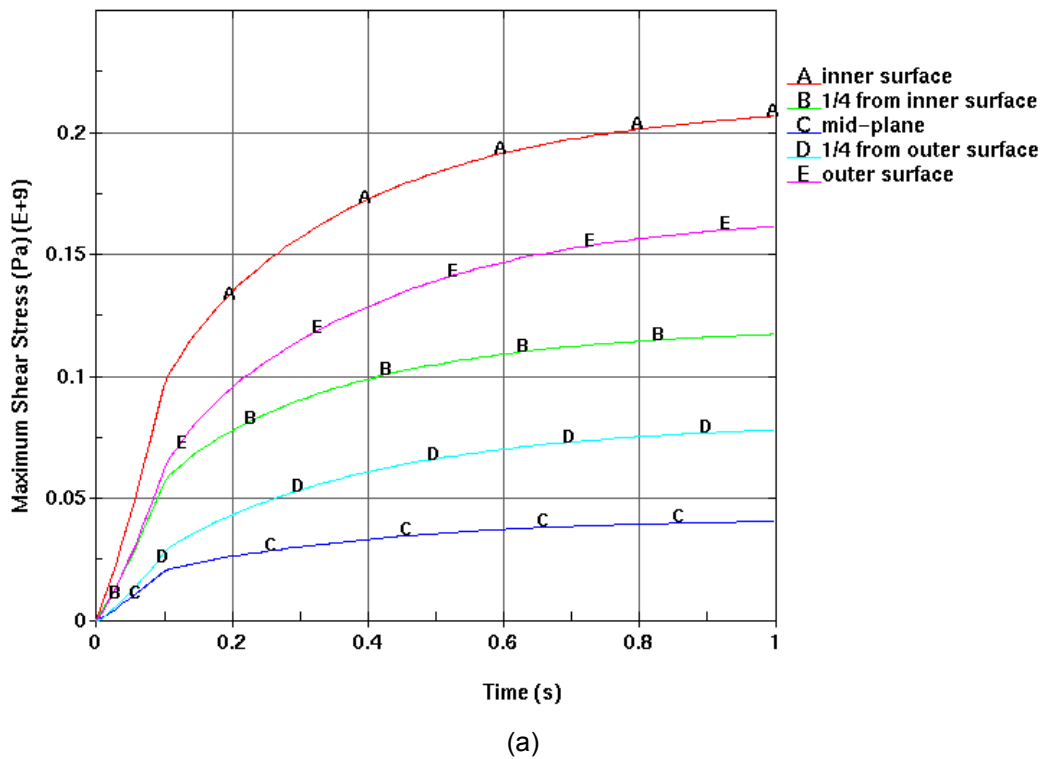
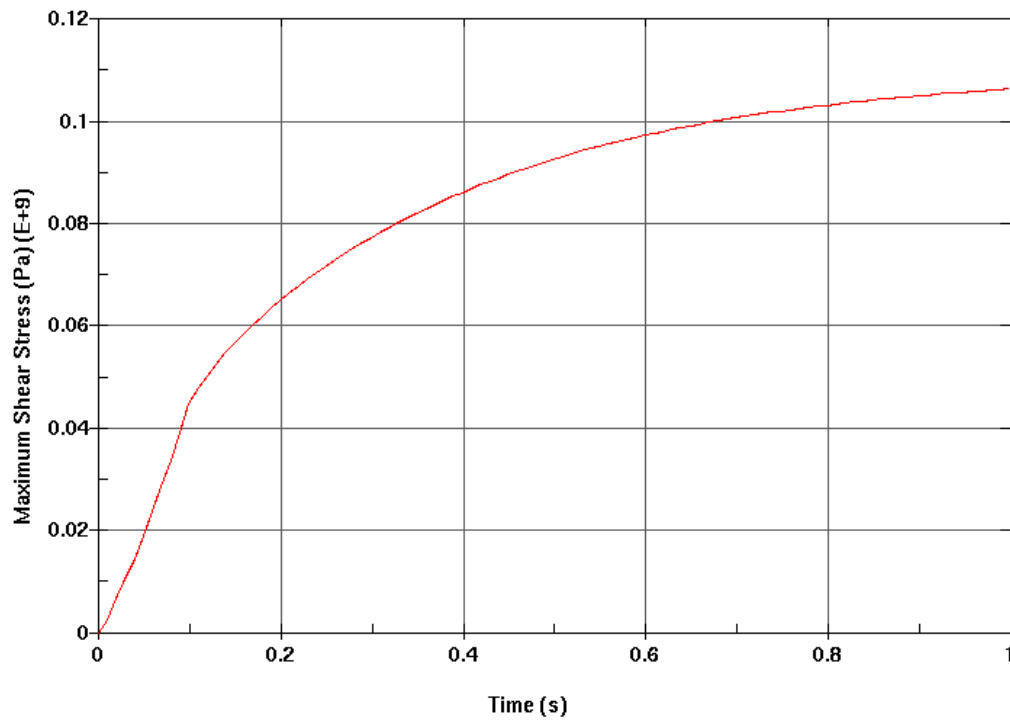


Figure III-4. Maximum Shear Stress (Pa) Plot of the Bulkhead for Realization 3





(b)

Figure III-5. Maximum Shear Stress History Plots of the Bulkhead for Realization 3: (a) Maximum Shear Stress through the Cross-Section, and (b) Average of the Shear Stress through the Cross-Section

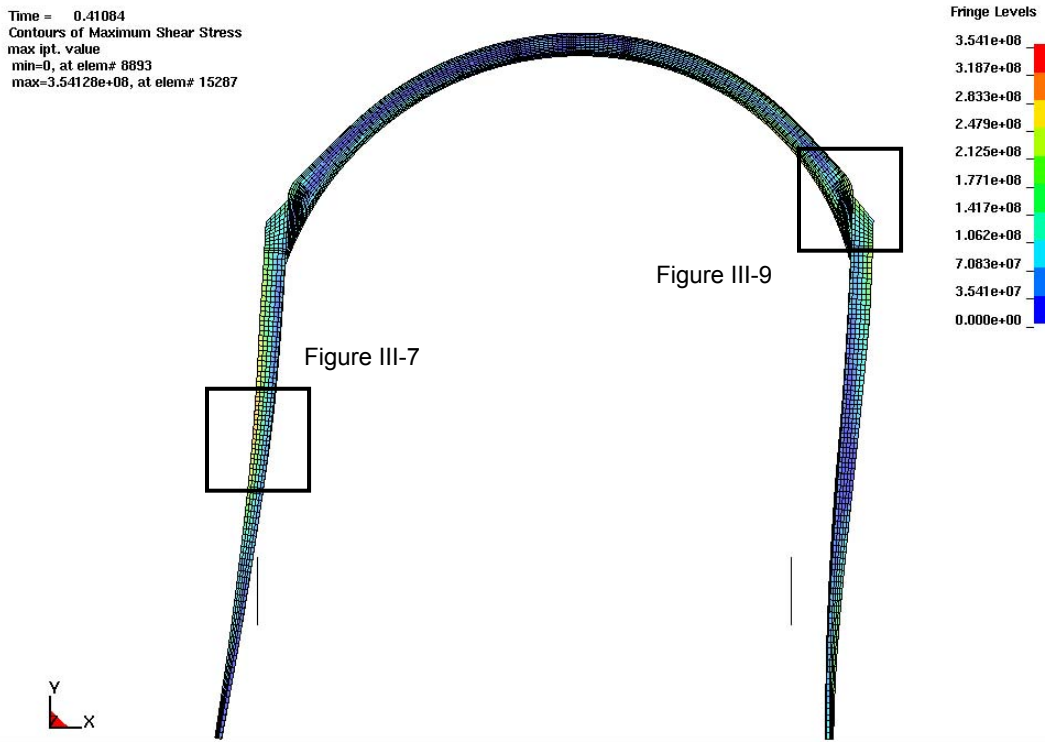


Figure III-6. Maximum Shear Stress (Pa) Plot for the Average of all Realizations with Density of Surrounding Rock Multiplied by 2.5

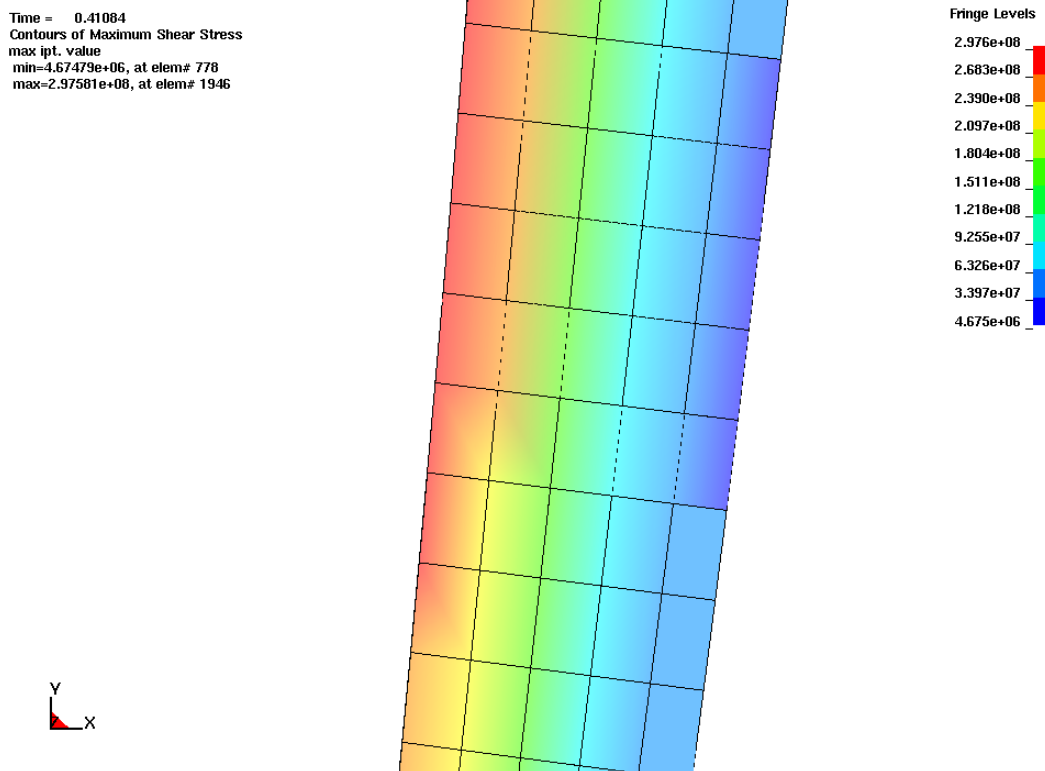


Figure III-7. Maximum Shear Stress (Pa) Plot of the Large Support Beam for the Average of all Realizations with Density of Surrounding Rock Multiplied by 2.5

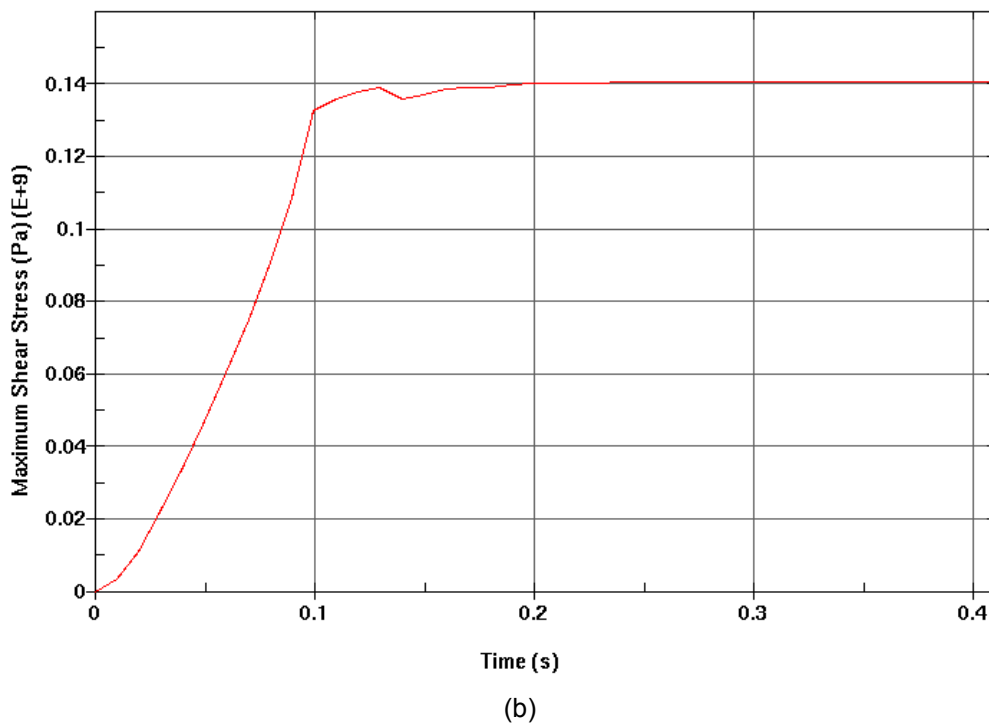
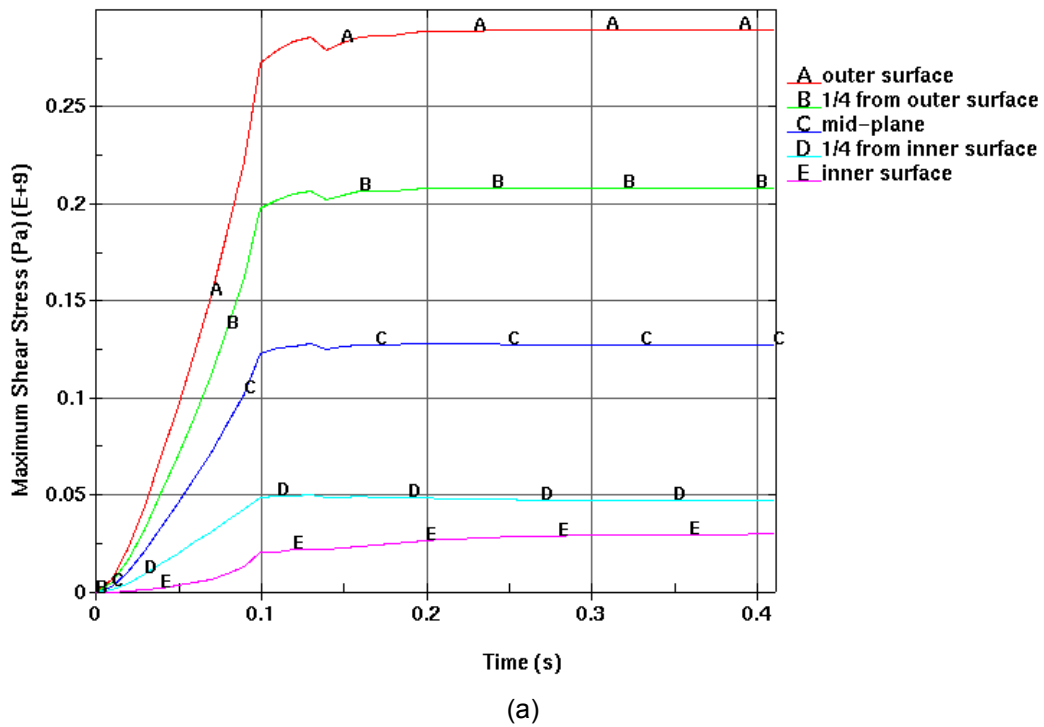


Figure III-8. Maximum Shear Stress History Plots of the Large Support Beam for the Average of all Realizations with Density of Surrounding Rock Multiplied by 2.5:
 (a) Maximum Shear Stress through the Cross-Section, and (b) Average of the Shear Stress through the Cross-Section

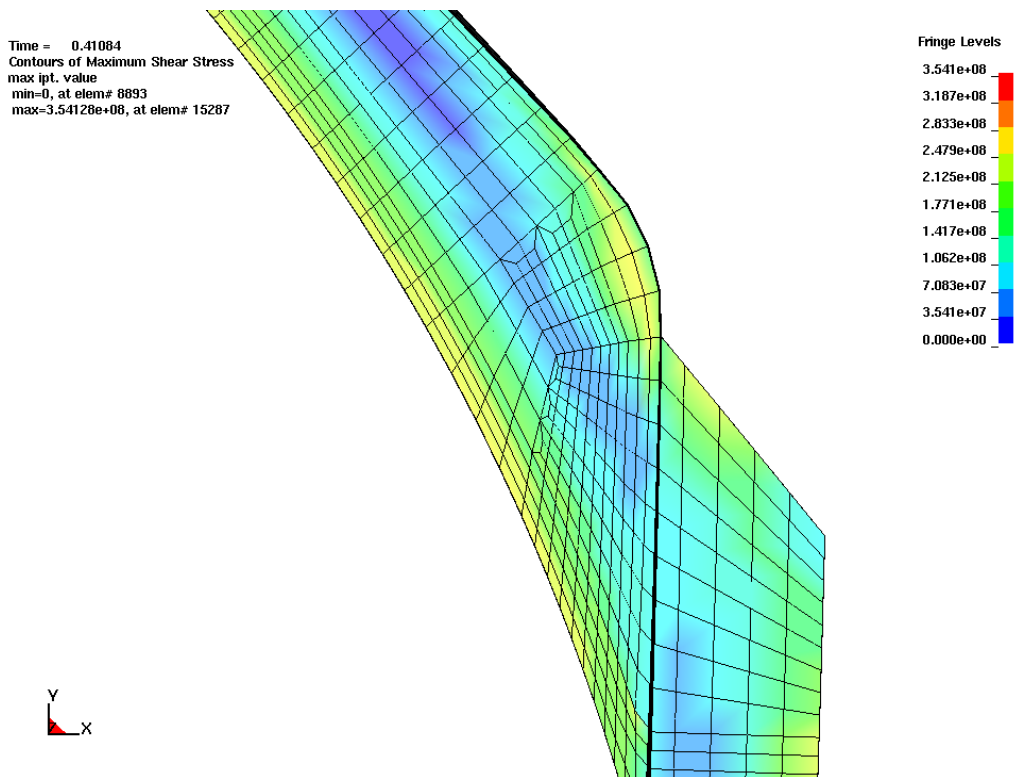
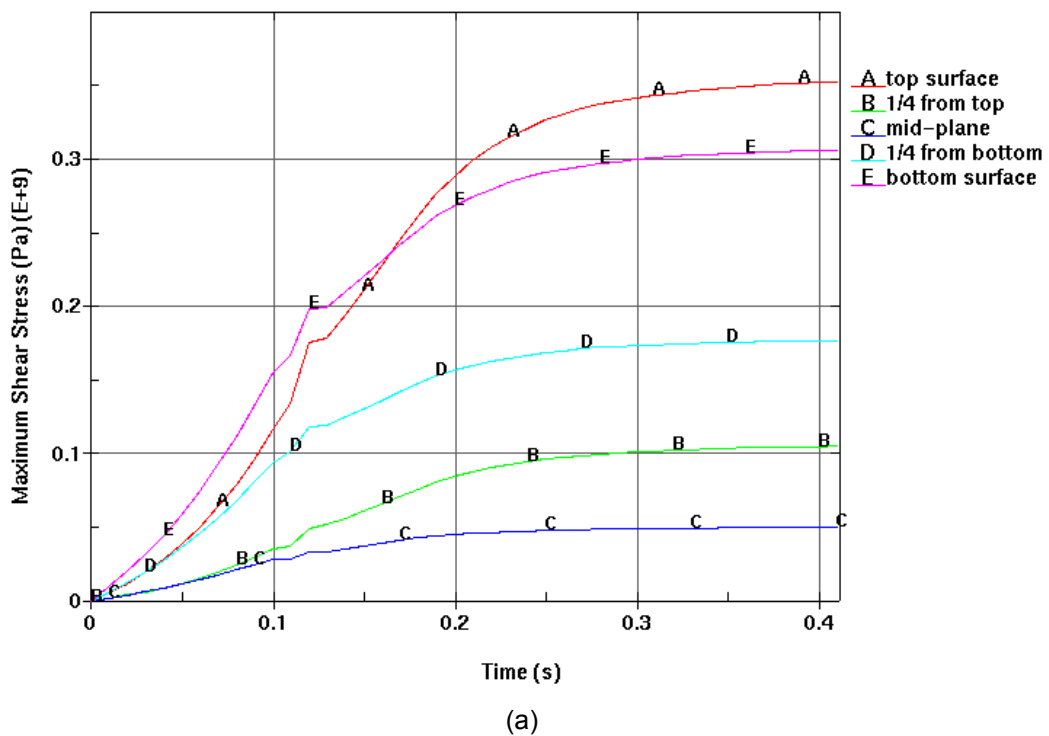
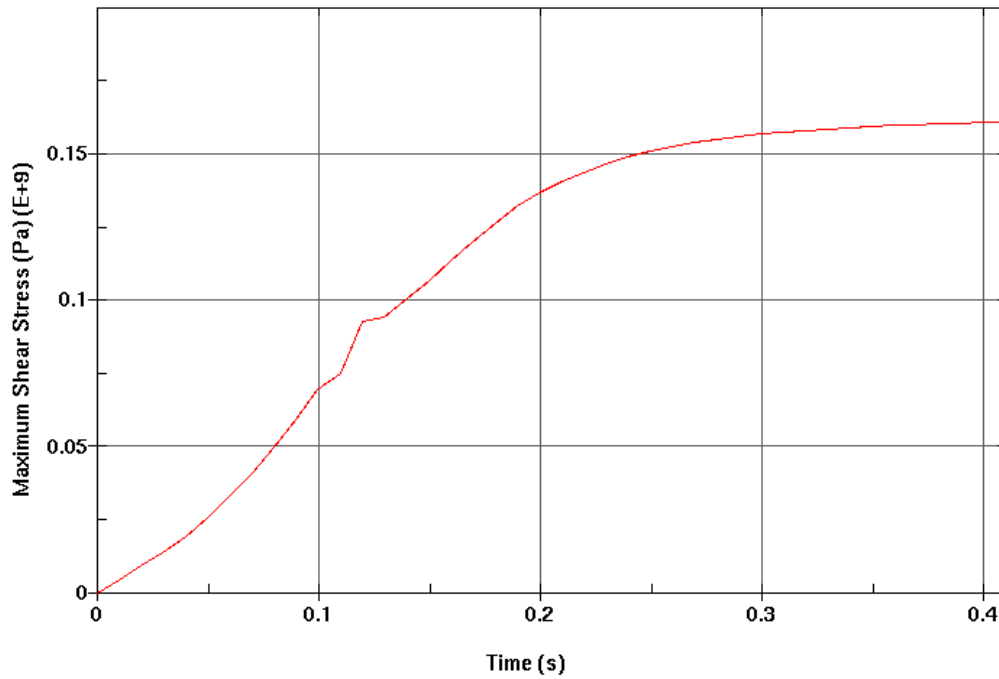


Figure III-9. Maximum Shear Stress (Pa) Plot of the Bulkhead for the Average of all Realizations with Density of Surrounding Rock Multiplied by 2.5





(b)

Figure III-10. Maximum Shear Stress History Plots of the Bulkhead for the Average of all Realizations with Density of Surrounding Rock Multiplied by 2.5:

(a) Maximum Shear Stress through the Cross-Section, and (b) Average of the Shear Stress through the Cross-Section

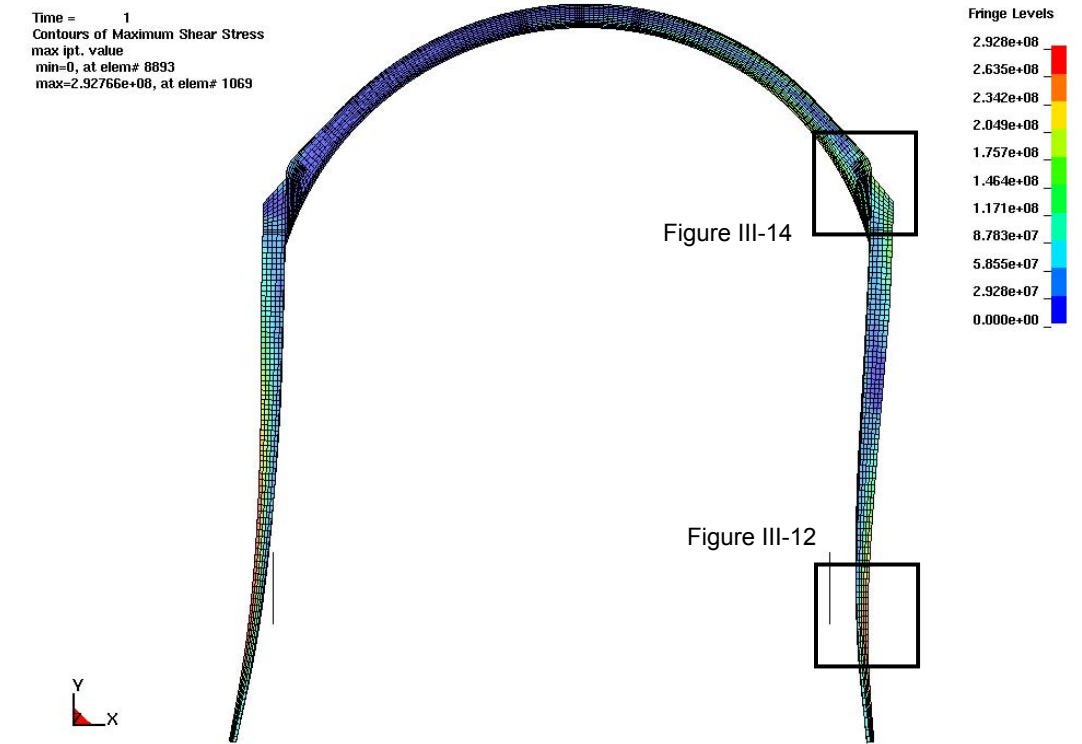


Figure III-11. Maximum Shear Stress (Pa) Plot for the Average of all Realizations with Density of Surrounding Rock Multiplied by 3.0

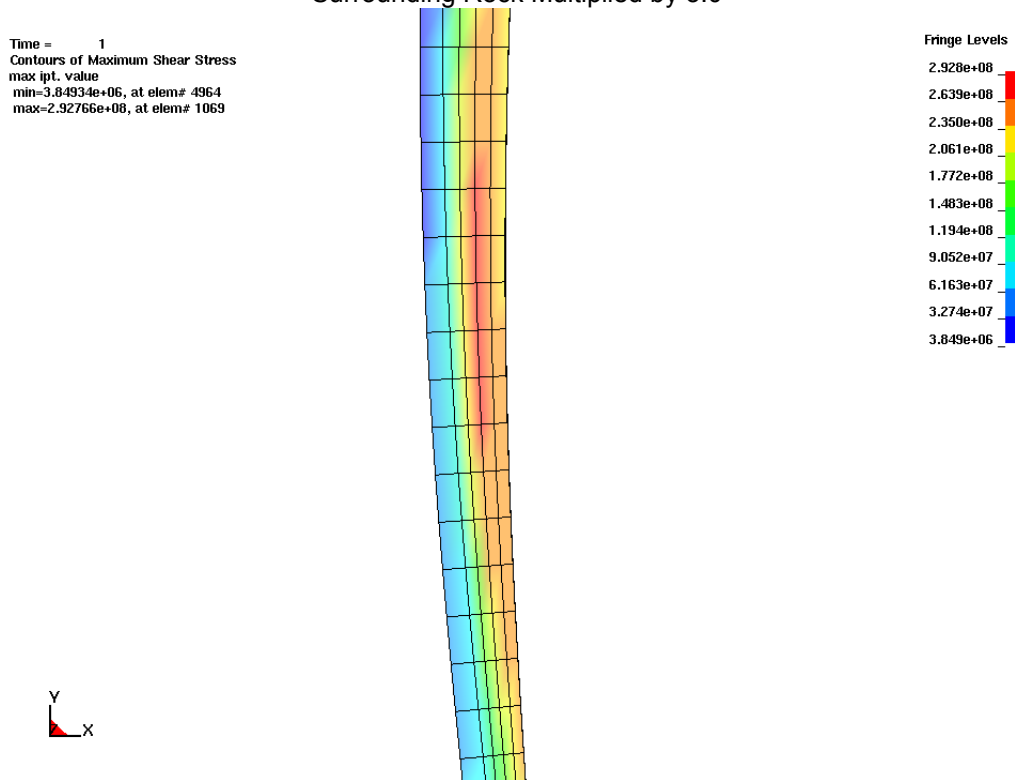


Figure III-12. Maximum Shear Stress (Pa) Plot of the Large Support Beam for the Average of all Realizations with Density of Surrounding Rock Multiplied by 3.0

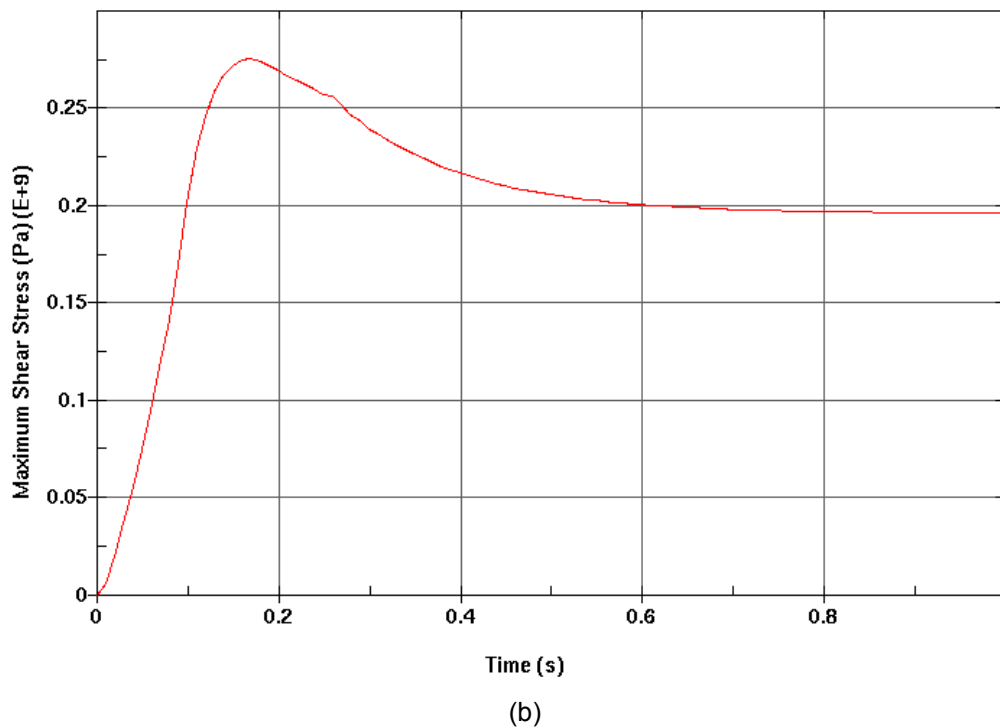
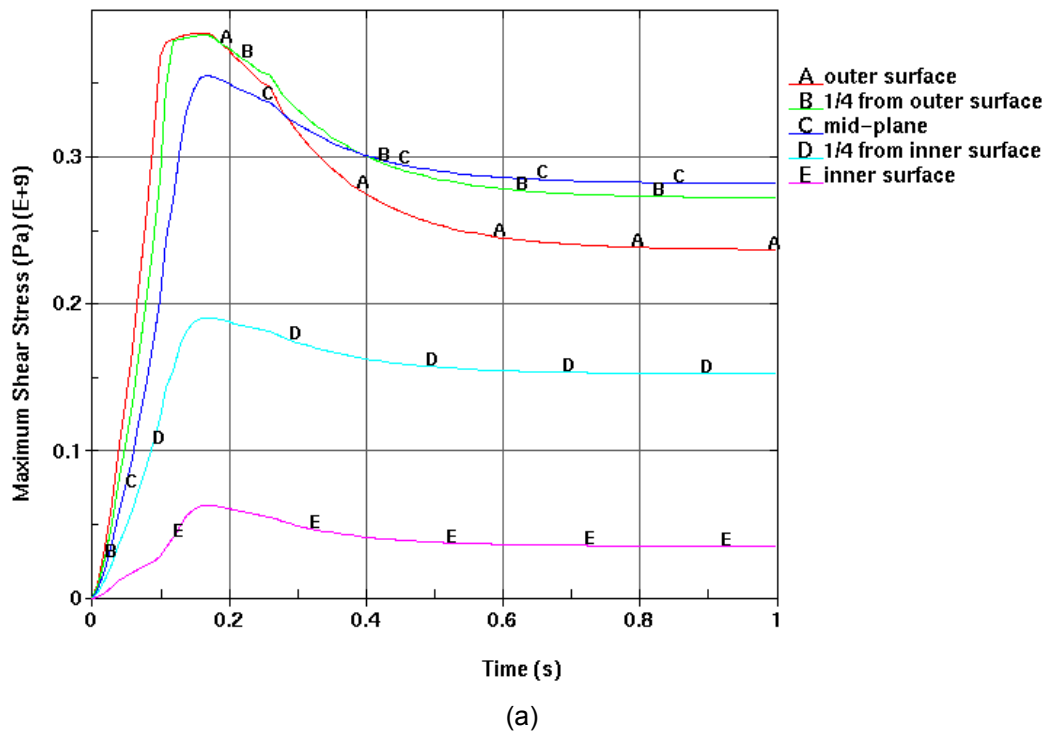


Figure III-13. Maximum Shear Stress History Plots of the Large Support Beam for the Average of all Realizations with Density of Surrounding Rock Multiplied by 3.0: (a) Maximum Shear Stress through the Cross-Section, and (b) Average of the Shear Stress through the Cross-Section

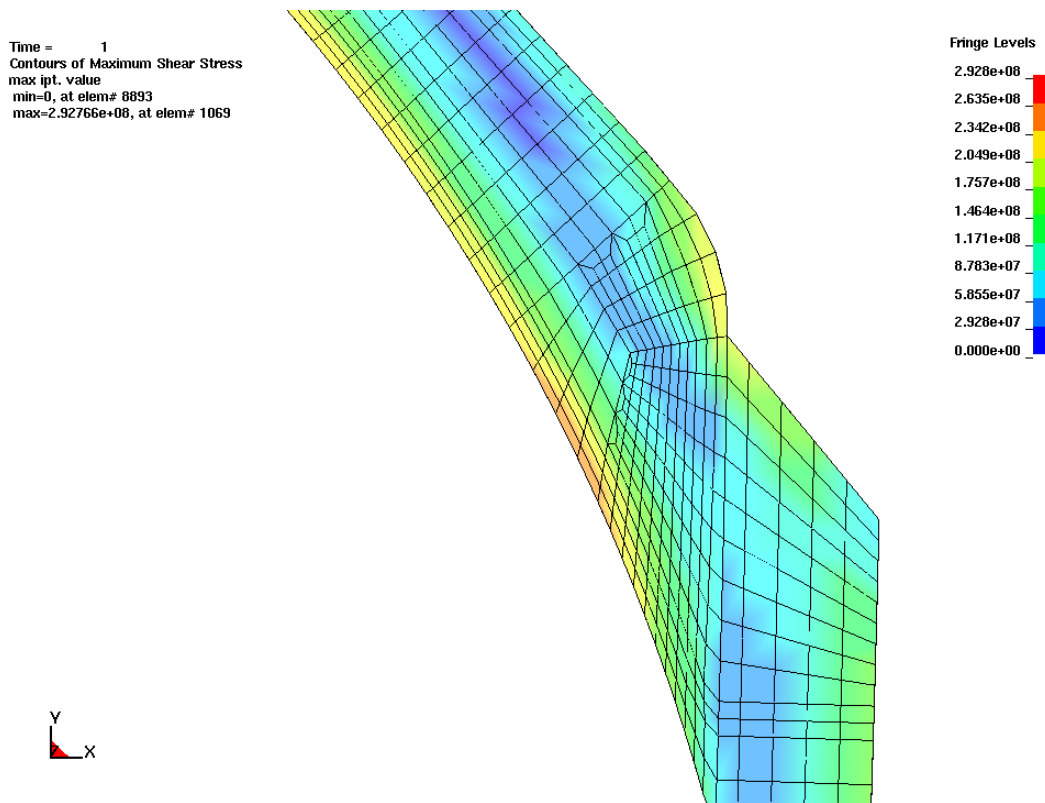
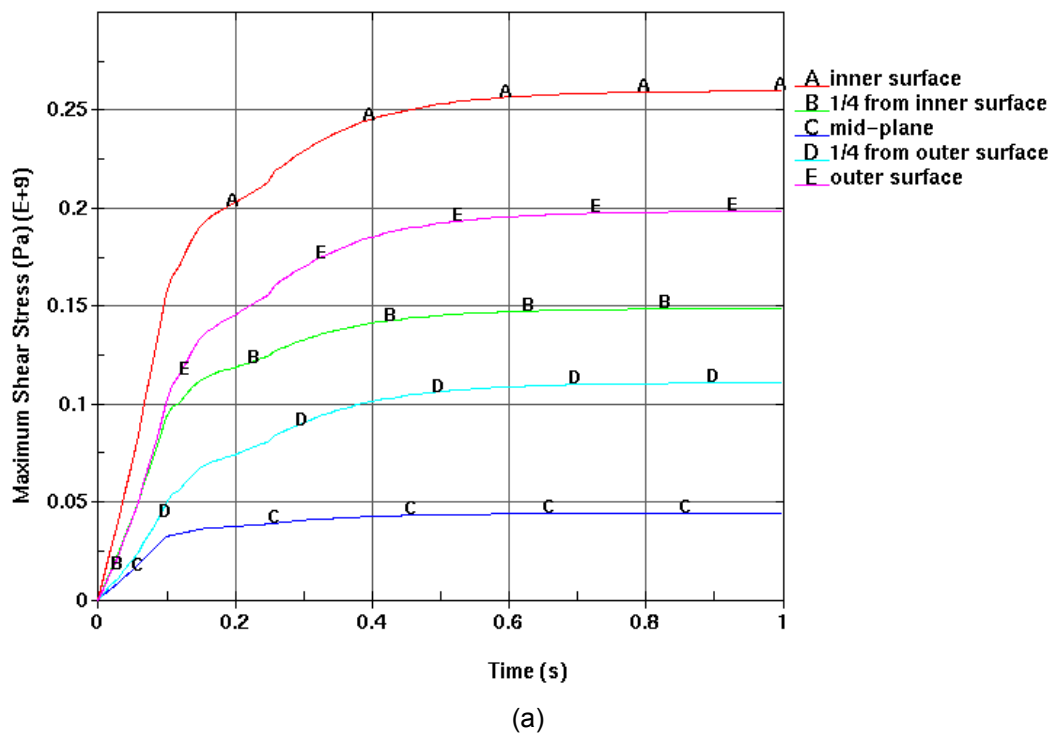
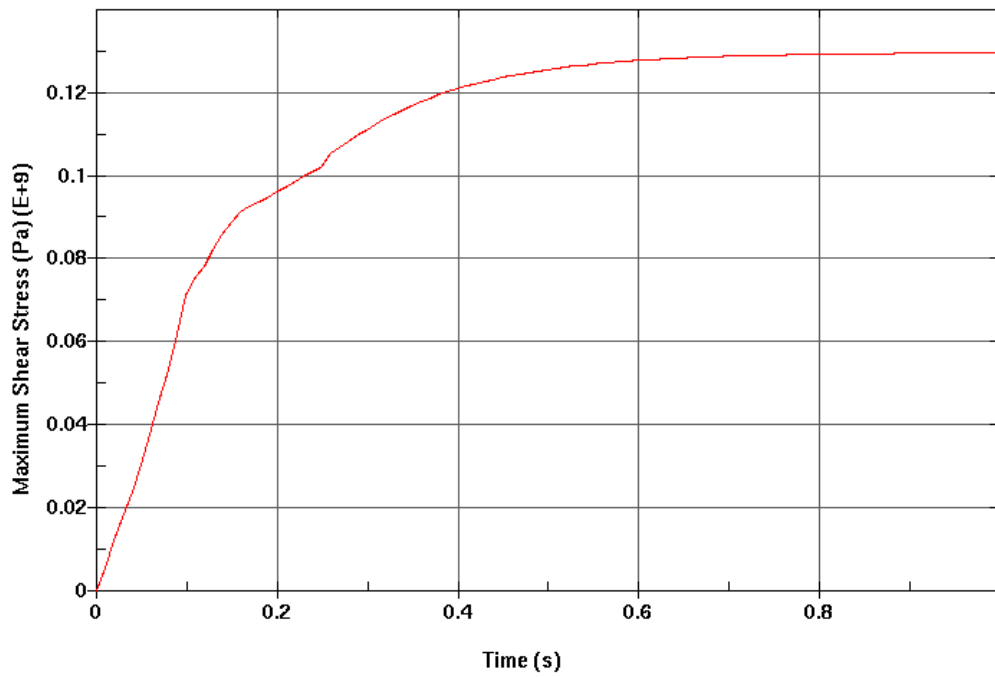


Figure III-14. Maximum Shear Stress (Pa) Plot of the Bulkhead for the Average of all Realizations with Density of Surrounding Rock Multiplied by 3.0





(b)

Figure III-15. Maximum Shear Stress History Plots of the Bulkhead for the Average of all Realizations with Density of Surrounding Rock Multiplied by 3.0:

(a) Maximum Shear Stress through the Cross-Section, and (b) Average of the Shear Stress through the Cross-Section

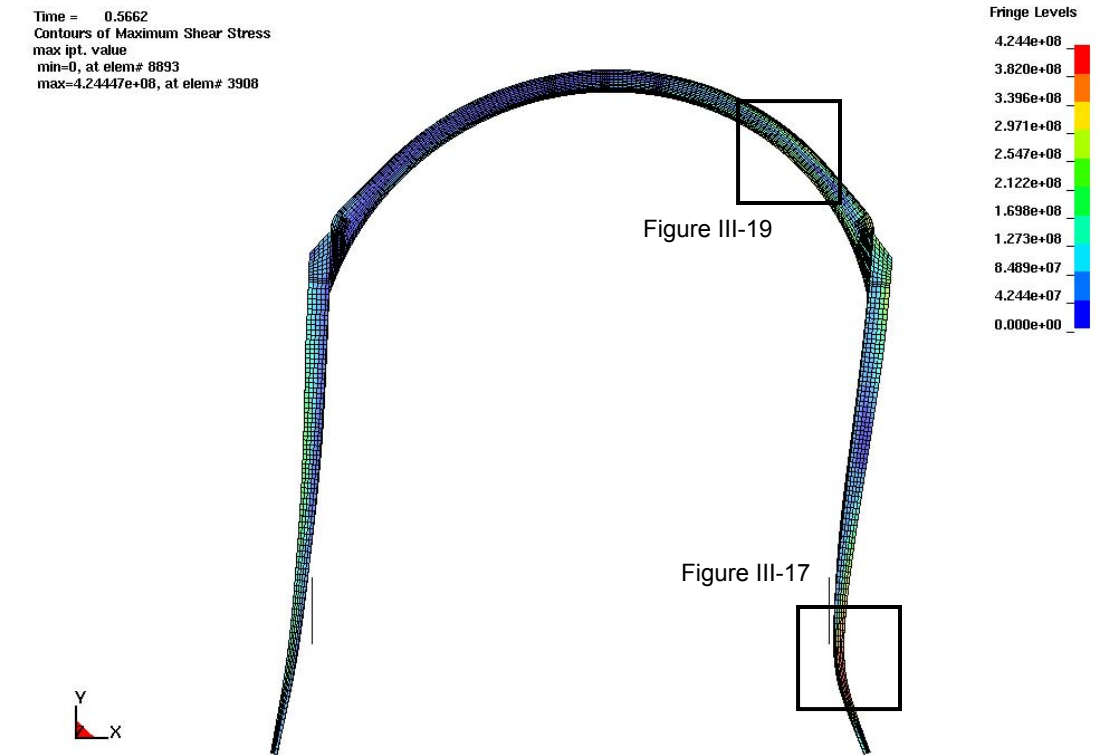


Figure III-16. Maximum Shear Stress (Pa) Plot for the Average of all Realizations with Density of Surrounding Rock Multiplied by 4.0

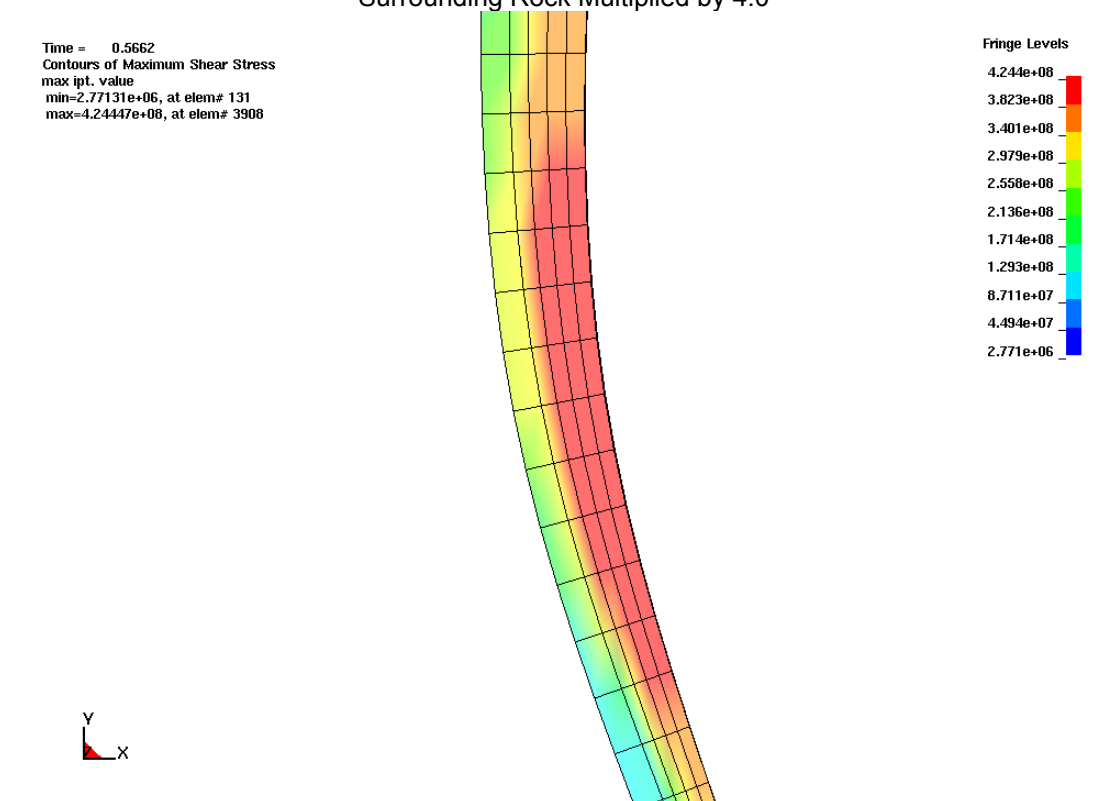
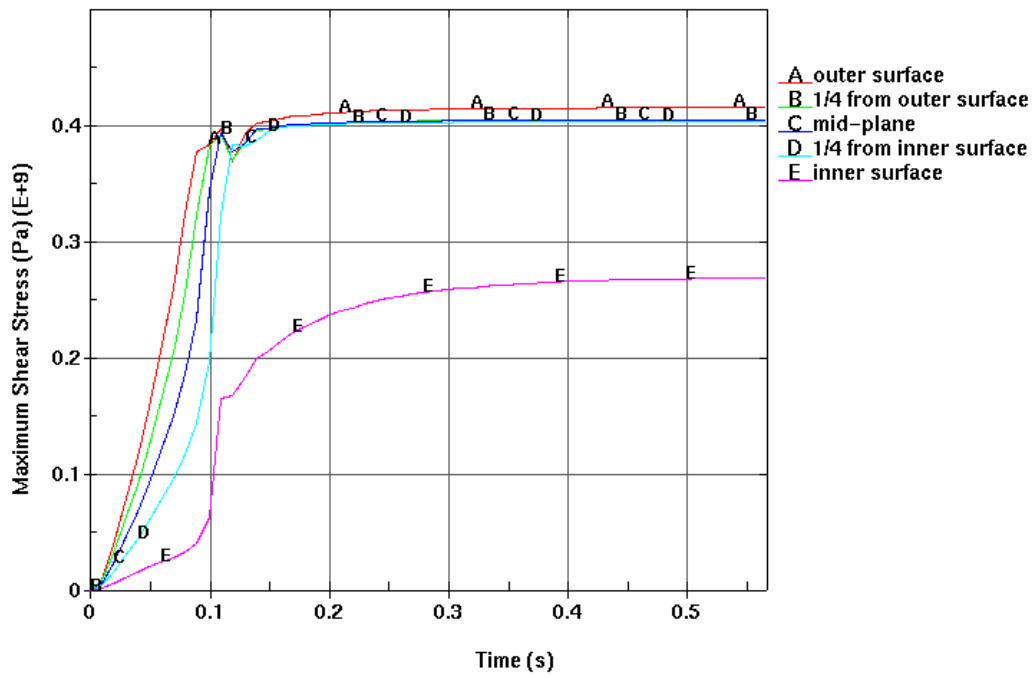
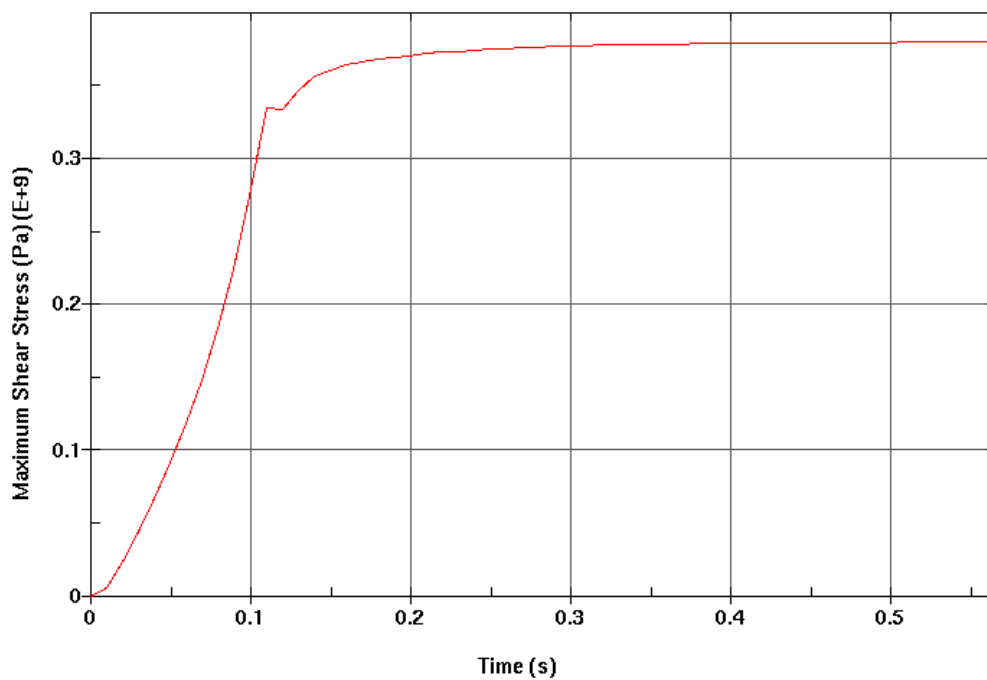


Figure III-17. Maximum Shear Stress (Pa) Plot of the Large Support Beam for the Average of all Realizations with Density of Surrounding Rock Multiplied by 4.0



(a)



(b)

Figure III-18. Maximum Shear Stress History Plots of the Large Support Beam for the Average of all Realizations with Density of Surrounding Rock Multiplied by 4.0: (a) Maximum Shear Stress through the Cross-Section, and (b) Average of the Shear Stress through the Cross-Section

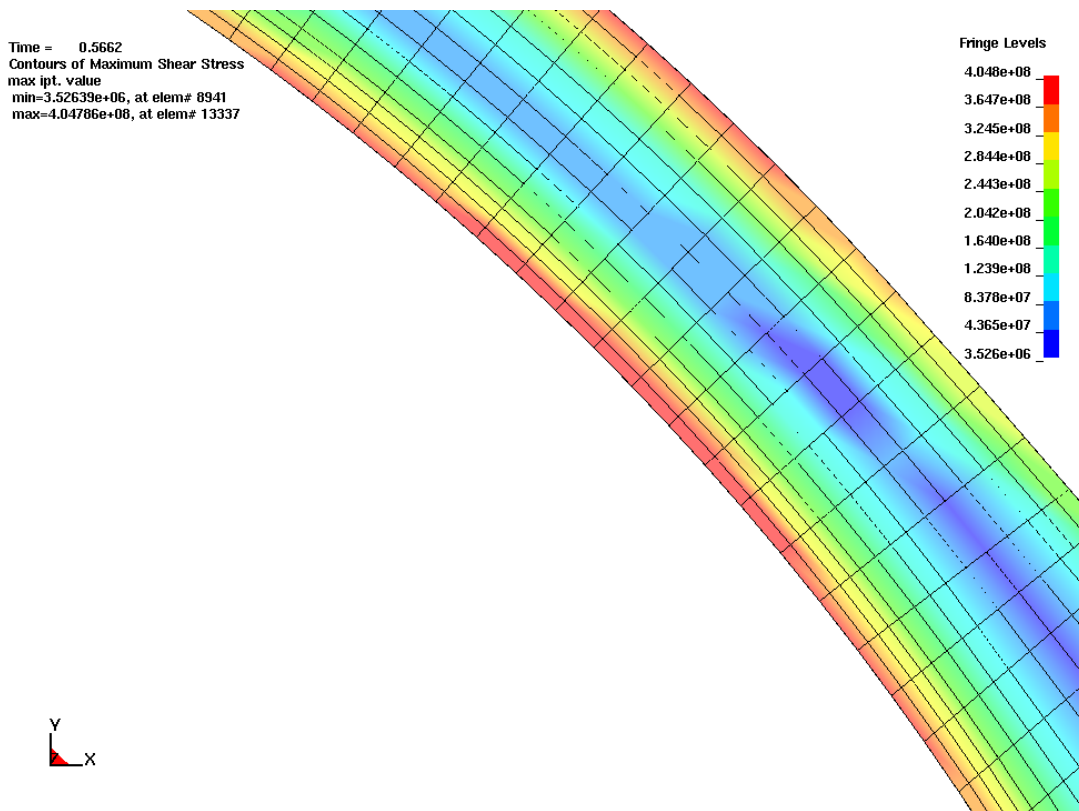
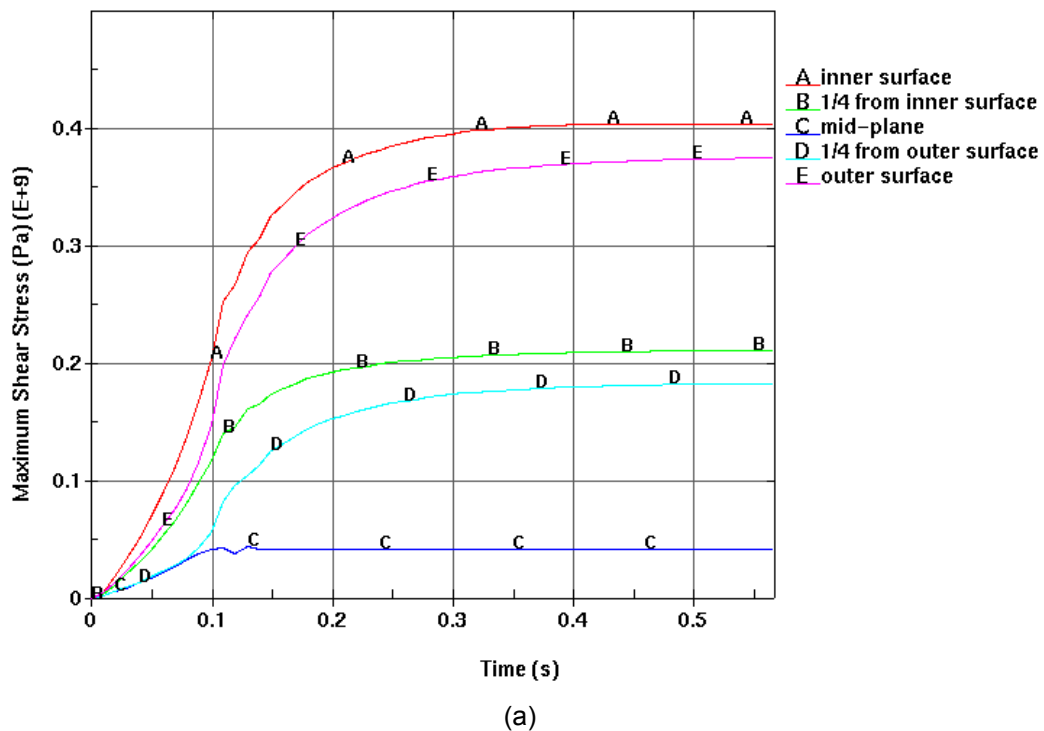
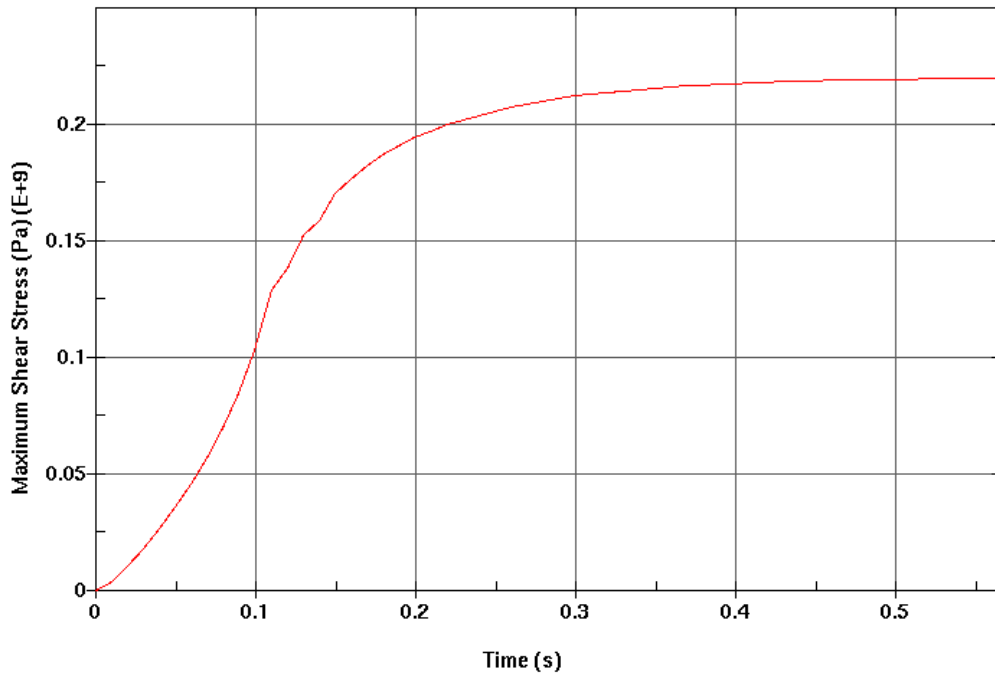


Figure III-19. Maximum Shear Stress (Pa) Plot of the Bulkhead for the Average of all Realizations with Density of Surrounding Rock Multiplied by 4.0





(b)

Figure III-20. Maximum Shear Stress History Plots of the Bulkhead for the Average of all Realizations with Density of Surrounding Rock Multiplied by 4.0:

(a) Maximum Shear Stress through the Cross-Section, and (b) Average of the Shear Stress through the Cross-Section

ATTACHMENT IV

DAMAGED AREA

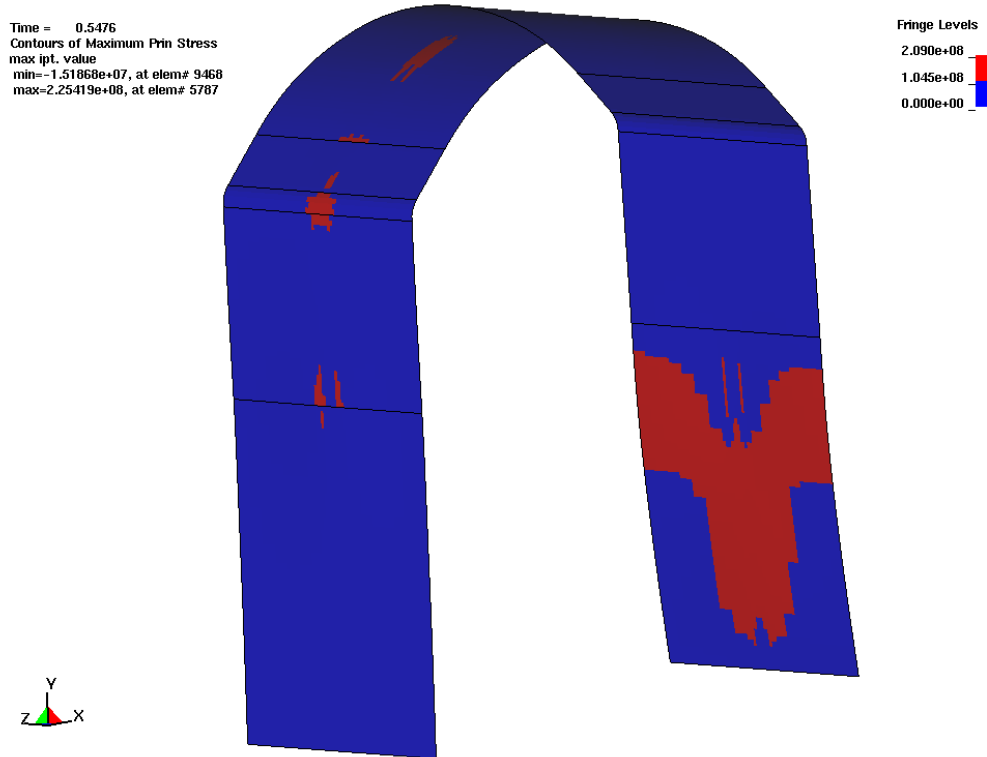


Figure IV-1. Damaged Area of the Ti-7 Plates for Realization 1

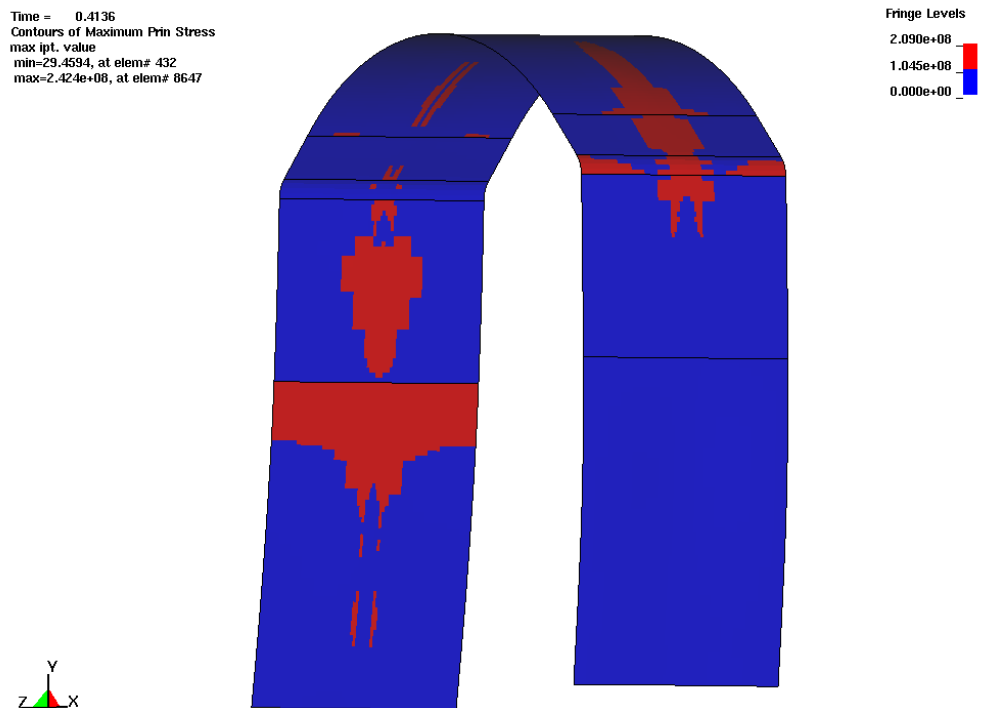


Figure IV-2. Damaged Area of the Ti-7 Plates for Realization 2

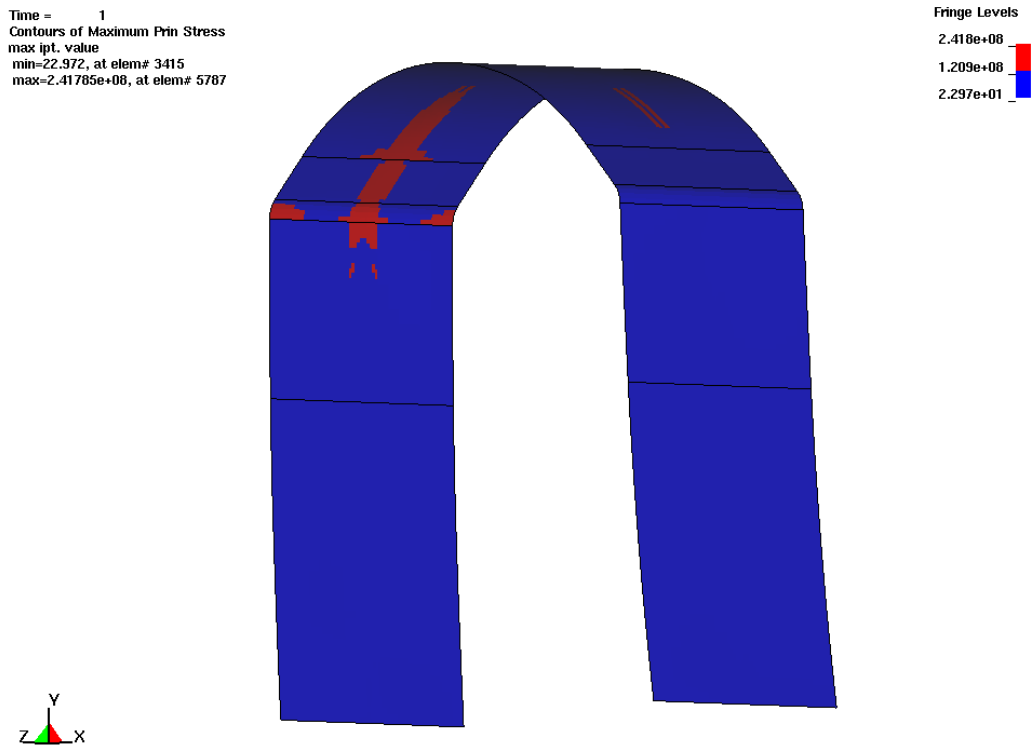


Figure IV-3. Damaged Area of the Ti-7 Plates for Realization 3

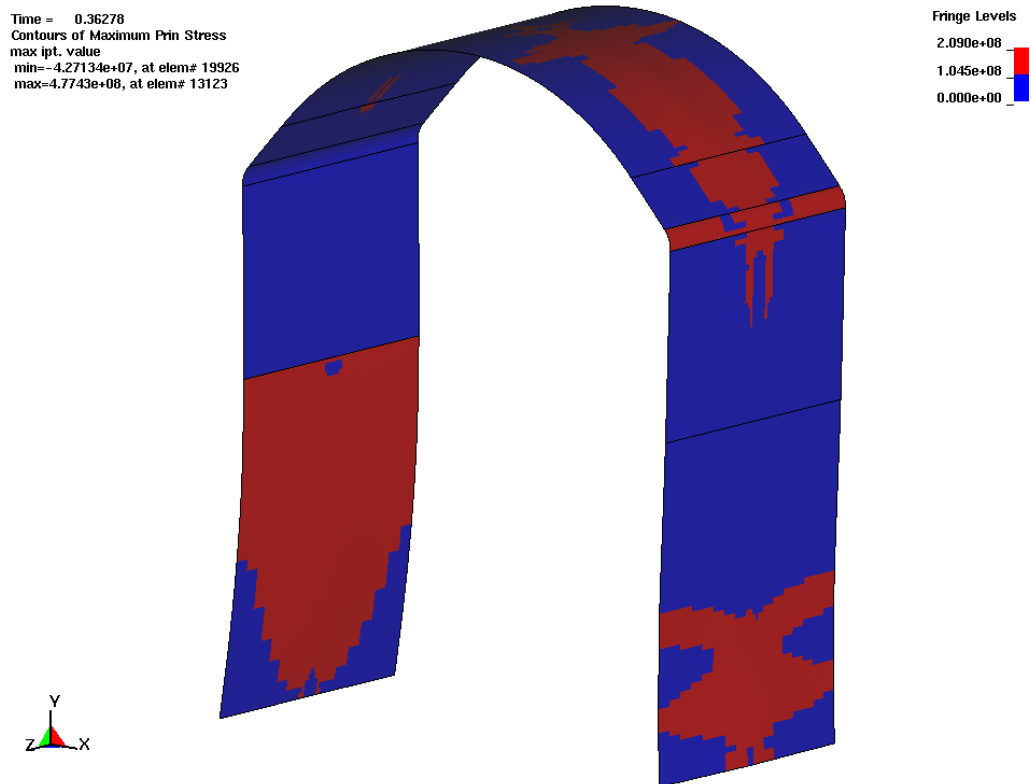


Figure IV-4. Damaged Area of the Ti-7 Plates for Realization 4

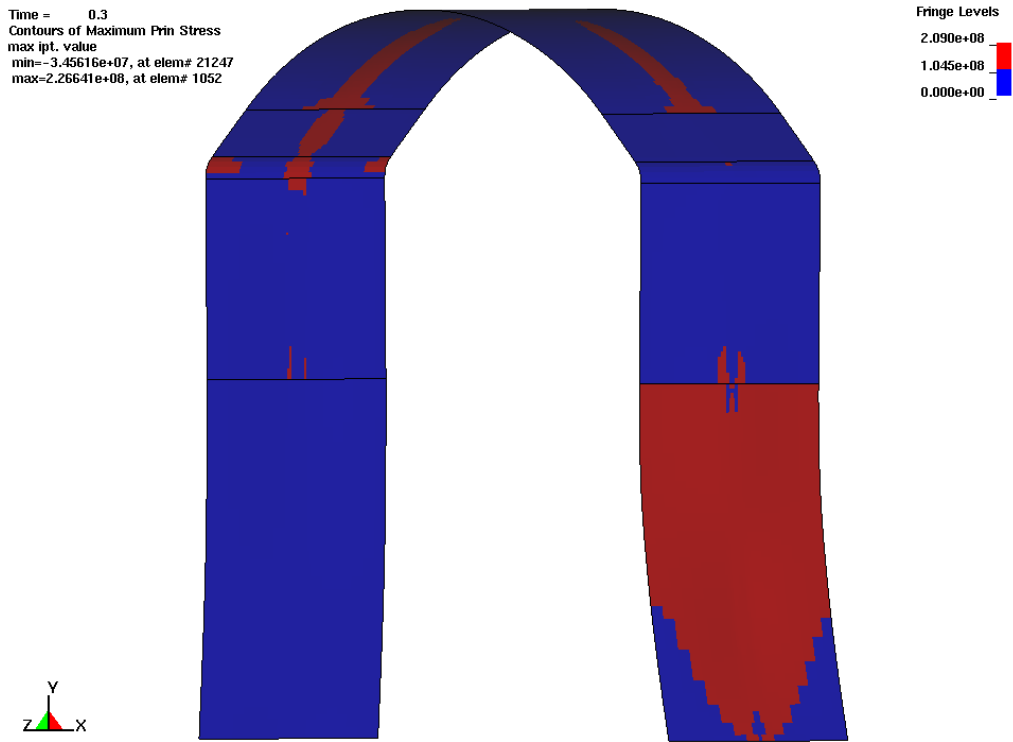


Figure IV-5. Damaged Area of the Ti-7 Plates for Realization 5

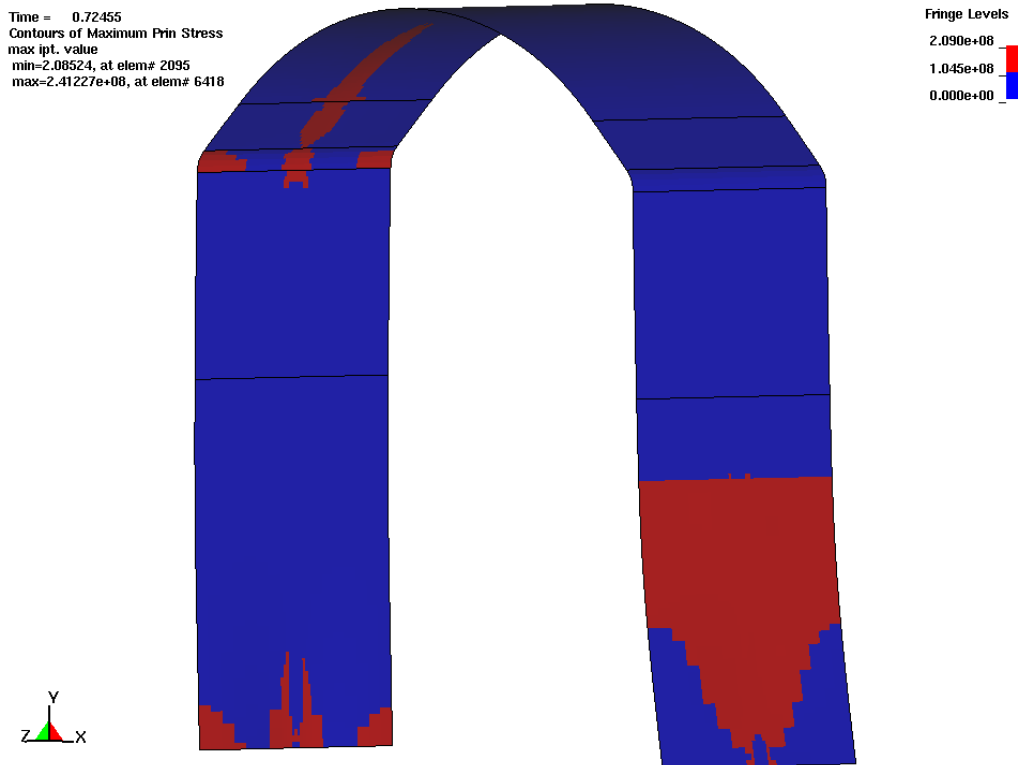


Figure IV-6. Damaged Area of the Ti-7 Plates for Realization 6

ATTACHMENT V

MESH OBJECTIVITY

The purpose of this inquiry is to verify the objectivity of the mesh (i.e., that the calculation results are not mesh-sensitive). An approach used to achieve this goal is presented in detail in Reference 15 (Section 6.2.3). The maximum vertical displacement of the drip shield top (see Figures 7 and V-2a for the location of node 38 [n# 38]) is presented in this section for two different meshes. The obtained results are considered mesh-objective (i.e., mesh-insensitive) if the relative difference of results between the first and the second mesh are much smaller (approximately an order of magnitude smaller) than the relative difference of volumes of their representative (average, typical) elements.

The first mesh is obtained by following the guidance in Reference 15 (Section 6.2.3). The second mesh is refined version of the first mesh. The first mesh is uniformly refined in all three directions. The volumes of the typical elements for the support beam and bulkhead are presented in Table V-1. The numbers presented in Table V-1 in parentheses represent the number of the element that is considered typical (see Figures V-1 and V-2).

The mesh sensitivity is studied for the average of all realizations with the density of the surrounding rock multiplied by 2.5. The choice of this realization is arbitrary: the mesh-objectivity results should not depend on the particular pressure distribution. The calculation with the density of the surrounding rock multiplied by 2.5 is interesting because it illustrates a stability safety margin for that pressure distribution. The results are presented in Table V-2. (Numbers of divisions in the axial, tangential, and thickness directions in the first mesh and the second mesh directions are available in Attachment VII. For the first mesh, check Attachment VII, folder: RNavg2.5 and for the second mesh Attachment VII, folder: RNavg_ref.)

Table V-1. Volume of Typical Element for Two Different Finite Element Meshes

Drip Shield Component	Volume of Typical Element ($1 \cdot 10^{-6} \text{ m}^3$)		
	First Mesh	Second Mesh	Relative Difference (%)
Bulkhead	1.38 (e# 6453)	0.85 (e# 15798)	62
Support Beam	2.47 (e# 4800)	1.46 (e# 12614)	69
	5.21 (e# 4888)	1.92 (e# 12854)	171

Table V-2. Maximum Vertical Displacement of Drip Shield Top for Two Different Finite Element Meshes

Maximum Vertical Displacement ($1 \cdot 10^{-3} \text{ m}$)		
First Mesh	Second Mesh	Relative Difference (%)
19.08	18.92	0.8

According to results presented in Tables V-1 and V-2, the calculation results are not mesh-sensitive.

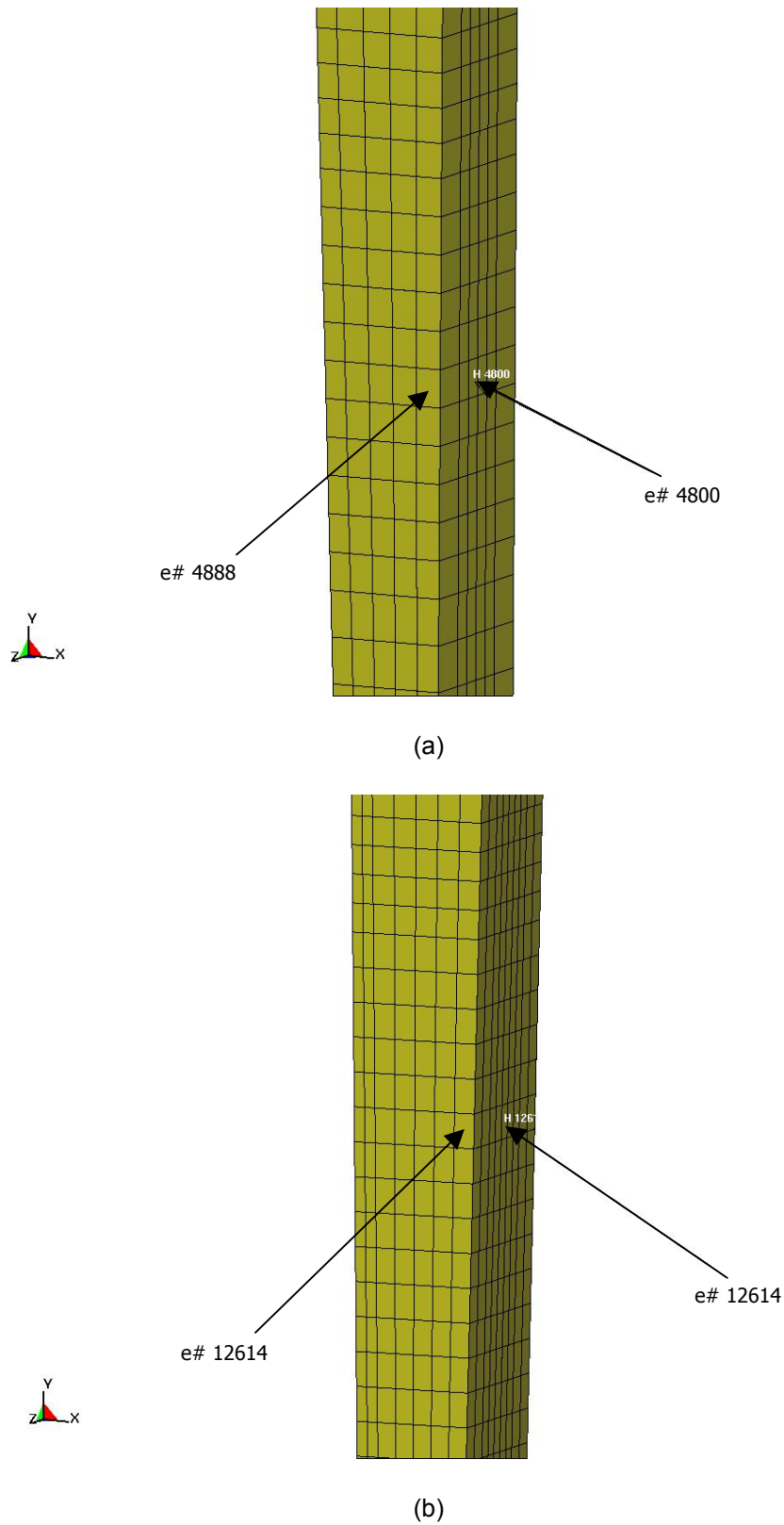
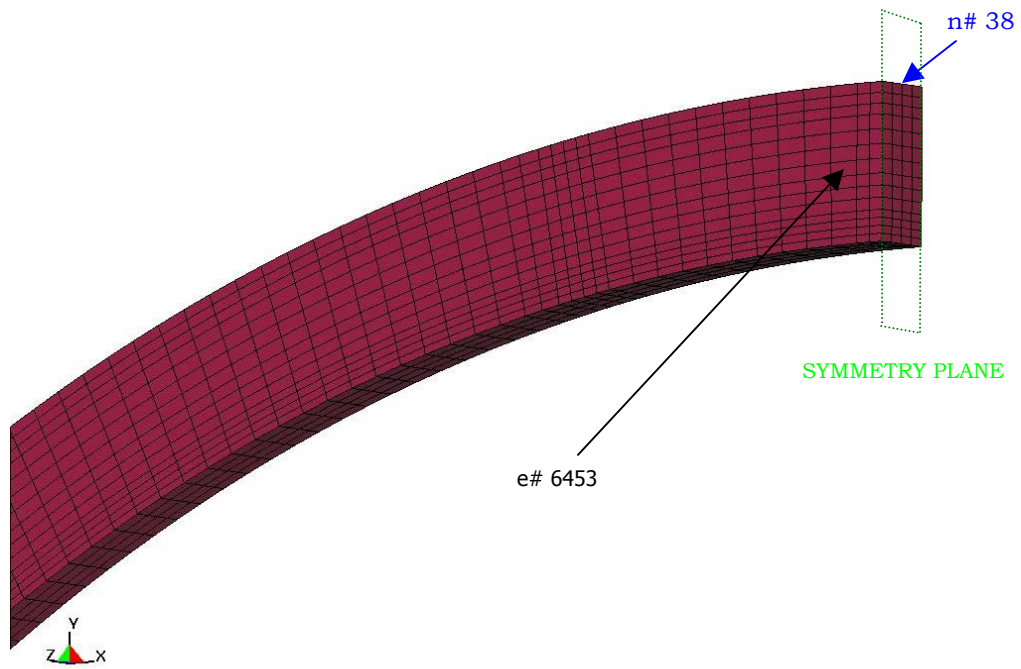
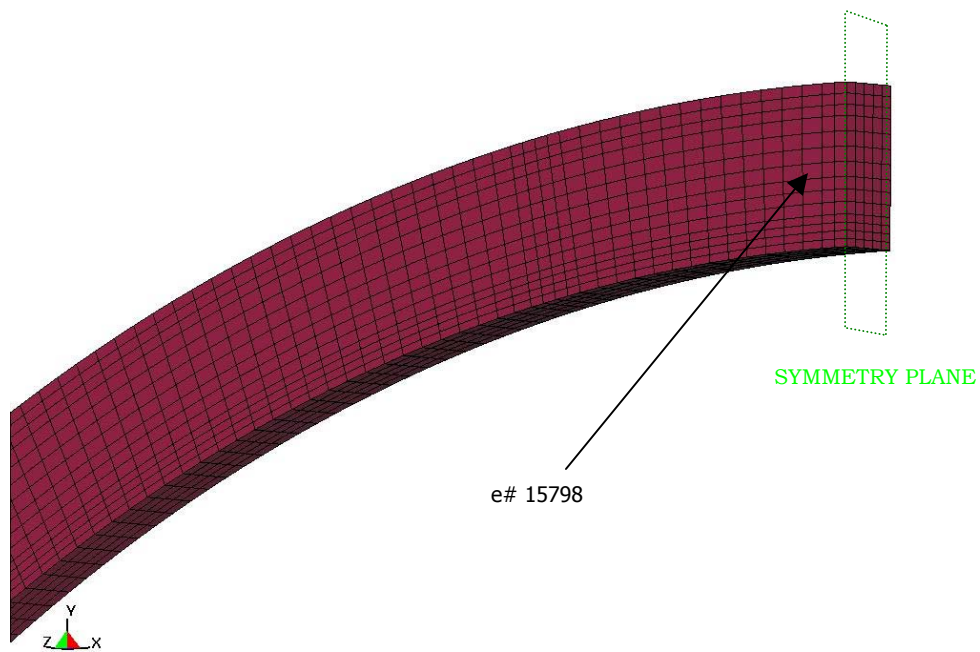


Figure V-1. Details of Finite Element Representation of the Drip Shielded Support Beam: (a) The First Mesh, and (b) The Second Mesh



(a)

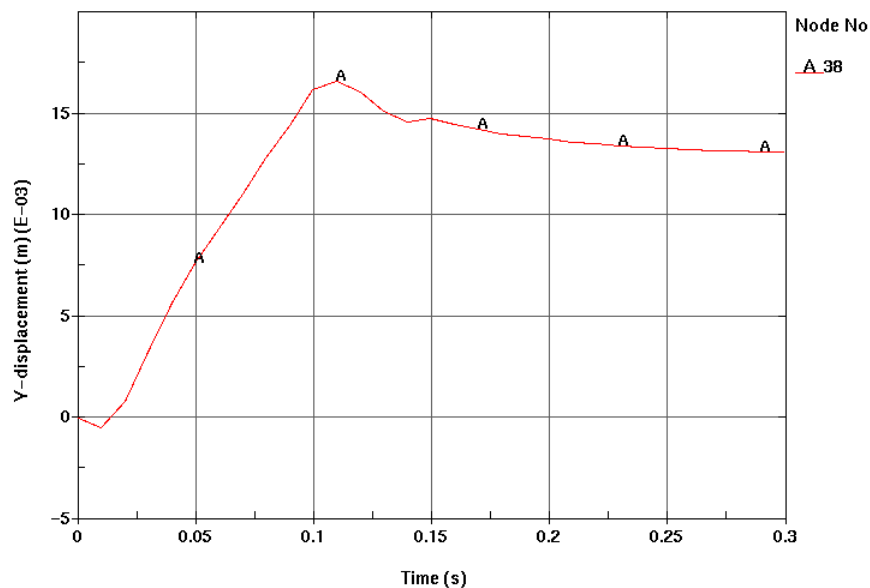


(b)

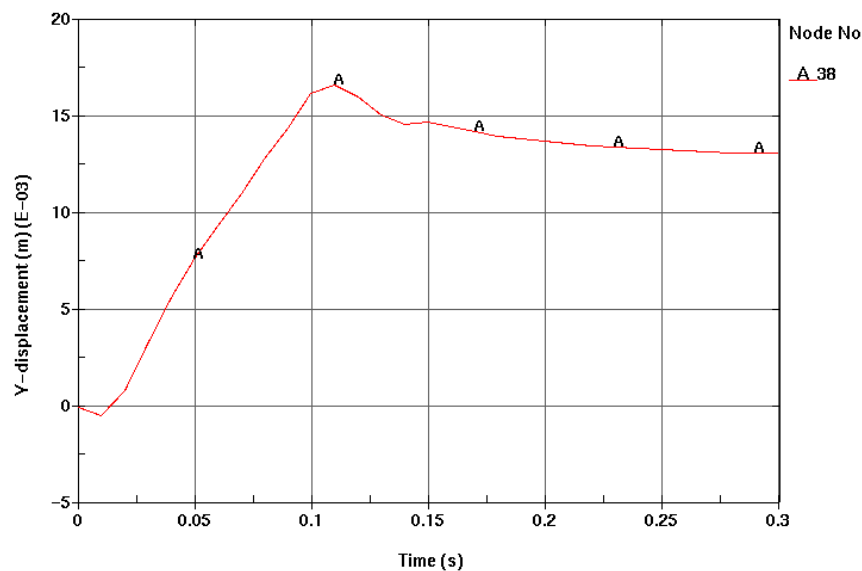
Figure V-2. Details of Finite Element Representation of the Drip Shielded Bulkhead: (a) The First Mesh, and (b) The Second Mesh

ATTACHMENT VI**COMPARISON OF RESULTS OBTAINED BY USING DIFFERENT LS-DYNA VERSIONS**

The purpose of this inquiry is to verify the objectivity of the results with respect to the use of different LS-DYNA versions. Realization 5 is arbitrarily selected for that purpose. The additional calculation is performed by using LS-DYNA V970 and the results are compared with the previously obtained results (LS-DYNA V960). Figure VI-1 shows a comparison of the vertical displacement of the drip shield top for both versions.



(a)



(b)

Figure VI-1. Vertical Displacement of Drip Shield Top:
(a) LS-DYNA V960, and (b) LS-DYNA V970

Title: Structural Stability of a Drip Shield Under Quasi-Static Pressure

Document Identifier: 000-00C-SSE0-00500-000-00A

Page VI-2

According to results presented in Table VI-1, the calculation results are not sensitive to the LS-DYNA Version.

Table VI-1. Maximum Vertical Displacement of Drip Shield Top for Two Different LS-DYNA Versions

Maximum Vertical Displacement ($1 \cdot 10^{-3}$ m)		
LS-DYNA V960	LS-DYNA V970	Relative Difference (%)
16.679	16.680	0.006